Faculty of Science and Engineering
Department of Spatial Sciences

Spatial and Temporal Characterisation of Ecosystems in Landscapes Surrounding Granite Outcrops

Goran Alibegovic

This thesis is presented for the Degree of
Doctor of Philosophy
of
Curtin University

October 2016

DECLARATION

To the best of my knowledge and belief this thesis contains no material previously published by any other person except where due acknowledgment has been made.

This thesis contains no material which has been accepted for the award of any other degree or diploma in any university.

Signature:

Date: 7 October 2016

ABSTRACT

This study examines the characteristics of granite outcrops (GOs) to identify potential climate change refugia for flora of the South-west Western Australian Floristic Region (SWAFR) (Byrne & Hopper, 2008), a global biodiversity hotspot (Myers et al., 2000). Refugia are habitats that components of biodiversity retreat to, persist in, and can potentially expand from under changing climatic conditions (Keppel et al., 2012). Three hypotheses about refugia habitats near GOs were formulated (Wardell-Johnson et al., 2009): 1) they provide more water and nutrient resources, 2) habitats on and near granite outcrops are more diverse than in the surrounding landscape, and 3) granite outcrops with a large diversity of habitats are more likely to contain refugia.

The study develops and implements geospatial techniques to test these hypotheses using remotely sensed imagery at the landscape scale. Firstly, a methodology to map GOs across the SWAFR using biannual Landsat TM imagery is developed. Secondly, patterns of ecosystem greenspots are modelled to predict refugia in landscapes surrounding GOs. Thirdly, phenological characteristics are quantified to identify habitat differences in growing conditions and responses to a current climatic trend of warming and drying that began in the mid-1970s (Bates et al., 2008).

Knowledge of the location and extent of GOs across the SWAFR is important to further study their potential role as refugia. An adaptive vegetation cover mask capitalising on seasonal differences of the low growth cover (e.g. lichen, algae and moss), combined with a supervised classification, allowed differentiation of granite from other land covers on five GOs across the rainfall gradient. This methodology provided high classification accuracy (Overall Kappa ranged from 0.83 to 0.91) irrespective of location. There is potential to use these methods to compile a more complete GO inventory over the region via calibration of the vegetation mask parameters.

GOs in the SWAFR support a wide range of taxa, vegetation types and habitats. An approach to identify potential refugia based on a time series of remotely sensed imagery was developed and applied. A novel means for identification of potential refugia is presented, based on fuzzy standardisation and the weighted fuzzy combination (WFC) of the time series data. A detailed map of vegetation response over the twelve year

period was generated to relate growth to environmental variables indicative of local resource availability. Potential ecosystem greenspots were identified using available landscape stratifications, Land zones and the Interim Biogeographical Regionalisation for Australia (IBRA) subregions. The approach was tested on five GOs across the SWAFR. It showed that land zone stratification based on underlying geology, geomorphology, soils and vegetation is best suited for mapping ecosystem greenspots. Overall Kappa ranged from 0.86 to 0.95 compared to 0.72 to 0.78 for IBRA subregions stratification and 0.56 to 0.64 when no stratification is applied.

Vegetation phenology of annual plants corresponds most strongly to light, temperature and water availability and any changes may, therefore, signal important year to year climatic variations or global environmental change. Here, the hypothesis that aprons near GOs across the SWAFR provide insulation from climatic fluctuations relative to the areas away from them is tested by assessing key phenological metrics. The approach was tested at the Porongurup Range at the fringes of the GOs (apron sites) and on non-apron sites. Apron sites at this location are areas with tall open forests of Karri *(Eucalyptus diversicolor)*, whereas non-apron sites are located away from the GOs and here are dominated by open forests of Jarrah *(Eucalyptus marginata)*. Results showed that vegetation located on GO aprons have a longer growing season that starts earlier than at the surrounding landscapes as a direct result of additional resources and protection provided by GOs. Results strongly indicate that spatial and temporal patterns of phenological metrics such as length of growing season and start of growing season are effective indicators of isolated refugia across the SWAFR.

The improved ability to map GOs and ecosystem greenspots has enhanced the ability to study them in more detail and enriched the understanding of the importance of refugia under a warming and drying climate trend. Quantification of the different levels of resources available to flora identified by studying the phenological patterns at GO apron locations and away from GOs, is increasingly important in conservation planning as a climate change adaptation strategy.

ACKNOWLEDGEMENTS

I have been fortunate by having received enormous support and assistance from a great many people throughout my research whom I acknowledge hereafter. For those that I might overlook, please accept my gratitude for the role that you have played.

First, I give my upmost gratitude to Dr Grant Wardell-Johnson and Dr Todd Robinson of Curtin University for their tireless assistance as supervisors/advisers. I also want to thank Dr Antonius Schut of Wageningen University in the Netherlands, who provided mentorship during the difficult early stages of identifying an interesting research area for a PhD thesis.

A research project is hardly feasible without the necessary funding and I want to thank the Australian Research Council (ARC) for their support in the linkage project (LP0990914) entitled: 'Protecting the safe havens: will granite outcrop environments serve as refuges for flora threatened by anthropogenic climate change?'.

I want to thank all staff and students at Curtin University for providing such an inspiring environment during my time spent at the University. I would like to acknowledge the moral and practical support of Dr Gunnar Keppel, Ms Lori Patterson and Dr David McMeekin.

I am very grateful to my employer, Department of Water, and in particular my Manager Lindsay Preece for having supported my studies by means of a weekly study time allowance, which has significantly helped improve the feasibility for me to pursue further study. Department of Water gave me much freedom to pursue my academic interests and apply them to my work, for which I am grateful.

Last but most importantly I want to thank my wife Beth and my daughters Selma and Amira for their patience and support.

TABLE OF CONTENTS

LIST OF FIGURES

LIST OF TABLES

ACRONYMS

AL	Apron landscapes
ANOVA	Analysis of Variance
ASTER	Advanced Spaceborne Thermal Emission and Reflection Radiometer
AUC	Area under the curve
AVHRR	Advanced Very High Resolution Radiometer
BoM	Bureau of Meteorology
CSIRO	Commonwealth Scientific and Industrial Research Organisation
CVA-MVC	Constrained-view angle - maximum value composite
DAFWA	Department of Agriculture and Food Western Australia
DEM	Digital elevation model
DEM-H	Hydrologically enforced digital elevation model
DEM-S	Smoothed digital elevation model
DoE	Department of Environment
DPaW	Department of Parks and Wildlife
EROS	Earth Resource Observation and Science Centre
ESRI	Environmental Sciences Research Institute
ETM	Enhanced thematic mapper
FNR	False negative rate
fPAR	fraction of photosynthetically active radiation
FPR	False positive rate
GA	Geoscience Australia
GDA94	Geocentric datum of Australia 1994
GIS	Geographic information system
GO	Granite Outcrops
GSWA	Geological Survey of Western Australia
HSD	Honest significant difference
IBRA	Interim biogeographical regionalisation for Australia
LiDAR	Light detection and ranging data
MODIS	Moderate resolution imaging spectroradiometer
MOD13Q1	MODIS 16-day Level 3 global 250 m data
NASA	National Aeronautics and Space Agency

NDVI	Normalized difference vegetation index
NIR	Near infra-red band
OCBIL	Old, climatically buffered, infertile landscapes
OSL	Old stable landscapes
PC	Photosynthetic capacity
RGB	Red-green-blue
ROC	Receiver operating characteristic
SL	Surrounding landscapes
SPSS	Statistical package for the social sciences
SRTM	Shuttle radar topography mission
SWAFR	South-west Australian Floristic Region
TM	Thematic mapper
TPR	True positive rate
WFC	Weighted fuzzy combination
USGS	United States Geological Survey
VI	Vegetation index
YODFEL	Young, often disturbed, fertile landscapes

1. INTRODUCTION

1.1. Background

The South-west Australian Floristic Region (SWAFR) (Hopper & Gioia, 2004) of Western Australia is recognised as one of the top 25 global biodiversity hot spots (Myers et al., 2000) and is the only such region in Australia. This old, topographically subdued and nutrient-poor landscape has been considered to be a somewhat unusual location for such a rich diversity of plants (Hopper & Gioia, 2004). However, the region is interspersed with numerous GOs of the underlying Yilgarn Craton and the Albany-Fraser Orogen bedrock formations (Withers, 2000), which may provide habitat refuges and be partial drivers of the rich biodiversity and unique endemic flora observed there (Hopper et al., 1997; Porembski & Barthlott, 2000; Hopper & Gioia, 2004). Many taxa have survived past regional climate changes by contracting to dispersed refugia characterised by features that ameliorate impacts of climate change (Hansen et al., 2007; Yates et al., 2007). Such refugia will likely contribute to the persistence of species and ecological communities as the south-west of Western Australia has observed a drying climate trend. As such, protection of refugia in the south-west of Western Australia is a vital component of climate change adaptation strategies (Keppel & Wardell-Johnson, 2012).

The research project "Protecting the safe havens: will granite outcrop environments serve as refuges for flora threatened by anthropogenic climate change" (Wardell-Johnson et al., 2009), funded by the Australian Research Council (ARC), looks at determining and quantifying the extent to which GOs across the SWAFR have acted as refugia in the past and will be able to do so under predicted future climate change. This ARC project examines the characteristics of GOs as potential climate change refugia for the flora of the SWAFR, a global biodiversity hotspot in the face of global climate change. This highly weathered and flat landscape offers little scope for biota to migrate to altitudinal refugees (Wardell-Johnson et al., 2009). However, the landscape is characterised by numerous GOs scattered across this mesic to semi-arid rainfall gradient (Withers, 2000). These minor variations in topographic complexity may serve to ameliorate the impacts of climate change for the flora in this area (Wardell-Johnson et al., 2009).

GOs are home to many microhabitats of major importance to the specific assembly of flora and plant communities, and are true hotspots of biodiversity across the SWAFR. Microhabitats on GOs may provide cooler and wetter growth conditions than those available in the surrounding landscape. The diversity of microhabitats, microclimates and water availability on GOs across the SWAFR has enabled the persistence of species beyond their main range in the face of climatic fluctuations. These outcrops are dominated by woody and herbaceous perennials and have an unusually rich diversity of annuals (Hopper et al., 1997). This suite of unique microhabitats on GOs such as rock pools (gnammas), non-flooded soil pockets, vegetation mats, temporarily flushed rocky surfaces and aprons with influx of water and nutrients from the outcrop (Wardell-Johnson et al., 2009) are likely responsible for ameliorating climate change in these landscapes. These habitats are characterised by their own sets of ecological filters assisting in the assembly of flora and plant communities and form the substrate for evolutionary assembly process, including speciation, extinction and migration (Dean & Wardell-Johnson, 2010).

Four hypotheses have been formulated (Wardell-Johnson et al., 2009) about refugia habitats near GOs: 1) topographic complexity on GOs is associated with increasing plant community productivity and complexity, and micro-climatic variations within GOs buffer against regional climate change; 2) phylogeographic patterns are indicators that GOs have acted as refugees in the past and are important reservoirs of genetic diversity; 3) Soils and water resources at the base of GOs are higher than in the surrounding landscape matrix, and individual plants are under less stress than those in the matrix; and 4) plant communities are more resilient to anthropogenic climate change disturbances than the communities of the surrounding landscape matrix.

1.2. Granite outcrop mapping

Mapping the location of GOs using automated or semi-automated techniques is a fundamental, though important, step for further validating the aforementioned hypotheses. Some outcrops across the SWAFR have been identified in a native vegetation database derived from aerial imagery interpretation (Schoknecht et al., 2004). However, no comprehensive or accurate map is currently available for GOs across the

SWAFR despite recommendations for a granite atlas of the region in 2000 (Campbell et al., 2000).

The SWAFR is considered as one of the five Mediterranean-climate ecosystems biodiversity hot spots (Cowling et al., 1996). This old, highly weathered, topographically subdued and nutrient-poor landscape has been considered to be a unique and unusual location for such a rich diversity of plants (Hopper & Gioia, 2004). However, the landscape is interspersed with numerous GOs of the Yilgarn Craton and Albany-Fraser Orogen formations that form its base (Withers, 2000), which may provide habitat refuges and be partial drivers of the rich biodiversity and unique endemic flora observed there (Hopper et al., 1997; Porembski & Barthlott, 2000). A better knowledge of the location and extent of these GOs may allow further quantification of their role in maintaining favourable climatic conditions for refugia that are absent in the surrounding landscape (Yates et al., 2010; Keppel et al., 2012), and would therefore be important for conservation planning (Keppel & Wardell-Johnson, 2012).

Remote Sensing and image processing techniques have proven capability for mapping relatively bare (e.g. not covered in vegetative material) and exposed GOs. For example, Campbell et al. (2000) have tested the feasibility of granite likeness scores based on Landsat Thematic Mapper (TM) image sequences at prominent GOs in Kellerberrin (e.g. Mt Caroline and Mt Stirling). However, they indicated that whilst bare granite can be separated from native vegetation, it was less distinguishable from uncovered sandy soils. GOs across the SWAFR present a further challenge for semi-automated mapping in that they are typically covered with lichen, algae and mosses, which strongly mask the unique bare granite key absorption features (Satterwhite et al., 1985; Schut et al., 2010)

1.3. Greenspot modelling

Ecosystem greenspots are locations that have high and temporally stable levels of plant productivity relative to nearby locations (Mackey et al., 2012). These areas have potential to function as drought and fire refugia - areas that burn less often or at less intensity than surrounding areas (Yates et al., 2003; Reside et al., 2014). If soil and water resources around the GO aprons (fringes) are higher than in the surrounding

landscape matrix, and individual plants are under less stress than those in the matrix (Wardell-Johnson et al., 2009) then it is likely that plants on the apron will be greener for longer (i.e. greenspots).

Identifying potential greenspots using remote sensing techniques is relatively new (e.g. Mackey et al., 2012), partially validated (e.g. Gould et al., 2014) but desirable because it enables rapid investigation over large regions (Ashcroft et al., 2012). Previously, greenspots were identified from estimates of gross primary productivity derived from the remote sensing data (Klein et al., 2009).

Fundamental to this approach is the assumption that climate and geomorphology interact over time to produce characteristic landscape patterns and influence the distribution of soil and plant associations (Lawson et al., 2010). Consequently there are associations of these environmental components, and landscape can be classified and mapped into units with characteristic patterns and a degree of internal homogeneity (Schoknecht, 2002).

1.4. Phenological cycles of apron vegetation

Seasonal characteristics of plants, such as emergence and senescence, are closely related to the annual cycle of regional climate (Reed et al., 1994). A typical phenological pattern of native vegetation is a low rate of photosynthesis persisting in winter followed by a rapid increase to a maximum by late spring. Changes in phenological events may therefore signal important year to year climatic variations or global environmental change (Reed et al., 1994). The timing and progression of plant development may provide information about ecosystem composition, linked to the growing condition of plants and their environment. The phenological patterns of terrestrial ecosystems are related to long term regional climatic patterns (Jeganathan et al., 2010). However, annual variation in phenology can be used as a proxy of variation in climatic conditions (Schut et al., 2009; Huete & Saleska, 2010). The existing spatio-temporal models of spectral indices, using data collected across time and space (Smith et al., 2003), are capable of measuring broad scale changes in the landscape that may not be associated with phenological events of specific plants. However, controversies exist when quantifying landscape phenology with imagery due to differences in temporal patterns for various spectral indices (Huete & Saleska, 2010). Also, at smaller spatial scales, it

is yet unclear how the effects of the phenological response to regional climate can be differentiated from local differences in ecosystems. It is expected that phenological patterns are similar within climatic zones, however small differences in these phenological patterns may be indicative for ecological niches with specific habitat characteristics.

Remote sensing techniques offer great potential for monitoring and analysing vegetated areas at various spatial, spectral and temporal resolutions. Satellite imagery available globally with a daily repeat cycle such as Advanced Very High Resolution Radiometer (AVHRR), has provided data to examine and monitor phenological events over large regions (Richards, 1993). Remote sensing has also been used to monitor plant productivity and droughts on a national scale (Heumann et al., 2007), landscape scale (Hill & Donald, 2003) and local scales (Sakamoto et al., 2005).

Land surface phenology is typically used to quantify phenology of the overstorey canopy (Nagendra, 2001). However, when sufficient contrast is present between understorey and overstorey, it can also be used to map understorey vegetation (Tuanmu et al., 2010). Considering the already large changes in rainfall amounts and patterns in the last decade (CSIRO et al., 2007), it is essential to evaluate phenological responses to changes in rainfall patterns or fire regimes on longer time series in order to pick up differences in ecosystems rather than differences in response to recent climate change.

1.5. Problem statement

Many unique microhabitats are found on or near GOs with significant areas of bare rock and shallow soil at the surface. It is, therefore, essential to know where these are located in the landscape. Currently, maps provide insufficient detail on the abundance of granite rock at the surface (Porembski et al., 1997). Regional scale imagery such as Aster, Landsat Thematic Mapper (TM) and Enhanced Thematic Mapper (ETM) are likely suitable to characterise and map GOs (Gillespie et al., 2008). However, rock cover with lichen, algae and moss needs to be considered (Satterwhite et al., 1985; Schut et al., 2010). The microhabitats of GOs are linked to the abundance of granite at the surface in the typical granite domes. However, a detailed map of granite rock abundance at the surface is not available for the SWAFR. This abundance of granite may be mapped with

Landsat TM or ASTER data (Watts et al., 2005), but a methodology for this is yet to be developed.

A remote sensing approach to identifying patterns and processes in refugia involve greenspot modelling and evaluation of phenological and productivity responses to changes (i.e. rainfall patterns or fire regimes) using a long time-series of imagery (Smith et al., 2007). However, greenspot modelling and comparing apron to non-apron phenological cycles has not been formally studied across the SWAFR, particularly from a remote sensing perspective.

1.6. Research objectives

Based on the above problem statement, the aims of this study are threefold:

i) Develop and implement a methodology to map GOs;

ii) Map ecosystems greenspots to predict refugia in landscapes surrounding GOs. More specifically:
   a) Identify whether stratifying the region into available landscape subdivisions such as Land Zones or IBRA Subregions would improve ecosystem greenspots mapping;
   b) Identify which landscape stratification is better suited to map ecosystem greenspots;
   c) Compare seasonal distribution of vegetation vigour near the five GOs located across the rainfall gradient; and
   d) Portray the range of ecosystem greenspots that predict refugia in landscapes surrounding GOs.

iii) Derive inter-annual phenologies to portray moist refugia. More specifically:
   a) Compare the growing season in apron vegetation with that in the surrounding landscapes;
   b) Compare temporal dynamics of peak and onset of greenness on aprons with the surrounding landscape; and

c) Identify breaks in temperature and rainfall thresholds from chronological clustering.

1.6.1. Expected outcomes

The expected outcomes of this research include:

i) An effective, cost efficient and rapid methodology to map GOs across the SWAFR from satellite images by exploiting unique spectral properties of the low growth cover of lichen, algae and moss, and of appropriate spatial resolution;

ii) A spatio-temporal model of potential refugia hotspots based on fuzzy modelling and the weighted fuzzy combination (WFC) of the time series data approach by using available landscape stratifications; as well as

iii) A better understanding of inter-annual phenological cycles of biota by comparing refugial environments with the surrounding landscapes.

1.7. Significance and benefits of the research

Characterisation of GOs at the landscape scale provides essential knowledge to identify ecological niches and understand current and future ecosystem responses to climate change. It enables identification of GOs with unique characteristics that require specific attention to conserve biodiversity in Western Australia. It will also provide new insights into dynamics in insular ecosystems found on and near GOs.

The development and application of sophisticated spatial information techniques will enhance Australia's capabilities to model, predict and improve the understanding of correlating indicators present in the Remote Sensing imagery to assessment of biodiversity dynamics in insular ecosystems such as GOs.

1.8. Thesis structure

This thesis consists of six chapters. Chapter 1 introduces the need for spatial and temporal characterisation of landscapes surrounding GOs across the SWAFR and it describes how this information can be derived from digital data (e.g. geographic, climate and remotely sensed). It then reviews relevant literature and methodologies to satisfy the three objectives of the study (develop a methodology to map GOs; map ecosystems greenspots to predict refugia in landscapes surrounding GOs; and derive inter-annual phenologies to portray moist refugia using remotely sensed imagery and climate data).

Chapter 2 introduces the study area in the south-west of Western Australia, provides a brief overview of the location and characteristics of the GO landscapes and presents all data sources used in subsequent chapters. The main software packages used to analyse, model and present the various outputs are reviewed.

Chapter 3 focuses on how the Landsat TM imagery is used to develop a novel methodology to map GOs by exploiting unique spectral properties of the low growth cover of lichen, algae and moss (objective i). This work has been published in the Journal of Spatial Sciences (Alibegovic et al., 2014).

Chapter 4 describes a novel means for identification of potential refugia based on fuzzy modelling and the WFC of the time series data approach. Potential ecosystem greenspots were identified using available landscape stratifications, the land zones and IBRA subregions (objective ii).

Chapter 5 examines the potential of multitemporal VI imagery and climate data for differentiating inter-annual phenological cycles to compare known refugial environments with the surrounding landscapes (objective iii).

The thesis is concluded in Chapter 6, with a summary of the outcomes in relation to the stated research objectives and recommendations for further research and management implications.

2. STUDY AREA AND DATASETS

2.1. Introduction

This chapter describes the location and characteristics of the SWAFR under study located in the south-west of Western Australia. Reference is given to habitats and vegetation, most notably that of the environments surrounding GOs. Climatic data are presented illustrating the mesic to semi-arid environment of the study area. Remotely sensed and ground datasets are presented and are used for multiple purposes:

i) Develop a methodology to map GOs;
ii) Map ecosystem greenspots to predict refugia in landscapes surrounding GOs; and
iii) Derive inter-annual phenologies to portray moist refugia

Finally, an overview of the main software used for various analyses throughout the thesis is given.

2.2. Study area

The SWAFR is a biodiversity hotspot that includes the Mediterranean forests, woodlands, and scrub bioregions (Thackway & Cresswell, 1995; Hopper & Gioia, 2004) (Figure 2.1). The region has a wet-winter, dry-summer Mediterranean climate (Sander & Wardell-Johnson, 2011a) consisting of a broad coastal plain 20-120 km wide, transitioning to gently undulating uplands made up of weathered granite, gneiss and laterite (Porembski & Barthlott, 2000). Desert and xeric shrublands lie to the north and east (Thackway & Cresswell, 1997). These semi-arid systems are responsive to precipitation, resulting in rapid onset of greenness following spring rainfall.

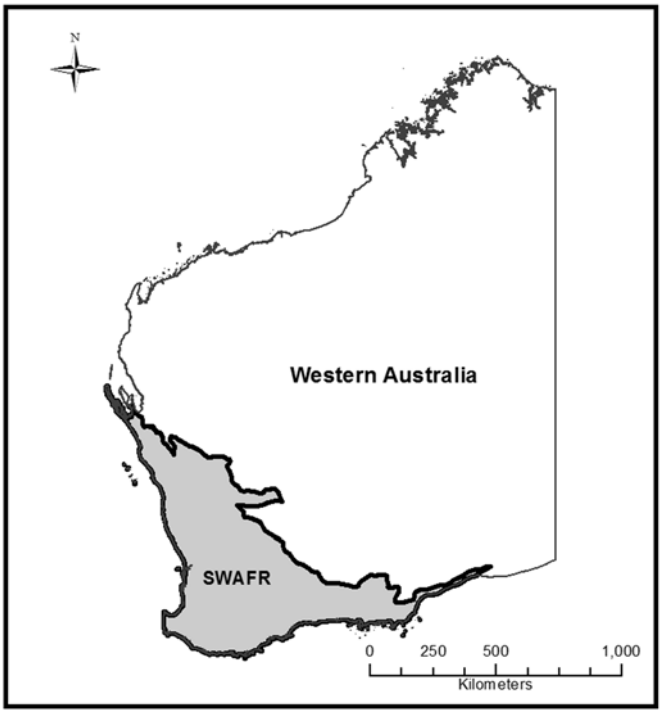

Figure 2.1 *Spatial and temporal characterisation was conducted on landscapes surrounding GOs located within the SWAFR*

The SWAFR is characterised by the ancient granite-based landscapes of the Yilgarn Craton and Albany-Fraser Orogen (Twidale, 1997). The Yilgarn Craton is an old and stable Archean part of the continental lithosphere. The Albany-Fraser Orogen is a Proterozoic orogenic belt that lies along the southern and south-eastern margin of the Yilgarn Craton (Myers, 1997b). GOs are topographically complex in comparison with the subdued surrounding landscape.

2.2.1. Habitats and vegetation

Predominant vegetation types across the SWAFR include eucalypt forests, woodlands, eucalyptus-dominated mallee shrublands (lignotuberous, multistemmed eucalypts) and kwongan shrublands and heathlands (Beard et al., 2000). The rich diversity of the flora is evident primarily among families of woody, sclerophyll shrubs (Myrtaceae, Proteaceae, Fabaceae and Epacridaceae). Dominant species in the high rainfall Warren and Jarrah Forest bioregions include tall open-karri (*Eucalyptus diversicolor*) forests at the GO aprons, whereas non-apron sites are dominated by open forests of jarrah *(Eucalyptus marginata)*. Non-apron sites in the Swan coastal and Avon regions include

paperbark (*Melaleuca quinquenervia*) and marri (*Corymbia calophylla*). Jam (*Acacia acuminata*) shrublands are dominant at Avon Wheatbelt bioregion. Predominating plant taxa across the SWAFR low nutrient interconnected landscapes were characterised by Wardell-Johnson et al., (2016).

The region has generally nutrient-poor sandy or lateritic soils, which have encouraged rich speciation of plants adapted to specific ecological niches. Relationships between vegetation structure and environmental variables were established by Schut et al., (2014) to relate growth to environmental variables indicative of local resource availability and growth constraints.

GOs are rich in areas with shallow soils that provide a wide range of habitats, are highly biodiverse and foster many endemic plant species. Rock surfaces provide ephemeral habitats for many species of lichen, algae and mosses. Typically there is little uncovered rock present.

Across the SWAFR, more than 17% of the State's vascular flora is represented on GOs and associated environments, including approximately 10% of the State's threatened flora (Brown et al., 1998). In addition, many species in the wider landscape are found in plant communities fringing these outcrops and many of these species have been restricted to the GO environment during past climate change (Yates et al., 2007; Byrne, 2008).

One reason for the disproportionately high number of species associated with GOs, in comparison with the surrounding landscape, lies in the variety of microhabitats that they provide (Hopper et al., 1997; Porembski et al., 1997). This suite of unique microhabitats includes: rock pools (gnammas), non-flooded soil pockets, vegetation mats, temporary flushed rocky surfaces that provide ephemeral habitat (lichens, algae and mosses) and aprons with influx of water and nutrients from the outcrop. The importance of GOs is even greater in disturbed agricultural landscapes, where they constitute important habitat remnants for the biota (Michael et al., 2010), and gene pools for surrounding landscapes under restoration.

2.2.2. Climate

The SWAFR experiences a Mediterranean type climate (Cowling et al., 1996; Medail & Quezel, 1999). Up to 80% of annual rainfall falls in the winter half-year from May to October. Rainfall amounts are higher and the wet season is longer than similarly exposed regions in other continents owing to the advection of moist air by strong westerly winds, influenced by the presence of a warm southward flowing offshore current (Leeuwin Current) and the modest orographic uplift provided by the Darling Scarp, of 250 to 300 m elevation running parallel with the west coast for over 300 km (Gentilli, 1972).

The region is already experiencing climate change, with a strong reduction in rainfall (Figure 2.2), attributed in part to global warming (Svenning & Condit, 2008; Charles et al., 2010), and it is predicted to become warmer and drier in the near future (Smith et al., 2007; Bates et al., 2008). Genetic studies indicate that many taxa have survived past regional climate changes by contracting to dispersed refuges (Byrne & Hopper, 2008; Yates et al., 2010). Such refuges will likely contribute to the persistence of species and ecological communities under anthropogenic global warming.

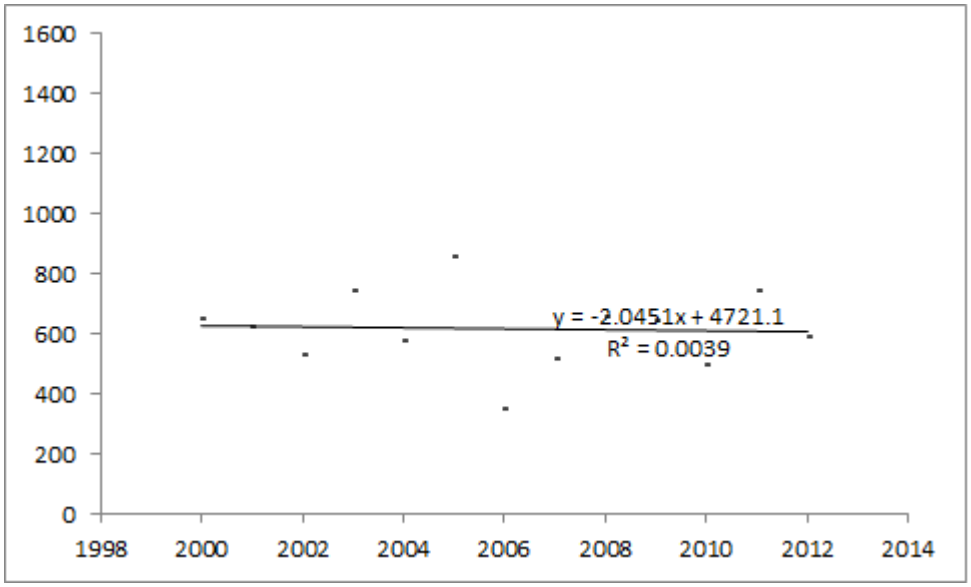

Figure2.2 *Daily averaged annual rainfall for the southern SWAFR*

2.2.2.1. Rainfall

Observational data for total annual rainfall recorded at meteorological stations across the SWAFR have been obtained from the National Climate Centre, Australian Bureau of Meteorology (BoM). The SWAFR has a strong rainfall gradient, ranging from mesic to semi-arid from the SW corner in a NE direction (Figure 2.3). The majority of the SWAFR is dominated by winter and early spring rainfall (June-October).

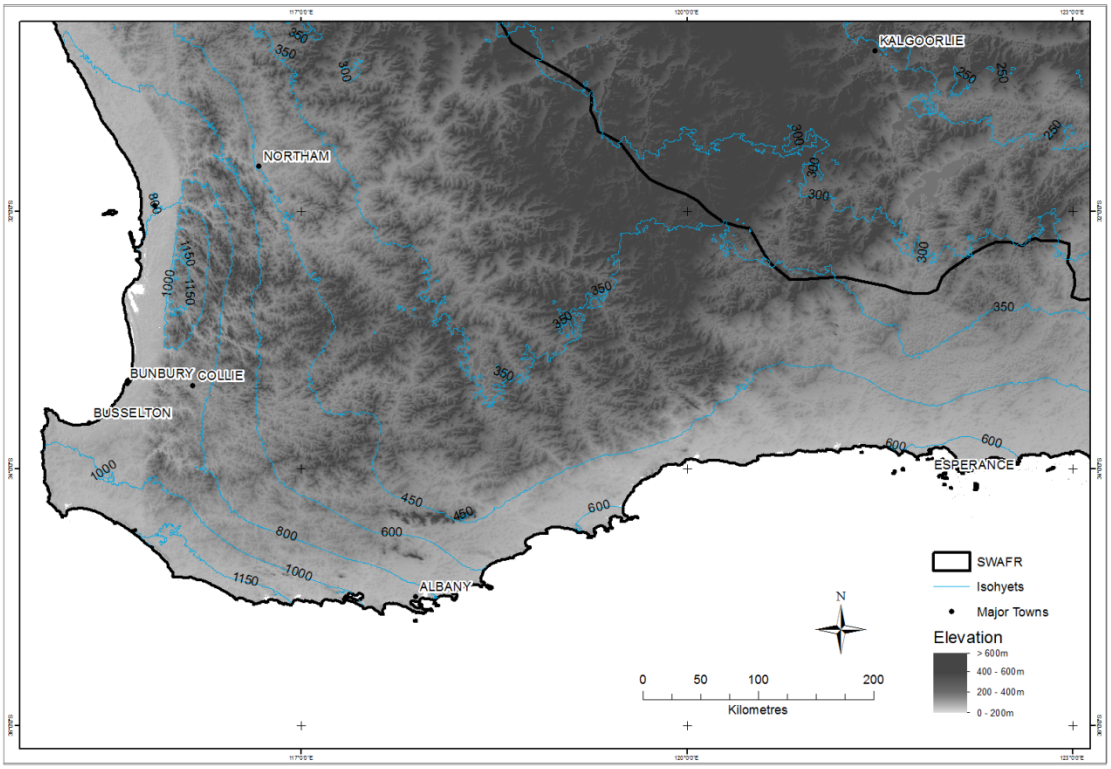

Figure 2.3 *Subdued topography with isohyets showing decreasing rainfall in the north-easterly direction*

Rainfall decreases rapidly inland to the north-east from 1,150 mm to 300 mm per year (Figure 2.3). Hopper (1992) advocated a division of the SWAFR into three broad rainfall zones, the high rainfall (800-1150 mm), the transitional rainfall (300-800 mm) and the arid zone (less than 300 mm), reflecting a diversity of land cover.

The SWAFR has become more arid in the last 30 years, attributed to factors including natural variability, and changes in land use and atmospheric circulation (Macfarlane et al., 2010). This trend is predicted to continue throughout the 21st century as a result of

global climate change. Long-term averages of rainfall allowed the detection of a sudden decrease in autumn and winter precipitation commencing in the 1990s (Delworth & Zeng, 2014). The SWAFR is expected to be drier and warmer in the future with total reductions in autumn and winter precipitation of approximately 40% by the late twenty-first century (Hennessy et al., 2006).

2.2.2.2. Temperature and humidity

Observational data for daily maximum temperature, daily minimum temperature and daily mean temperature recorded at meteorological stations across the SWAFR have also been obtained from BoM. Five weather stations across the SWAFR were selected for their high quality of long term meteorological records, and the measurements averaged for each dataset. The period of time for which temperature and relative humidity data were acquired for the stations is from 2000 to 2012. These observations have been taken from the BoM's real time system where the data are generated and handled automatically. Statistics are calculated for the "total rainfall" and "mean maximum temperature". The mean air temperature is the average of the daily maximum and minimum temperatures.

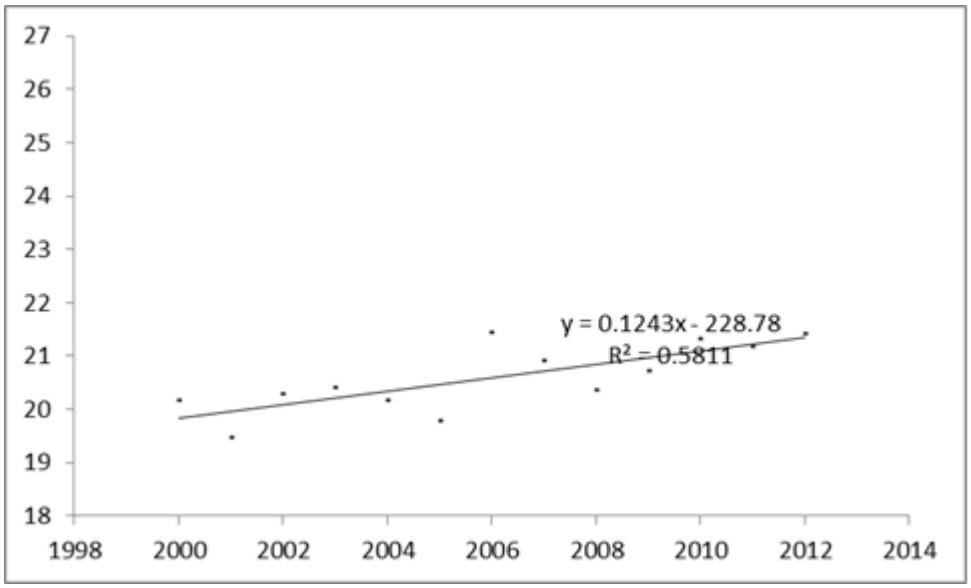

Figure 2.4 *Daily averaged annual mean air temperature for the southern SWAFR*

The spatial distribution of air temperature has a strong north to south gradient, with a less pronounced gradient with distance from the coast. Coastal moderation effects are

particularly evident in winter. Relative humidity similarly has a strong north to south gradient and distance from coast gradient, as expected given that onshore flow is the major source of atmospheric moisture (Trewin, 2013).

BoM has established and maintains a denser rainfall observation network than the air temperature observation network because of the importance and spatial inhomogeneity of rainfall relative to that of air temperature (Charles et al., 2010).

2.2.3. Topography

The relatively subdued ancient landscape across the SWAFR, with the exception of the Stirling Range, offers little scope for biota to migrate to altitudinal refuges (Figure 2.3). The regions topography is however dominated by the Yilgarn Craton and where erosion exposes the bedrock GOs rise above the landscape creating topographic complexity which influences resource flows and microclimates. Numerous GOs are scattered across the mesic to semi-arid rainfall gradient and are a conspicuous feature of the SWAFR landscape (Withers, 2000).

2.3. Remotely sensed data

Several remotely sensed datasets were acquired for this study. Moderate resolution Landsat TM imagery was acquired to determine their effectiveness at accurately separating GOs covered with low vegetative growth from all other land cover and types across the study area. A multi temporal sequence of MODIS was sourced to provide a record of the spatial coverage of 275 temporal rates of the SWAFR landscape. LiDAR surveys and aerial red-green-blue (RGB) imagery of prominent GOs across the SWAFR was used for ground truthing and validation purposes. Ground data and elevation models needed for separating GO's from other land covers and for mapping the greenspots were acquired. These datasets are described in more detail hereafter.

2.3.1. Aerial and surface reflectance imagery

High resolution aerial RGB imagery was acquired for prominent GOs across the SWAFR using a DSS439 camera and 60 mm lens recording 16 bit imagery. The spatial

resolution of images acquired was approximately 0.2 m at nadir. Radiance was recorded within a spectral range of 400-500 nm (Blue band), 500-600 nm (Green band) and 600-700 nm (Red band).

Reflectance of areas covered with lichen, algae and moss typical for GOs was measured in the field. The radiances were also recorded which cover the spectra range between 350-2500 nm with a 3-30 nm bandwidth. Reflectance was calculated using radiance. Spectra were recorded from a height of 1.7 m above ground, using a fibre-optic cable with a field of view of 8^0. Means of 10-30 readings were calculated and stored for each sampling point. For each sampling point a description was recorded of the lichen/algae/moss present and a geocoded digital image was taken.

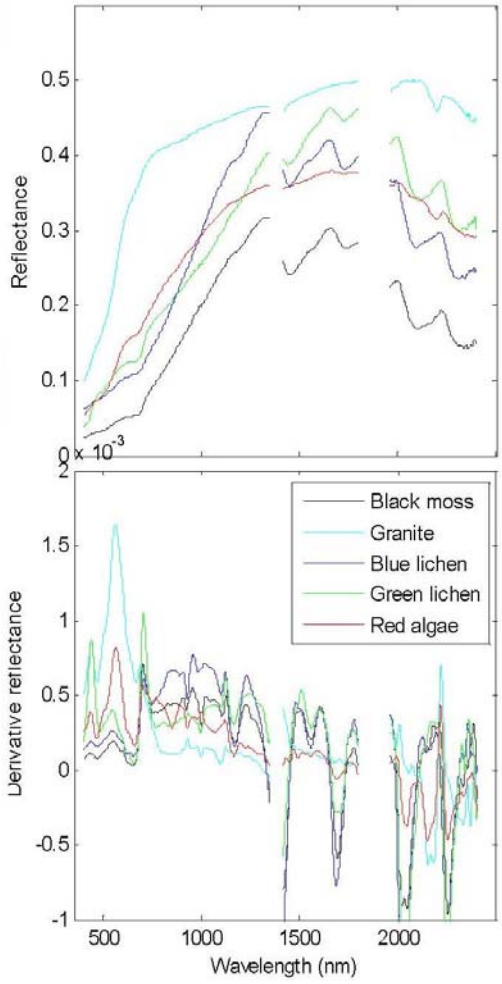

Figure 2.5 *Spectral properties of Granite and low growth cover*

2.3.2. Airborne LiDAR

High resolution airborne LiDAR was simultaneously acquired with aerial RGB imagery. The average distance between laser strikes on the ground was approximately 1.2 m, with a vertical accuracy of 0.15 m and horizontal accuracy of altitude times 1/5500, resulting in accuracy better than 0.35 m. A total of up to four returns were recorded for each pulse. The intensity of the return was also recorded. As a first step, laser strikes were classified as ground or non-ground. From this, a DEM is extracted for selected GOs. The first return laser strikes were classified as non-ground.

The LiDAR data provide an excellent high resolution DEM suitable for groundtruthing and validation. The vegetation height, extracted from the first return laser strikes shows that taller vegetation is present in the valleys and near the GO aprons, indicating more abundant resources than in the surrounding landscape.

2.3.3. Satellite imagery

The source data for Chapter 3 were Landsat TM imagery acquired from the Earth Resource Observation and Science Centre (EROS) for winter and summer seasons (U.S. Geological Survey, 2012). The images acquired were processed to standard terrain correction level (level 1T), providing systematic radiometric and orthometric corrections by incorporating ground control points while employing a Digital Elevation Model for topographic accuracy (Neigh et al., 2008).

The source data for Chapters 4 and 5 were continental time series of Normalized Difference Vegetation Index (NDVI) values from the MODIS 16-day L3 Global 250 m (MOD13Q1) composite gridded data (Paget & King, 2008) acquired from the EROS from 18 February 2000 to 8 May 2012 (U.S. Geological Survey, 2012). The MOD13Q1 NDVI values were built using the constrained-view angle - maximum value composite (CVA-MVC) algorithm on a 16-day compositing period described in Huete et al. (2002). The data are at 250 m spatial resolution and in 16-day time intervals resulting in 23 images per year. Each time series consists of a total of 276 observations (over 12 years). The MODIS NDVI data are computed from atmospherically corrected bi-

directional surface reflectance that have been masked for water, clouds, heavy aerosols, and cloud shadows.

2.3.4. Digital elevation and surface models

The digital surface data covering the entire study area were the Hydrologically Enforced digital elevation model (DEM-H) (Gallant et al., 2011). The dataset was derived from the Shuttle Radar Topography Mission (SRTM) data acquired by National Aeronautics and Space Agency (NASA) in February 2000 and was publicly released under Creative Commons licensing from November 2011 in ESRI Grid format (Dowling et al., 2011) and was acquired from the Geoscience Australia (GA).

Digital elevation model (DEM) represents ground surface topography, with vegetation features removed. Smoothed DEM (DEM-S) represents ground surface topography, excluding vegetation features, and has been smoothed to reduce noise and improve the representation of surface shape. This dataset supports calculation of local terrain shape attributes such as slope, aspect and curvature that could not be reliably derived from the original 1 second DEM because of noise (Gallant, 2011).

Hydrologically Enforced DEM (DEM-H) is a hydrologically enforced version of the smoothed DEM-S. The DEM-H captures flow paths based on SRTM elevations and mapped stream lines, and supports delineation of catchments and related hydrological attributes. The dataset was derived from the DEM-S by enforcing hydrological connectivity, using selected 1:250,000 scale watercourse lines and lines derived from DEM-S to define the watercourses (Gallant et al., 2012). The drainage enforcement has produced a consistent representation of hydrological connectivity with some elevation artefacts resulting from the drainage enforcement. Areas with poor spot height coverage were removed from the DEM-H dataset.

2.4. Ground data

Several ground level captured datasets were also acquired for this study. Surface geology was sourced to provide a base for identifying areas with granitic rock occurring near surface. Land use data was sourced to provide a record of native vegetation to

separate it from agricultural areas, and land types data of the Interim Biogeographical Regionalisation for Australia (IBRA) and Land systems were acquired to determine their effectiveness at mapping greenspots. These datasets are described in more detail hereafter.

2.4.1. Surface geology

Detailed geological mapping at 1:250 000 providing information on geological units, structural geology and fault lines was acquired from Geological Survey of Western Australia (GSWA). A total of 28 map sheets were needed to cover the entire study area. The data were published in 1978. These datasets have been compiled from information collected from field notes and input from aerial photo interpretation. Map data were scanned and vectorised. The data were originally created in the Clarke 1858 projection and later de-projected to decimal degrees of the Geocentric Datum of Australia 1994 (GDA94) coordinate system. Positional accuracy of the data is approximately 10 metres.

Geological units are classified by standard geological nomenclature showing rock types (together with the lithographical formations in pre 1984 series). The accuracy of the attribute information on all datasets covering the SWAFR is estimated at 98% (Geological Survey of Western Australia, 2008).

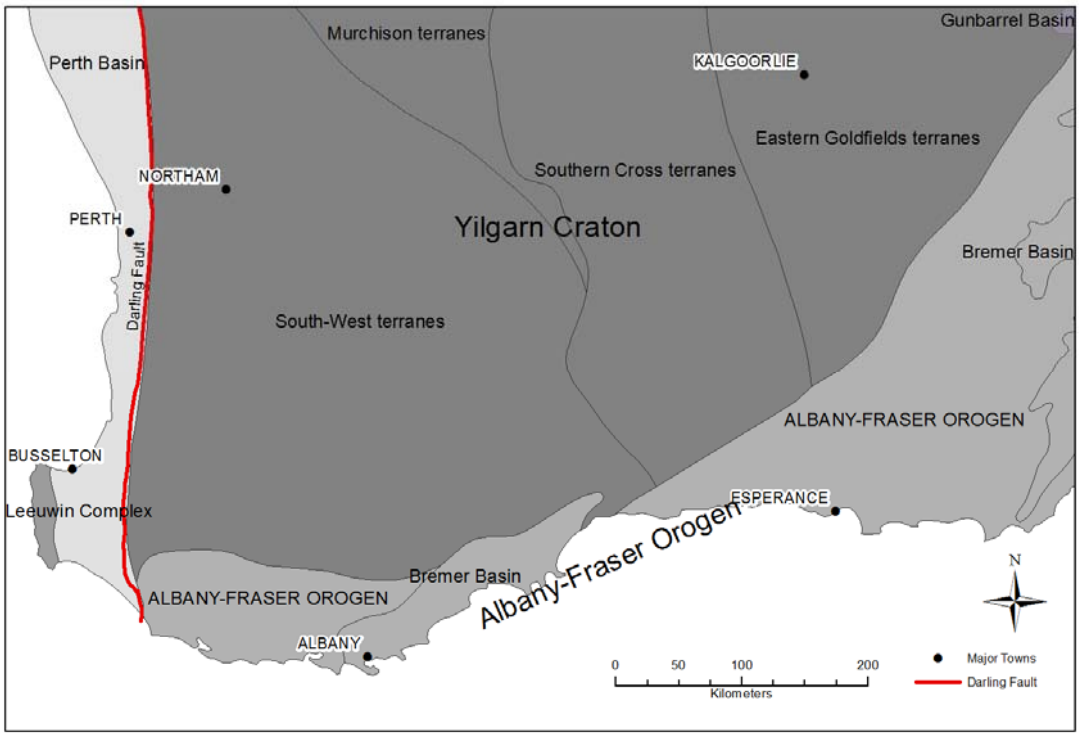

Figure 2.6 *Simplified Geology of the southern SWAFR*

2.4.2. Land types and classes

Two types of landscape sub-divisions exist across the SWAFR, the IBRA and the Land Systems classification of Western Australia. The IBRA is based on biogeographic regionalisation, and the Land System classification primarily on underlying soils and geology. The IBRA data were acquired from the Commonwealth Department of Environment (DoE), and the Land System data from the Department of Agriculture and Food Western Australia (DAFWA).

The IBRA defines 89 biogeographic regions and 419 subregions across the country, 18 of which fall wholly or partly in the in the SWAFR. Land Systems classification of Western Australia defines 74 categories, 39 of which fall in the SWAFR. From the above datasets, the IBRA subregions and the land zones were used as units of stratification as these are the areas defined on geomorphological and geological criteria, suitable for regional perspectives.

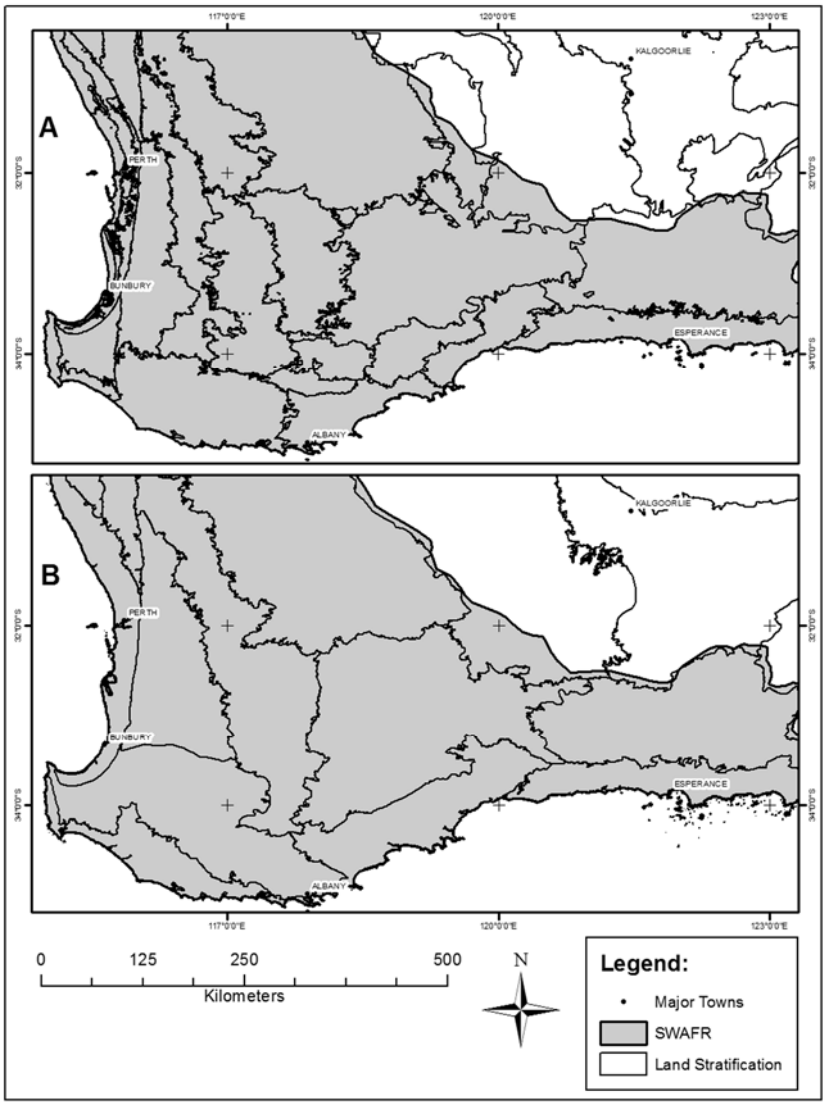

Figure 2.7 *Land stratification across the SWAFR by A) Land Systems and B) IBRA subregions*

2.4.3. Land use

The land use data were acquired from the DAFWA and includes native vegetation extent (from the mapping of remnant vegetation in Western Australia) and pre-European vegetation types, a broad-scale mapping of what was present before clearing. The data for the intensive land use zone in south-western Australia were originally derived from 1995 Landsat TM imagery and corrected using digital aerial photography acquired from 1996 to 2014. The data were non-projected (geographic coordinates) in the GDA94 datum.

These data were combined with the Managed Lands and Waters data, acquired from the Department of Parks and Wildlife (DPaW), to exclude the agricultural areas. Tenure categories of this dataset include National Parks, Nature Reserves, Conservation Parks, State Forest and Timber Reserves, ex Pastoral Lease and Freehold areas managed by DPaW. Positional accuracy of the data is approximately 50 metres.

2.5. Software

ArcGIS (version 10.2) (ESRI, 2014) was used to carry out the majority of Geographic Information Systems (GIS) operations throughout this thesis. IDRISI Taiga (Clark Labs, 2012) and ER Mapper (version 2014) (Hexagon Geospatial, 2015) were used for all image processing/classification routines. TimeSat (Jönsson & Eklundh, 2004) was used for time-series data processing to extract phenology metrics. Brodgar (version 2.7.4) (Highland Statistics Ltd, 2013), an interface to R, was used for advanced statistical analyses and for chronological clustering. Microsoft Excel and SPSS (IBM, 2015) were used for data synthesis.

2.6. Summary

In general terms, the study area is the SWAFR located in the south-west Region of Western Australia. The study looks into the topics from a landscape perspective to explain phenomena occurring at localised scale, i.e. GOs scattered across the SWAFR which are rich in biodiversity and foster many endemic plant species. The methodologies are based on spatial and temporal characterisation of these ecosystems surrounding GOs using remote sensing data.

The summer and winter series of Landsat TM data were used to develop a methodology to separate GO's from other land covers. Time-series of MODIS NDVI data were selected to map greenspots which include the refugial environments and to study the phenological cycles of apron and non-apron sites.

3. MAPPING GO ABUNDANCE

Abstract

GOs are key environments for biodiversity richness across the SWAFR and may provide habitat refugia under variable climatic conditions and extremes. GOs are scattered extensively throughout this region but there is no up to date or comprehensive inventory of them available. One challenge in using a generic approach for mapping GOs is that they are often partially covered in vegetative material (e.g. lichen, algae and moss) obscuring a 'pure' granite spectral response. This chapter develops and tests a methodology that incorporates the seasonal differences of this vegetative material to enable differentiation from co-existing land covers. Five granite outcrops were targeted, occurring across climate zones to test the robustness of the developed methods using summer and winter Landsat TM imagery. A crude threshold was used to eliminate most land covers other than granite, which was later fine-tuned using Receiver Operating Characteristic (ROC) analysis. The remaining, substantially reduced, areas were classified using an enhanced maximum likelihood routine. Overall Kappa calculated using all land covers ranged from 0.77 to 0.95 and from 0.9 to 0.97 for the granite versus non-granite class. Our approach allows differentiation of GOs from other environments, and hence provides low-cost and accurate mapping of these important habitats across the region.

3.1. Introduction

The five Mediterranean-climate ecosystems (Cowling et al., 1996; Klausmeyer & Shaw, 2009) are all recognized as global biodiversity hotspots (Myers et al., 2000). The SWAFR (Hopper & Gioia, 2004) is the least topographically complex of these regions (Sander & Wardell-Johnson, 2012) and is characterised by ancient granite-based landscapes of the Yilgarn Craton and Albany Fraser Orogen (Twidale, 1997). Granite inselbergs or outcrops (GOs) are topographically complex in comparison with the subdued surrounding landscape (Schut et al., 2014), are rich in biodiversity (Hopper et al., 1997), and of great conservation importance in the region (Withers, 2000). These GOs may provide habitat refuges and be partial drivers of the rich biodiversity and endemic flora observed there (Hopper et al., 1997; Porembski & Barthlott, 2000; Hopper & Gioia, 2004). A better knowledge of the location and extent of these GOs may allow further quantification of their role in providing climatic conditions favourable for refugia that are absent in the surrounding landscape (Wardell-Johnson & Roberts, 1993; Yates et al., 2010; Keppel et al., 2012) and would therefore be important for conservation planning (Byrne, 2008; Byrne & Hopper, 2008; Keppel & Wardell-Johnson, 2012). Some outcrops in the region have been identified in a native vegetation database derived from aerial photographic interpretation (Schoknecht et al., 2004). However, no comprehensive or accurate map is currently available for granite outcrops in the SWAFR, despite recommendations for a granite atlas of the region (Campbell et al., 2000).

Remote Sensing and image processing techniques have demonstrated potential for mapping relatively bare (e.g. not covered with vegetative material) GOs. For example, Campbell et al. (2000) have tested the feasibility of granite likeness scores based on Landsat TM image sequences at two prominent GOs (Mt Caroline and Mt Stirling) in Kellerberrin in the SWAFR. However, they indicated that whilst bare granite can be separated from native vegetation, it was less distinguishable from bare sandy soils. GOs in the SWAFR present a further challenge for semi-automated mapping in that they are typically covered with lichen, algae and mosses, which strongly mask the unique bare granite key absorption features (Satterwhite et al., 1985; Schut et al., 2010). Notwithstanding, the reflectance of GOs covered with lichen, algae and moss remain relatively constant in reflectance throughout the year, in contrast to other land covers

(e.g. soil) which do show seasonal differences (Rollin et al., 1994). However, to our knowledge, no previous research has used these features together with seasonal differences in coexisting land covers to assist in the differentiation of GOs.

The aim of this research is to develop and test a methodology for the rapid identification of areas with granite outcropping at the regional scale of the southern Yilgarn Craton and western Albany-Fraser Orogen in the SWAFR (Schut et al., 2010). It is hypothesised that successful identification of granite is possible if spectral separation is only required for a small number of classes and seasonal differences are capitalised upon. To this end, we provide a methodology, novel to the application of GOs, which successively eliminates non-granite land covers (e.g. vegetated areas, bare in summer soil) from further classification using winter and summer imagery until only the granite class remains. In this research, we demonstrate the techniques using a case study from Boyagin Nature Reserve. We also provide a classified output and measure of accuracy for five granite landscapes encompassing the south-west climate gradient.

3.2. Materials

3.2.1. Study area

The study area covers the rainfall gradient on the southern margin of the Yilgarn Craton, east of the Darling fault, and the western side of the Albany-Fraser Orogen of the SWAFR; an area of about 160,000 km^2 (Figure 3.1). Rainfall decreases rapidly inland from the south-west to the north-east from about 1,150 mm to about 250 mm per year, respectively (Figure 3.1). The Yilgarn Craton was formed by the melting of older continental crust when the continent was assembled from a number of smaller rafts of continental crust between 2.7 and 2.6 billion years ago (Myers, 1997a). Granite of the Albany-Fraser Orogen is a product of continental collision between the Yilgarn Craton and the Mawson Craton in South Australia during two distinct episodes: 1) the older western Recherche granite intruded intermittently (about 1.3 billion years ago), or was formed in-situ by the melting of older granite (1.7 to 1.6 billion years old); and 2) the younger eastern Esperance granite intruded about 1.2 billion years ago (Myers, 1997a).

Five granite landscapes were selected for the development and testing of the methodology. These were located in the Boyagin Nature Reserve, Chiddarcooping Nature Reserve, Mount Frankland National Park, Mount Chudalup and Porongurup National Park (Figure 3.1) and were selected to ensure coverage of the rainfall gradient and the different ages and origins of the granites (i.e. the Yilgarn Craton and the Albany-Fraser Orogen) to determine if the methods were robust to these variations.

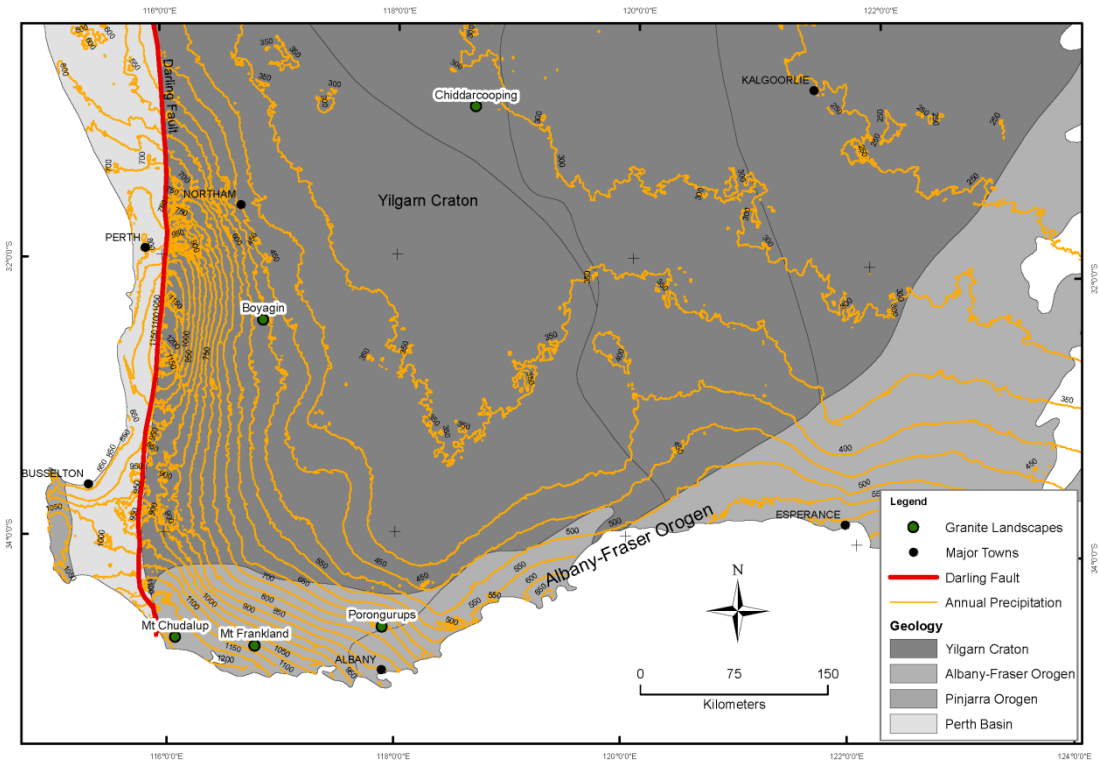

Figure 3.1 *Location of the five selected granite landscapes containing the studied granite outcrops in the SWAFR study area.*

3.2.2. General characteristics of granite

Granite is an intrusive, felsic, igneous rock which is granular and crystalline in texture comprising quartz (20-45%), feldspar (up to 60%), mica and/or amphibole or pyroxene (Blatt & Tracy, 1997). The crystals are generally large enough to be visible on exposed rock, and give granite its rough texture on weathered surfaces.

3.2.3. Spectral characteristics of granite and low growth cover

Granite formed at different times may differ in composition and grain size resulting in variable within class spectral reflectance (Baird, 1984; Clark, 1999). Nevertheless, bare granite rock surfaces generally do differ spectrally from other rock types (Campbell et al., 2000; Watts et al., 2005; van Ruitenbeek et al., 2006). However, in some locations granite can be so extensively covered by lichen and other surface cover such as moss and algae (Figure 3.2) that only a small percentage of the rock's surface is exposed. Consequently, reflectance characteristics represent some unknown mixture of rock and biological material (Satterwhite et al., 1985).

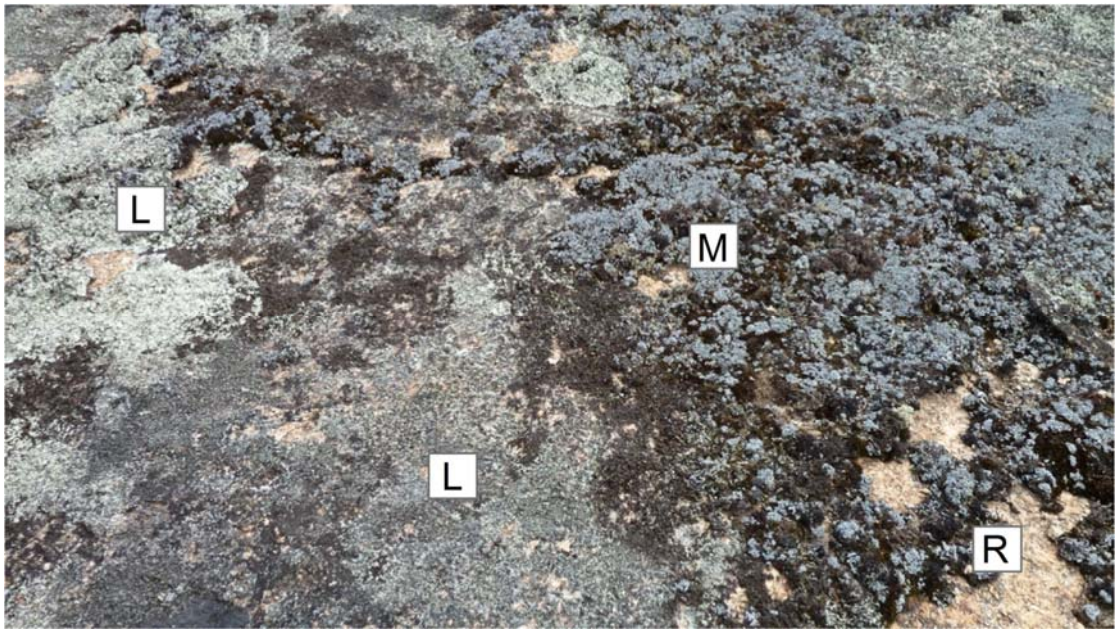

Figure 3.2 *Image of a granite rock surface (R), with relatively large amounts of lichen (L) and moss cover (M) at Boyagin Nature Reserve, in the SWAFR.*

3.2.4. Datasets

To test the hypothesis that rapid fine-scale differentiation between granite and coexisting land covers is possible regionally, it was considered that remotely sensed imagery needed to be: 1) available for both wet and dry seasons; 2) low cost; 3) capable of detecting smaller outcrops (and thus a suitable spatial resolution must be considered); and 4) acquired in at least the red and near infra-red (NIR) range of the spectrum to facilitate calculation of vegetation indices based on photosynthetic vigour to enable

masking of vegetated areas and the detection of seasonal changes. Landsat TM imagery were considered to satisfy these prerequisites and so were acquired from the Earth Resource Observation and Science centre of the United States Geological Survey (USGS) for winter and summer seasons (Table 3.1). A further requirement in their selection was to ensure that both the summer and winter season images were cloud free and from the same year. Occasionally, this required selecting imagery that was up to a decade old.

Table 3.1 *Landsat TM scenes sourced from the United States Geological Survey for five selected granite landscapes in the SWAFR.*

Granite Landscape	Path	Row	Summer	Winter
Boyagin Nature Reserve	112	82	15-Jan-2004	11-Sep-2004
Chiddarcooping Nature Reserve	111	81	11-Feb-2005	20-Sep-2004
Mt Frankland National Park	111	84	7-Jan-2007	18-Jul-2007
Porongurup National Park	112	84	9-Feb-2010	10-Sep-2010
Mt Chudalup	112	84	7-Jan-2007	18-Jul-2007

The images acquired were processed to standard terrain correction level (level 1T), providing systematic radiometric and orthometric corrections by incorporating ground control points while employing a Digital Elevation Model for topographic accuracy (Neigh et al., 2008). As all thresholds were developed separately for each season (see below), and supervised classification was performed on one twelve band image composite (stack), further atmospheric correction was deemed unnecessary (Turcotte et al., 1993).

3.2.4.1. Calibration and validation data

High spatial resolution aerial imagery acquired in the visible portion of the spectrum only (red-green-blue – RGB) and light detection and ranging data (LiDAR) were acquired for the five selected outcrops. This imagery was used to assist development of a point layer of 1,200 stratified random samples for each granite landscape of visually interpreted land covers to ensure sufficient sampling over the entire landscape. The interpretation was later corroborated and adjusted in the field, and then randomly

divided in half. One half was used to identify thresholds and the supervised classification ("calibration data"). The other 600 points ("validation data") were used for accuracy assessment (see below).

3.2.5. Software

Standard image processing software ERDAS ER Mapper (version 2011) (Hexagon Geospatial, 2015) was used for pre-processing, generating a series of summer-winter imagery, creating NDVI masks with various thresholds, and for classifications. Environmental Sciences Research Institute's (ESRI) ArcGIS (v. 10) (ESRI, 2014) was used to perform GIS tasks. These included generating stratified random point samples to develop the calibration and validation datasets. ROC analyses and assessment of the spectral differences between land-covers were carried out using the Statistical Package for the Social Sciences (SPSS) (IBM, 2015). Kappa statistics were calculated using Microsoft Excel.

3.3. Methods

A series of sequential steps were conducted to successively eliminate non-granitic land covers, leading to a final supervised classification pass (Friedl & Brodley, 1997; Mulder et al., 2011).

3.3.1. Spectral separation and transformation

Spectral signature graphs were derived from both summer and winter imagery to visualise the spectral separation of the four major cover types (seasonal vegetation, native vegetation, bare in summer soil, and granite outcrops), and the likelihood of capitalising on the seasonal differences (Sonnenschein et al., 2011; Cracknell & Reading, 2014). The significance of these differences (α=0.01) was tested with Tukey's Honest Significant Difference (HSD) test (Barbosa et al., 2006) for the Boyagin Nature Reserve study site using the calibration dataset.

Both the summer and winter imagery were transformed using the Normalised Difference Vegetation Index (NDVI) (Tucker, 1979), following the approach of Cingolani et al.

(2004). These images were used to generate a series of masks with various thresholds for removal of areas that contain evergreen vegetation (a high Normalised Difference Vegetation Index - NDVI value in summer and winter), or are strongly greening up in winter (a strong change in NDVI from summer to winter).

3.3.2. Initial thresholds

Initial thresholds were chosen as a crude division of the granite and non-granite classes. These were developed manually by identifying the NDVI value at which all granite outcrops would remain, while removing as much of the other land covers as possible. Equation 3.1 was then used to mask all areas greater than the chosen winter and summer thresholds, and to ensure that any change greater than the range between summer and winter thresholds (t_s - t_w) is not classified as granite.

$$Mask = \left(NDVIs_{ij} < t_s\right) AND \left(NDVIw_{ij} < t_w\right) \\ AND \ (NDVIw_{ij} - NDVIs_{ij}) < (t_s - t_w), \quad (3.1)$$

where $NDVIs_{ij}$ is the NDVI for summer at pixel location at row i and column j, $NDVIw_{ij}$ is the NDVI for winter at pixel location ij, t_s is the threshold for summer, t_w is the threshold for winter and (t_s - t_w) is the range between the summer and the winter thresholds.

3.3.3. Calibrated thresholds and supervised classification

The thresholds used in Equation 3.1 (t_s and t_w) were further refined for the remaining land covers (e.g. granite, bare in summer soil and light vegetation cover with low vigour) using Receiver Operating Characteristic (ROC) curves (Bradley, 1997; Kerekes, 2008). The ROC curve works by plotting the false positive rate (FPR – the prediction of a granite pixel when no granite pixel is present) against the true positive rate (TPR – the prediction of a granite pixel when a granite pixel is present). The optimum threshold is then found by identifying the FPR, TPR combination in the northwest corner of the curve (Fawcett, 2006; Malatesta et al., 2013) and matching it to the NDVI value to which it corresponds.

An enhanced maximum likelihood classifier was applied to the composite twelve band image stack of the summer and winter imagery to remove spurious non-granite pixels from the classified image. Spectral signatures were defined from the calibration data to eliminate commission error caused by bare areas being identified as GOs.

3.3.4. Accuracy assessment

The Overall Kappa statistic (Bishop et al., 1975; Congalton, 1991) was calculated for each granite landscape using the validation dataset to quantify the agreement between the validation data and the classified image. Overall Kappa was first calculated based on points in all four classes to assess overall accuracy. However, misclassification of other classes will mask the accuracy of the target class (GOs) when assessed together. Therefore, all other classes were grouped as "non-granite" and Overall Kappa was recalculated using only this class and the granite class.

3.4. Results

3.4.1. Spectral separation and transformation

Spectral response graphs were derived from both summer and winter imagery to visualise spectral separability of the four major cover types (Figure 3.3). According to Tukey's HSD test (Table 3.2), spectral separation was significant ($p < 0.01$) in bands 2 (green) and 3 (red) for all land covers in summer (Figure 3a, Table 3.2) and for band 4 (near infrared) in winter (Figure 3.3b, Table 3.2). There is also significant separation between granite and all other land covers in winter (Table 3.2). Granite and native vegetation had a similar response in the near infrared (band 4) in summer, but due to differences in the red band, the NDVI was considered to be useful for further discrimination of land covers in both seasons.

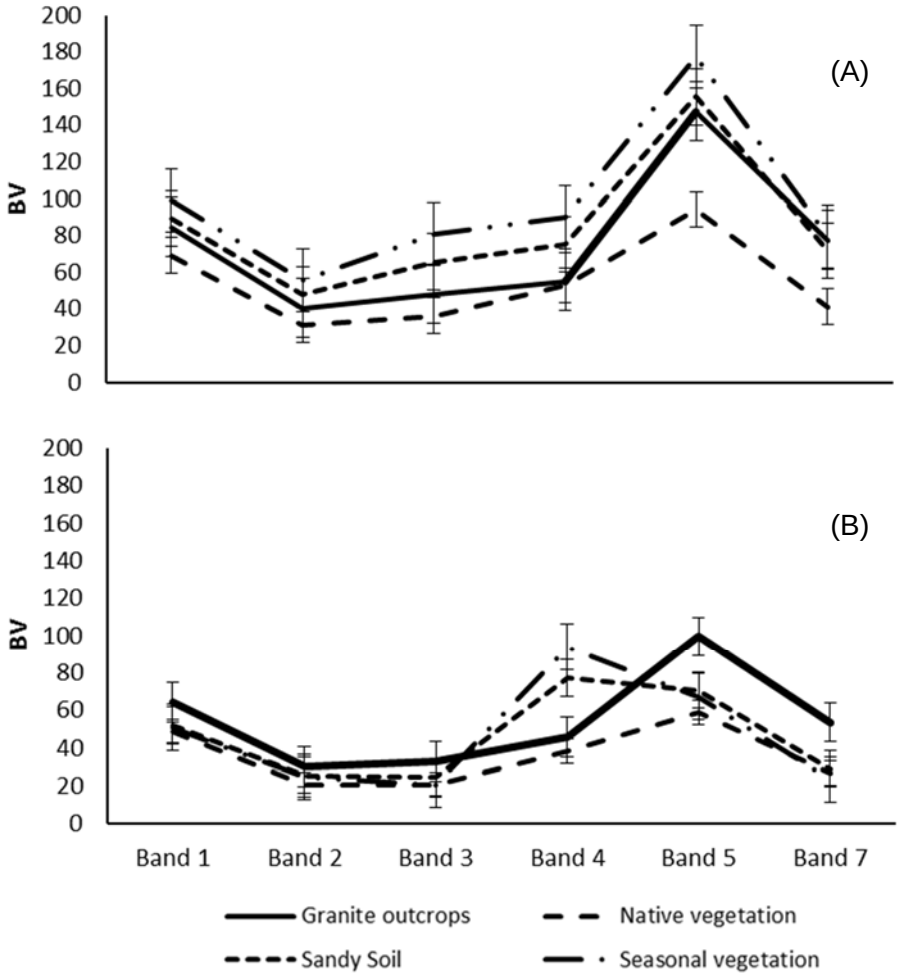

Figure 3.3 *Responses in Landsat TM spectral bands for four land cover types at Boyagin Nature Reserve for a) summer and b) winter imagery. BV is the average brightness value (digital number) of each band. The vertical bars indicate one standard error.*

Table 3.2 *Mean spectral responses for each land cover for the summer and winter seasons at the Boyagin Nature Reserve study site. Land covers with the same superscripts are not significantly different (p<0.01).*

Season	Band	Granite Outcrops	Bare in Summer Soil	Native Vegetation	Seasonal Vegetation
Summer	1	84.73[a]	89.46[a]	69.22[c]	98.92[d]
	2	40.55[a]	47.93[b]	31.35[c]	56.05[d]
	3	48.45[a]	65.93[b]	36.41[c]	80.96[d]
	4	55.05[a]	75.33[b]	52.98[a]	90.29[d]
	5	147.61[a]	155.58[a]	94.35[c]	177.63[d]
	7	77.84[a]	71.98[a]	41.41[b]	79.33[a]
Winter	1	64.34[a]	52.28[b]	48.75[c]	50.90[b]
	2	30.11[a]	25.67[b]	20.58[c]	24.77[b]
	3	32.82[a]	24.40[b]	20.37[c]	20.91[c]
	4	46.00[a]	77.23[b]	38.20[c]	93.94[d]
	5	99.48[a]	70.58[b]	58.85[c]	67.28[b]
	7	53.64[a]	29.00[b]	26.62[b]	23.49[c]

3.4.2. Initial thresholds

Initial thresholds for each of the selected areas are shown in Table 3.3 below. Equation 3.1 was then used to eliminate a large proportion of non-granite areas using these values.

Table 3.3 *Initial NDVI threshold identified for five granite outcrops in the SWAFR. These thresholds (t_s, t_w and range t_s - t_w) are used in Equation 3.1.*

Granite Landscape	Summer (t_s)	Winter (t_w)	Range (t_s - t_w)
Boyagin Nature Reserve	0.05	0.22	0.17
Chiddarcooping Nature Reserve	0.07	0.22	0.15
Mt Frankland National Park	0.12	0.25	0.13
Porongurup National Park	0.09	0.25	0.16
Mt Chudalup	0.12	0.25	0.13

3.4.3. Calibrated thresholds and supervised classification

The calibrated thresholds (NDVI values) identified from the ROC curves are shown in Table 3.4. For example, NDVI values less than 0.06 in summer and 0.22 in winter were identified for the Boyagin Nature Reserve and 0.09 (summer) to 0.22 (winter) were

found for the Chiddarcooping Nature Reserve (Table 3.4). These mask thresholds excluded a majority of seasonal vegetation, as well as a vast proportion of evergreen native vegetation (Figure 3.4a), while leaving all major granite outcrop areas for further processing using the enhanced maximum likelihood routine (Figure 3.4b). Differentiation between granite and surrounds was also achieved at all of the selected sites across the SWAFR climatic zone, and images are shown in Figure 3.5 (a-d).

Table 3.4 *ROC based NDVI threshold identified for five granite outcrops in south-western Australia. These thresholds (t_s, t_w and range t_s - t_w) are used in Equation 3.1.*

Granite Landscape	**Summer (t_s)**	**Winter (t_w)**	**Range ($t_s - t_w$)**
Boyagin Nature Reserve	0.06	0.22	0.16
Chiddarcooping Nature Reserve	0.09	0.22	0.13
Mt Frankland National Park	0.20	0.28	0.08
Porongurup National Park	0.20	0.28	0.08
Mt Chudalup	0.20	0.28	0.08

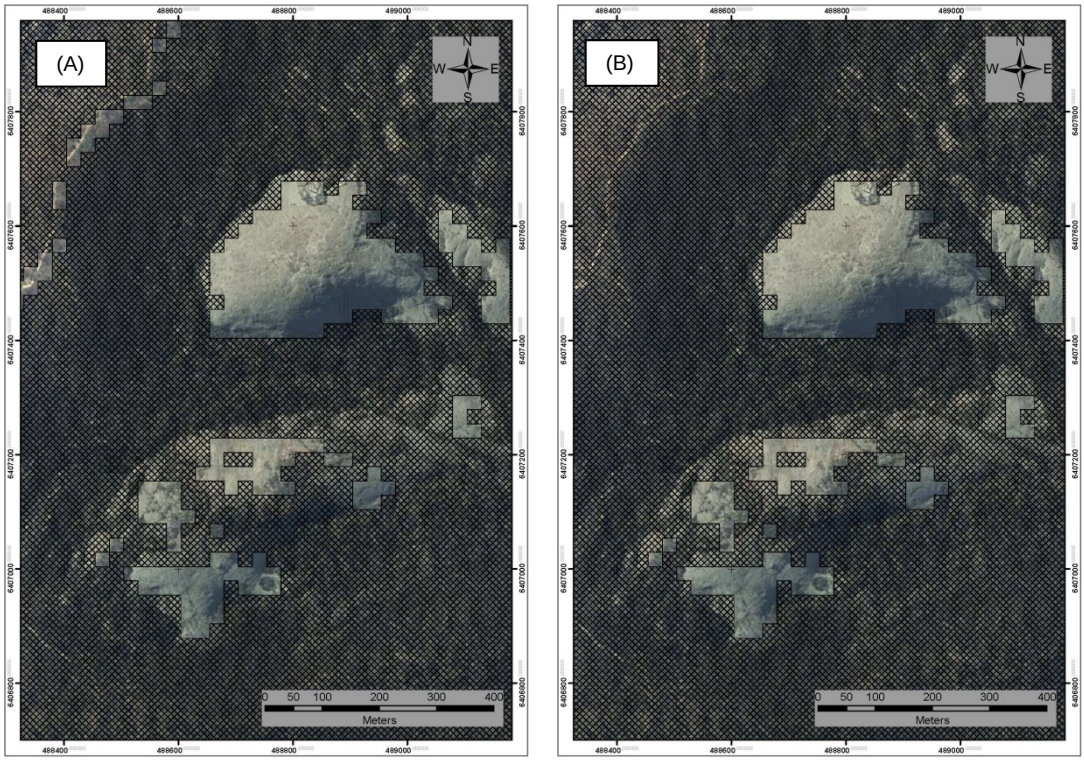

Figure 3.4 *Mask using (a) a ROC-based threshold of 0.06 (Summer NDVI) and 0.22 (Winter NDVI) and an NDVI difference of < 0.17 and b) Final result using the Maximum likelihood enhanced supervised classification applied to unmasked areas of the Boyagin Nature Reserve in the SWAFR. Note that the pixels errantly classed as granite in the northwest have been removed following the supervised classification.*

3.4.4. Accuracy assessment

Overall Kappa values for all classes and for the granite class versus non-granite class are shown in Table 3.5. Overall Kappa ranged from 0.77 (Mt. Chudalup) to as high as 0.89 (Porongurup National Park – Table 3.5) and averaged 0.83 over the five landscapes when assessed using all classes. Overall Kappa increased for all landscapes (mean = 0.88) when assessed for just the granite and non-granite class (Table 3.5).

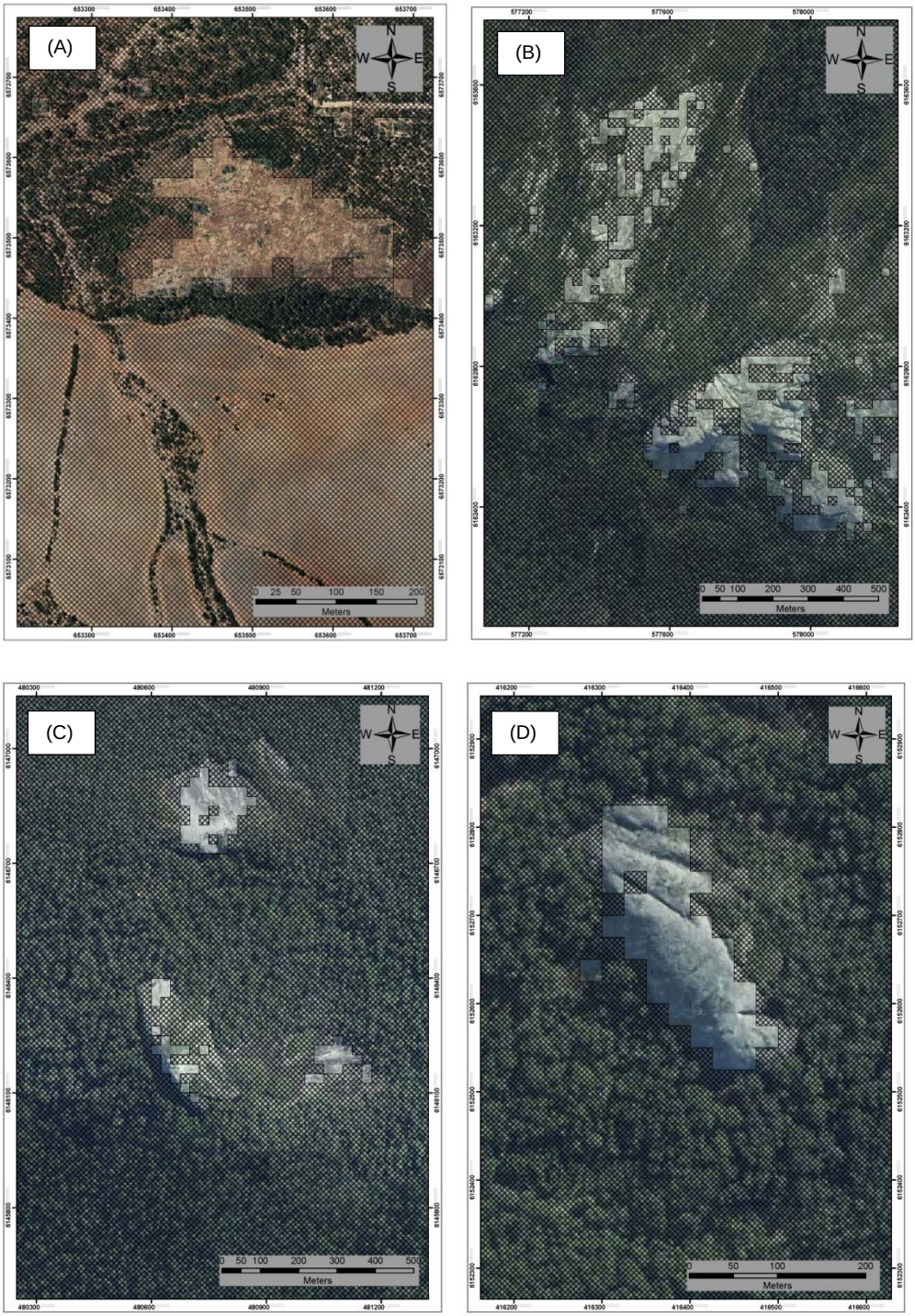

Figure 3.5 *Optimised masks for granite outcrops and surrounds across the SWAFR: a) Chiddarcooping Nature Reserve, b) Porongurup National Park, c) Mount Frankland National Park, and d) Mount Chudalup.*

Table 3.5 *Overall Kappa for all classes (Kc) and for the granite vs non-granite (Kg) for the five granite landscapes in the SWAFR.*

Granite Landscape	Kc (All)	Kg (granite vs non-granite)
Boyagin Nature Reserve	0.86	0.87
Chiddarcooping Nature Reserve	0.81	0.91
Mt Frankland National Park	0.79	0.83
Porongurup National Park	0.89	0.90
Mt Chudalup	0.77	0.88

3.5. Discussion

Vegetation indices such as the NDVI show limited variation in greenness of granite surfaces covered by lichen, mosses and algae. We used this characteristic to develop and test a methodology to differentiate areas with outcropping granite from their surroundings. Overall kappa ranged from 0.77 to 0.89 (interpreted as "very good" to "excellent") (Monserud & Leemans, 1992) when assessed on all land covers, and averaged 0.83 ("excellent") over the five landscapes studied. Accuracy levels improved when assessed on only two classes (granite and non-granite) ranging from 0.83 to 0.91 (mean = 0.88), which can also be interpreted as an "excellent" level of classification and denotes that the lower Overall Kappa for all classes was due, in part, to confusion within the other classes. Such confusion is of little concern as only high accuracy of the target class (GOs) was required.

It is evident that the three granite landscapes located in the south-west portion of the Albany-Fraser Orogen (i.e., Mt Chudalup and the Mt Franklin and Porongurup National Parks) required masks developed using relatively large NDVI values from both the summer (e.g. 0.20) and winter images (e.g. 0.28). Consequentially, the range between the summer and winter images in these locations was considerably lower than inland areas. This is indicative of a relatively stable moss mat cover that may be linked to the higher rainfall at these locations (e.g. 700 to 1,150 mm), relative to the inland areas (e.g. 300 to 500 mm). The two granite landscapes located further inland (Boyagin nature Reserve and Chiddarcooping Nature Reserve) had lower NDVI values in winter (0.22)

and in summer (e.g. 0.06 to 0.09), suggesting less photosynthetic vigour in winter and a drying of the moss mat during the summer. These variations across the rainfall gradient over contrasting seasons also illustrate that a one-size fits all approach for state-wide mapping would not be suitable, as these parameters vary spatially and temporally.

Other authors have also used remotely sensed imagery for mapping rocky outcrops. For example, multispectral ASTER (Advanced Spaceborne Thermal Emission and Reflection Radiometer) data are widely used to map different lithological units (Rowan & Mars, 2003; Rowan et al., 2005; Baldridge et al., 2009). These approaches often rely on an extensive spectral library (Baldridge et al., 2009), and have demonstrated the potential to assist the mapping of lithological units in well exposed areas (Rowan et al., 2005; van Ruitenbeek et al., 2006; Massironi et al., 2008). However, such signatures do not exist for granite covered by moss, lichen and algae. ASTER data does have the potential to improve on the spatial resolution used in this study. However, it was not available for all granite landscapes in our study area, and therefore could not be used over the entire rainfall gradient. Thermal sensors are another potential means of separating granite from other cover if there are significant differences in the temperature of granite from its surroundings (Ninomiya et al., 2006), although this was not investigated in this study.

The methods presented in this study make it possible to map exposed granite surfaces not covered by vascular plants effectively, and with minimal cost. Using imagery from summer and winter, the majority of seasonal and native vegetation was masked. Initial thresholds were identified visually by assessing histograms, while the optimum thresholds required to separate vegetation from granitic and sandy surfaces were identified using ROC curves (Kerekes, 2008). The major advantage of this methodology is that it allows the differentiation of granite outcrops from other environments (e.g. different annual rainfall), and hence enables low-cost and accurate mapping of GOs across the region. It has potential to be used to provide a more accurate and contemporary inventory of GOs at the landscape scale (Landsat TM) for the SWAFR than currently exists.

Investigation of other vegetation indices was beyond the scope of this study. However, examination of the spectral characteristics over the two seasons suggest that there were

significant differences in the spectral response of various land covers in the middle-infrared portion of the spectrum and, in particular, band 5 ($p < 0.01$ for Boyagin) for winter seasons. These differences are most likely due to the moisture levels in the different land covers, with granite remaining relatively moisture resistant. Therefore, there appears to be potential to use other indices that incorporate band 5, such as the i35, which was utilised by the Land Monitor Project across the south-west of Western Australia (Allen & Beetson, 1999).

A limitation of the approach presented here is that it cannot detect granite surfaces partly or completely covered with vascular vegetation and that the margins of outcrops are potentially excluded, possibly due to scattered vegetation coverage in these areas. A method for overcoming this shortcoming could be the use of region growing and boundary forming algorithms (Hoffmann & Boehner, 1999; Zhang et al., 2014) where outcropping areas could be expanded to where the outcrop flattens to show the full extent of outcrops with dense vegetation cover or to the exact boundary of vegetated areas in less undulated terrain. The availability of high-resolution imagery covering the full SWAFR region will help to refine this process.

4. ECOSYSTEM GREENSPOT MODELLING TO PREDICT REFUGIA IN LANDSCAPES SURROUNDING GOs ACROSS THE SWAFR

Abstract

Identification of refugia is increasingly important in conservation planning as a climate change adaptation strategy. Granite outcrops (GOs) have long been regarded as potential refugia where conditions have remained relatively constant and stable during times of climatic fluctuations. GOs support a diverse range of flora, including a wide range of vegetation types and habitats across the SWAFR. In this study a time series of remotely sensed imagery, combined with land stratification data (Land Zones and IBRA subregions) were used to develop a greenspot model to identify potential refugia. The primary data for this analysis were NASA MODIS 16-day L3 Global 250 m (MOD13Q1) satellite imagery. A novel means for identification of potential refugia is presented, based on fuzzy modelling and the weighted fuzzy combination (WFC) of the time series data approach. A detailed map of vegetation response over the twelve year period was generated to relate growth to environmental variables indicative of local resource availability. The approach was tested on five GOs across the SWAFR and showed that land zone stratification based on underlying geology, geomorphology, soils and vegetation is best suited for mapping ecosystem greenspots (Kappa = 0.86) in old stable landscapes (OSLs). The approach is relevant to other regions of the world where the role of refugia in the persistence of species is recognised, including across the world's arid zones and, in particular, for the Australian, southern African, and South American continents. Refugia networks may play an important role in maintaining betadiversity at the regional scale and contribute to the stability, resilience, and adaptive capacity of ecosystems under rapid anthropogenic climate change, land use, and other threatening processes.

4.1. Introduction

Refugia are habitats that facilitate species persistence during large scale and long-term climatic change (Keppel et al., 2012), and are increasingly important in conservation planning as a climate change adaptation strategy. Identifying the geographic location of refugia requires a spatially explicit understanding of the relationships between biodiversity, environment and climate at appropriate spatial and temporal scales. The SWAFR (Hopper & Gioia, 2004) is a globally significant ancient subdued landscape characterised by granites of the Yilgarn Craton and Albany Fraser Orogen (Withers, 2000) where moisture deficits, nutrient impoverishment, and acidity are typical features of local soils (Lambers et al., 2010). Granite outcrops (GOs) scattered across the SWAFR are topographically complex in comparison with the subdued surrounding landscape. The region has experienced a decrease in precipitation (CSIRO et al., 2007; Wardell-Johnson et al., 2011) thus microclimatic variations due to soil moisture variability (Ashcroft & Gollan, 2013) within GOs could buffer against regional climate change and could continue to provide habitats for species occurring around them. The importance of GOs is even greater in disturbed agricultural landscapes (Schut et al., 2014) where they form important habitats for remnant native vegetation.

Hopper (2009) introduced a term OCBIL to define old, climatically buffered, infertile landscapes and to contrast them from relatively young, often disturbed, fertile landscapes (YODFELs). According to Hopper (2009) OCBILs are rare, but prominent primarily in the SWAFR, South Africa's Greater Cape, and Venezuela's Pantepui Region of the Guyana Highlands (Takhtajan, 1986). Mucina and Wardell-Johnson (2011) built on this theory to introduce the concept of old stable landscapes (OSLs) to define areas found on the intersection of the three key dimensions: a) age of landscape (correlated with increasing nutrient impoverishment), b) climatic stability, and c) predictability of fire regime. According to this concept OSLs are relatively wide-spread but due to naturally stringent criteria, limited in spatial extent and highly fragmented at the continental scale. Considering the three dimensions suggested by Mucina and Wardell-Johnson (2011) SWAFR provides examples of OSLs with laterites and exposed rocky surfaces such as GOs and banded-iron formations of the Yilgarn Craton (Hopper, 2009), but the region also includes valley floors and swampy terrain in some areas

underlain by old surfaces including whole catenas from hilltop to valley (Mucina & Wardell-Johnson, 2011).

Ecosystem greenspots are locations within OSLs that have relatively high and temporally stable levels of plant productivity in the fragmented landscapes such as SWAFR compared to other locations of the same vegetation (Mackey et al. 2012). These areas have potential to function as drought and fire refugia, areas that burn less often or at less intensity than surrounding areas (Yates et al., 2003; Reside et al., 2014). Their identification is a research and conservation priority (Hopper & Gioia, 2004; Pressey et al., 2007; Game et al., 2011).

GOs have long been regarded as potential refugia where conditions have remained relatively constant and stable during times of anthropogenic climatic fluctuations (Byrne, 2008; Ashcroft, 2010; Stewart et al., 2010; Schut et al., 2014). The elevated nature and geological constitution of GOs means that they channel water, nutrients and plant residues to the fringes of the rock (apron), where growing conditions are more favourable for plants. Weathering on exposed GOs provides nutrients and sediments to associated colluvial and alluvial fans surrounding the outcrops, further reducing local constraints on plant growth (Verboom & Pate, 2003). In addition, slope and shallow soils of GOs reduce waterlogging, and basement rock beneath the fringe prevents water seeping away into deeper aquifers. Therefore, it is expected that aprons should be conducive to denser, healthier (greener) and more resilient (persistent) vegetation than that of the surrounding landscape (Burke, 2002). If this is to be supported then they should be distinguishable by means of modelling multitemporal based sets of remotely-sensed imagery.

Classification of the SWAFR landscapes into units with characteristic underlying geology, geomorphology, soils and vegetation provides a foundation for conservation and management (Tille et al., 1998). Stratification of the landscape has been practiced worldwide and classifications are refined or updated as more information and data become available (Townshend et al., 1991; Jongman et al., 2006; Mücher et al., 2010). In Australia integrated landscape approaches to environmental stratification traces its origins to the integrated land system survey embodied in the Commonwealth Scientific and Industrial Research Organisation's (CSIRO) Land Use Series (e.g. Christian &

Stewart, 1953), later improved by Thackway and Cresswell (1995) as a framework for establishing the national system of reserves. Currently two landscape stratification approaches have been developed in Australia. The Interim Biogeographical Regionalisation for Australia (IBRA) defines 89 biogeographic regions and 419 subregions across the country, 18 of which fall wholly or partly in the in the SWAFR. Land Systems classification of Western Australia defines 74 categories, 39 of which fall in the SWAFR. The units are defined on the basis of climate, geology, landform, soils, vegetation and fauna (Thackway & Cresswell, 1997). Fundamental to this approach is the assumption that climate, geology and geomorphology interact over time to produce characteristic landscape patterns and influence the distribution of soil and vegetation associations (Lawson et al., 2010; Lawley et al., 2011). Consequently there are associations of these environmental components, and landscape can be classified and mapped into units with characteristic and recurring patterns and a degree of internal homogeneity (Schoknecht, 2002).

SWAFR is mostly characterised by arid environments underlain by granites of the Yilgarn Craton but also includes moist forests to the south (Wardell-Johnson & Horwitz, 1996; Dean & Wardell-Johnson, 2010). These forests are located in the areas where soils are product of granites of the Albany-Fraser orogen. Mapping of vegetation response on a landscape scale in a region that includes both the moist forests and semi-arid vegetation of OSLs has a potential to result in fragmented stable landscapes within OSL to be subdued by stronger responses from the moist forests to the south. A well accepted approach to assist interpretation of environmental indicators across variable landscapes is landscape stratification, dividing the landscape into regions within which homogeneity of response may be expected (Hutchinson et al., 2005). Focus on stratifying landscape based on either bioregions (Thackway & Cresswell, 1997) or land characteristics (land system zonation) (Schoknecht, 2002) may therefore be needed for detailed study of OSL environments to highlight the vegetation response and to map any potential fragmented but stable moist environments within the subdued landscapes of the SWAFR. Spatial and temporal modelling of subdued but highly heterogeneous ecosystem greenspots within the more homogenous landscape subdivisions will allow investigation of the interactions between vegetation response and climate over a broad geographic area.

Multi-temporal satellite imagery can be composited over a season (or other time period) to produce imagery which is representative of that period, using techniques which will reduce contamination by cloud and other problems. The notion of a composite satellite image, created from multiple images acquired on multiple dates, is widely used. Huete at al. (2002) introduced the method of using a composite defined by the maximum value of the NDVI for use with the MODIS instrument in combination with other constraints to help exclude other undesirable artefacts from extreme view angles, cloud contamination, and other sources, producing a 16 day vegetation index composites. Identifying potential greenspots using remote sensing techniques is relatively new, partially validated (e.g. Gould et al., 2014) but desirable because it enables rapid investigation over large regions (Ashcroft et al., 2012). On the east coast of Australia, Mackey at al. (2012) have identified potential ecosystem greenspots within the Great Eastern Ranges based on the fPAR over a ten year time period, stratified by major vegetation type.

In this study, I sought to generate a detailed map of vegetation response over a twelve year period as a means to relate growth to environmental variables indicative of local resource availability in topographically complex areas on a landscape scale. The number of sites required to meaningfully estimate the relationships between vegetation and environmental variables using multi-temporal satellite imagery to identify potential refugia was examined. The five prominent GOs across the SWAFR which cover the rainfall gradient and occur on different land sub-divisions within the study area were selected to validate the results. Here four specific aims and associated hypotheses are explored.

1) Identify whether stratifying the region into available landscape subdivisions such as Land Zones or IBRA Subregions would improve ecosystem greenspots mapping. It is expected that stratifying the region into homogenous units of underlying soils, geomorphology and geology would improve identification of ecosystem greenspots.
2) Identify which landscape stratification is better suited to map ecosystem greenspots. It is expected different landscape patterns to emerge reflecting variation in resource availability when different landscape stratifications are

applied. A stronger response is expected in emerging patterns when landscape stratification with more homogeneous units is applied.

3) Compare seasonal distribution of vegetation vigour near the five GOs located across the rainfall gradient. The largest difference in vegetation vigour on GO aprons and surrounding landscape during summer months is expected, reflecting the impact of run-on areas that receive additional resources at the base of GOs.
4) Portray the range of ecosystem greenspots that predict refugia in landscapes surrounding GOs. It is expected that sites closest to GOs will retain more vigorous vegetation than sites further away from them particularly in the arid areas to the north-east. It is also expected that areas other than GOs, i.e. swamps, estuaries, edges of salt lakes and groundwater dependent ecosystems, where conditions are favourable, support stable environments that ameliorate effects of climate change.

4.2. Materials

4.2.1. Study area

The study area consists of the central and southern parts of the SWAFR and covers a rainfall gradient on the southern margin of the Yilgarn Craton and the western side of the Albany Fraser Orogen (Twidale, 1997). The SWAFR forms the south-west global biodiversity hotspot (Figure 4.1) (Myers et al., 2000). The area occupies approximately 160,000 km^2 and contains a wide range of ecosystem types including a) shrubland/woodland, b) dune vegetation, c) swamps and outcrops, d) open forests, and e) tall open forest communities (Beard, 1984; Wardell-Johnson & Williams, 1996). The region is a relatively wet continental refuge, bordered on two sides by ocean, and isolated by arid areas to the north and east (Hopper, 1979). It encompasses a temperate, Mediterranean climate, with a strong declining south-west to north-east precipitation regime, and complex subdued topography and landform characterised by numerous scattered GOs (CSIRO et al., 2007; Sander & Wardell-Johnson, 2012; Reside et al., 2014).

Within the study area five GO landscapes have been selected to test and validate the mapping of the SWAFR greenspots for three main reasons: a) their locations cover the

entire climate gradient of the study area (Bureau of Meteorology, 2015); b) they are located within a different landscape subdivisions, such as bioregions and soil landscape units (Thackway & Cresswell, 1995); and c) vegetation types in the surrounding landscape of the five selected outcrops vary significantly from open forests in the south-west (i.e. Mount Frankland, Mt Chudalup) to semi-arid shrubland in the north-west (i.e. Chiddarcooping) (Hopper et al., 1997).

Mean annual rainfall decreases rapidly inland to the north-east from 1,150 mm to 300 mm per year. Rainfall is highly seasonal with up to 80% of the rain being recorded during a 6 month period from May to October (Bureau of Meteorology, 2014). The average rainfall is 600 mm, with local maxima on the western escarpment in excess of 1000 mm. This differs from other locations at similar latitude on the western edges of landmasses such as southern Africa or South America which have cold coastal currents flowing toward the equator and receive less than 300 mm of rainfall annually (Timbal et al., 2006). Potential evaporation increases across the study area south-west to north-east, with very high potential evaporation in the summer months compared to winter months. Average pan evaporation rate for the south-west is 175 mm and for the north-east is 350 mm in January, compared to 50 mm and 100 mm respectively in June (Bureau of Meteorology, 2015).

Spatially, the study area was subdivided into more localised and homogenous units developed in response to the need to work with large geographic scales and biological cycles to plan and achieve biodiversity conservation (CSIRO, 1983). Subdividing landscape into more localised and homogenous units is useful in regional conservation planning and in the development of conservation that, if it is to be representative of the natural environment, needs to contain viable areas of the major ecosystems of each natural region. Landscape subdivisions enable data from localised areas to be assessed in a regional, state-wide or national context.

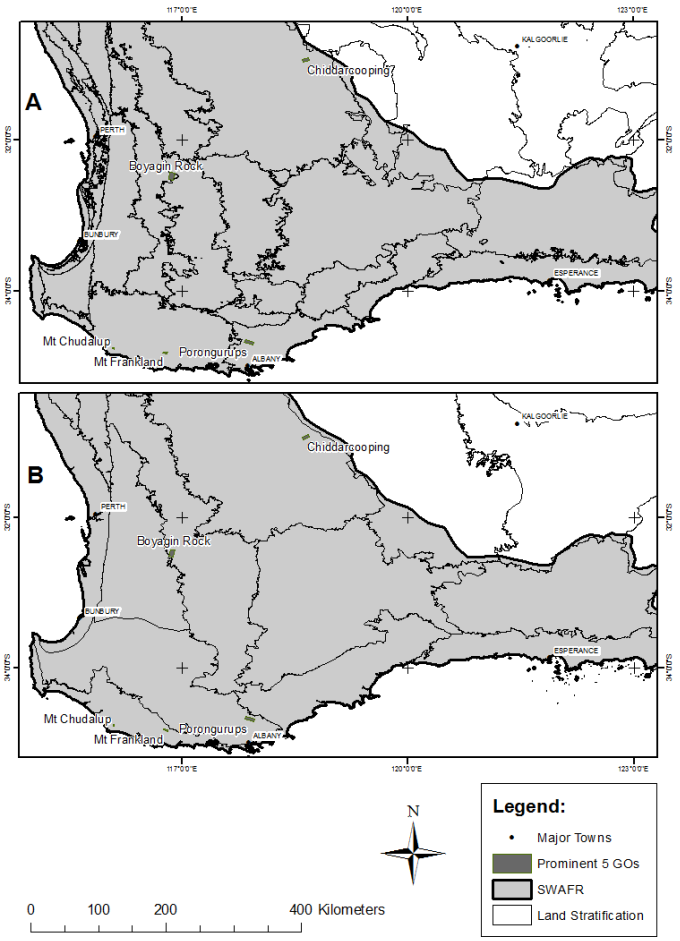

Figure 4.1 *Study area – SWAFR stratified by a) Land Zones and b) IBRA Subregions. Prominent five GOs covering rainfall gradient are also shown.*

Temporally the study was restricted to a 12 year period. During six of these years annual precipitation over south-west Australia was < 90% of the long term (1900 to 2013) average of 600 mm/year (Bureau of Meteorology, 2014). The most extreme drought conditions in south-west Australia occurred during 2010 with average precipitation of 390 mm/year (Delworth & Zeng, 2014).

Observations are used to develop a weighting scheme to emphasise these characteristics, which are applied to a summarised time series of remote-sensing based NDVI imagery. The technique is applied and tested on five GOs located throughout the SWAFR covering the rainfall and temperature range and granites of varying origins, from older Yilgarn craton bedrock to granites of the Albany-Fraser orogen.

4.2.2. Remotely-sensed imagery

The source data were continental time series of Normalized Difference Vegetation Index (NDVI) values from the MODIS 16-day L3 Global 250 m (MOD13Q1) composite gridded data (Paget & King, 2008) acquired from the Centre for Earth Resources Observation and Science (EROS) from 18 February 2000 to 8 May 2012 (U.S. Geological Survey, 2012). The MODIS NDVI product is computed from atmospherically corrected bi-directional surface reflectance that has been masked for water, clouds, heavy aerosols, and cloud shadows.

4.2.3. Land stratification data

Two types of landscape sub-divisions are available and were considered over the study area. IBRA is based on biogeographic regionalisation and geomorphology, and the Land System classification primarily on underlying soils and geology. Land stratification into more localised and homogenous units enables a consistent presentation and analysis of soil and landform data across the region and enables data from localised areas to be assessed in a regional, state-wide or national context.

Bioregions are relatively large land areas characterised by broad, landscape-scale natural features and environmental processes that influence the functions of entire ecosystems (Morgan & Terrey, 1992). They capture the large-scale geophysical patterns across Australia. These patterns in the landscape are linked to fauna and flora assemblages and processes at the ecosystem scale, thus providing a useful means for simplifying and reporting on more complex patterns of biodiversity. The bioregions are described in the interim Biogeographic Regionalisation for Australia (IBRA). The Australian land mass is divided into 89 bioregions and 419 subregions which are more localised and homogenous geomorphological units in each bioregion. Each region is a land area made up of a group of interacting ecosystems that are repeated in similar form across the landscape. IBRA is a more detailed subset of the global ecoregions and was developed as a framework primarily to identify deficiencies in the Australian network of protected areas and to set priorities for further enhancing the reserve system (Thackway & Cresswell, 1995).

Land System classification in soil landscape unit mapping hierarchy deals with differing levels of complexity in both landscape and soil patterns (Tille et al., 1998). It maintained a consistent approach across a range of mapping scales, and at varying levels of detail in the associated data. It included the development of a nested hierarchy of soil-landscape mapping units (Schoknecht, 1997). This hierarchy has six levels in order of decreasing spatial scale (Schoknecht et al., 2004). Each level of the soil-landscape mapping hierarchy is a subdivision of the preceding level with increasingly more detail relating to soil thickness, water storage, permeability, salinity, fertility, and erodibility (Tille, 2006). The highest two levels are regions and provinces, provinces being subdivisions of the regions. Both are based on a framework introduced by CSIRO (1983) for the whole of Australia. Provinces are in turn sub-divided in zones. The zones are subdivided into remaining three levels: systems, subsystems and phases (Thackway & Cresswell, 1997).

A hierarchy of mapping soil landscape units with six levels allows for descriptions from the lowest level of the hierarchy to feed into summaries at higher levels. Each land unit consists of a soil group of Western Australia and its qualifier as well as the landform position in which it occurs (Schoknecht, 2002). The characteristics of stratification units for both types of landscape sub-divisions for the 5 GOs is shown in Table 4.1.

Table 4.1 *Land stratifications characteristics for the five selected GOs modified from Thackway and Creswell (1997) and Tille (1998).*

	IBRA Subregion	**Land Zone**
Porongurups	**Southern Jarrah Forest** – Located on the Yilgarn Craton inland plateau and includes wooded valleys. On the west coast further south the sub-region covers the Leeuwin-Naturaliste Ridge. At the southern end of the plateau stands the Whicher Range and the lower Blackwood Plateau. The name refers to the sub-region's dominant ecosystem: Jarrah forest. Soils are fertile, but often salt laden.	**Albany Sandplain** - The zone is a gently undulating plain dissected by a number of short rivers flowing south. Eocene marine sediments are overlying Proterozoic granitic and metamorphic rocks. Soils are sandy duplex soils, often alkaline and sodic, with some sands and gravels.
Boyagin	**Avon Wheatbelt P2** - An area of active drainage dissecting a Tertiary plateau in Yilgarn Craton. It is the erosional surface of gently undulating rises to low hills with abrupt breakaways. Continuous stream channels that flow in most years. Colluvial processes are active. Soil formed in colluvium or in-situ weathered rock.	**Eastern Darling Range** - The zone is moderately to strongly dissected lateritic plateau on granite with eastward-flowing streams in broad shallow valleys and some surficial Eocene sediments. Continuous stream channels usually flow in most years where colluvial processes are active. Soils are formed in laterite colluvium or in-situ weathered granite.
Chidarcooping	**Avon Wheatbelt P1** – Located on the central Yilgarn Craton and comprises gently undulating landscape of low relief. Soils are fertile, but often salt laden.	**Zone of Ancient Drainage** – The zone is an ancient plain with low relief on weathered granite. There is no connected drainage, salt lakes occur as remnants of ancient drainage systems which only function in wet years. Lateritic uplands are dominated by sandplain.
Mt Frankland	**Warren** - Hilly topography caused by two factors: the underlying geology, which consists of infolded metamorphic rock of the Leeuwin Complex and Archaean granite of the Albany-Fraser Orogen; and the dissection of rivers such as the Blackwood, Warren and Frankland. Soil types include hard setting loamy soil, lateritic soil, leached sandy soil and Holocene marine dunes.	**Warren-Denmark Southland** - The zone is characterised by rises in a series of broad benches from the Southern Ocean north to the Blackwood Valley. It comprises deeply weathered granite and gneiss overlain by Tertiary and Quaternary sediments in the south. The zone is swampy in places.
Mt Chudalup	**Warren** - as above	**Warren-Denmark Southland** - as above

For validation purposes, land zones and IBRA subregions were tested as units of stratification as these are the areas defined on geomorphological and geological criteria, suitable for regional perspectives. Mount Frankland and Mount Chudalup GOs are both selected because Mount Frankland is situated within the southern forests amongst numerous other GOs while Mount Chudalup is isolated within the D'Entrecasteaux National Park. This setting will allow testing the greenspot mapping suitability across the Albany-Fraser Orogen area (Figure 2.6).

4.2.4. Digital surface data

The digital surface data used in this study were the Hydrologically Enforced Digital Elevation Model (DEM-H) (Gallant et al., 2011). The dataset was derived from the Shuttle Radar Topography Mission (SRTM) data acquired by NASA in February 2000 and was publicly released in November 2011 (Dowling et al., 2011).

Digital elevation model (DEM) represents ground surface topography, with vegetation features removed. Smoothed DEM (DEM-S) represents ground surface topography, excluding vegetation features, and has been smoothed to reduce noise, intensity spikes caused by errors in data transmission, and improve the representation of surface shape. This dataset supports calculation of local terrain shape attributes such as slope, aspect and curvature that could not be reliably derived from the original 1 second DEM because of noise (Gallant, 2011).

Hydrologically Enforced DEM (DEM-H) is a hydrologically enforced version of the smoothed DEM-S. The DEM-H captures flow paths based on SRTM elevations and mapped stream lines. The dataset was derived from the DEM-S by enforcing hydrological connectivity, using selected 1:250,000 scale watercourse lines and lines derived from DEM-S to define the watercourses (Gallant et al., 2012).

4.2.5. Software

Idrisi Taiga (Clark Labs, 2012; Warner & Campagna, 2013) geographic information system was used to: a) extract and convert the NDVI and the pixel reliability data from

the original MODIS files; b) de-project data from the original sinusoidal projection to GDA94 datum; c) concatenate data extents to fit the study area; and d) identify and correct grid cells affected by cloud contamination or sensor errors. For de-projecting data each MODIS pixel of 250 m square was allocated a 7.5 arc seconds for resampling of data following approach suggested by the US Geological Survey (Danielson & Gesch, 2011).

Spatial analyses, modelling, and automation tasks were completed using the ArcGIS 10.2 geographic information system, and ArcScene 10.2 for 3D analysis (ESRI, 2014). The spatial unit of analysis was a regular matrix of grid cells at ~250 m spatial resolution. SPSS (IBM, 2015) was used for statistical analyses.

4.3. Methods

The mapping approach in this study consists of eight steps if no landscape stratification is used. The first two steps comprise high temporal resolution NDVI data preparation and de-noising by calculating medians. This is followed by the calculation of seasonal median images and standardising of sensor data into standard NDVI value ranges (0, 1). The seasonal influence in fuzzy sets is then determined and appropriate weights calculated to adjust for it. In the final step NDVI images with adjusted seasonal influences are combined into a single weighted fuzzy combination image.

If landscape stratification is used, the additional two steps are introduced at the beginning of the process. These steps are needed to stratify time series data before de-noising. At the end of the process an additional step is also required to combine stratified units into a single weighted fuzzy combination image. The process is repeated until the most effective stratification is identified as shown in Figure 4.2.

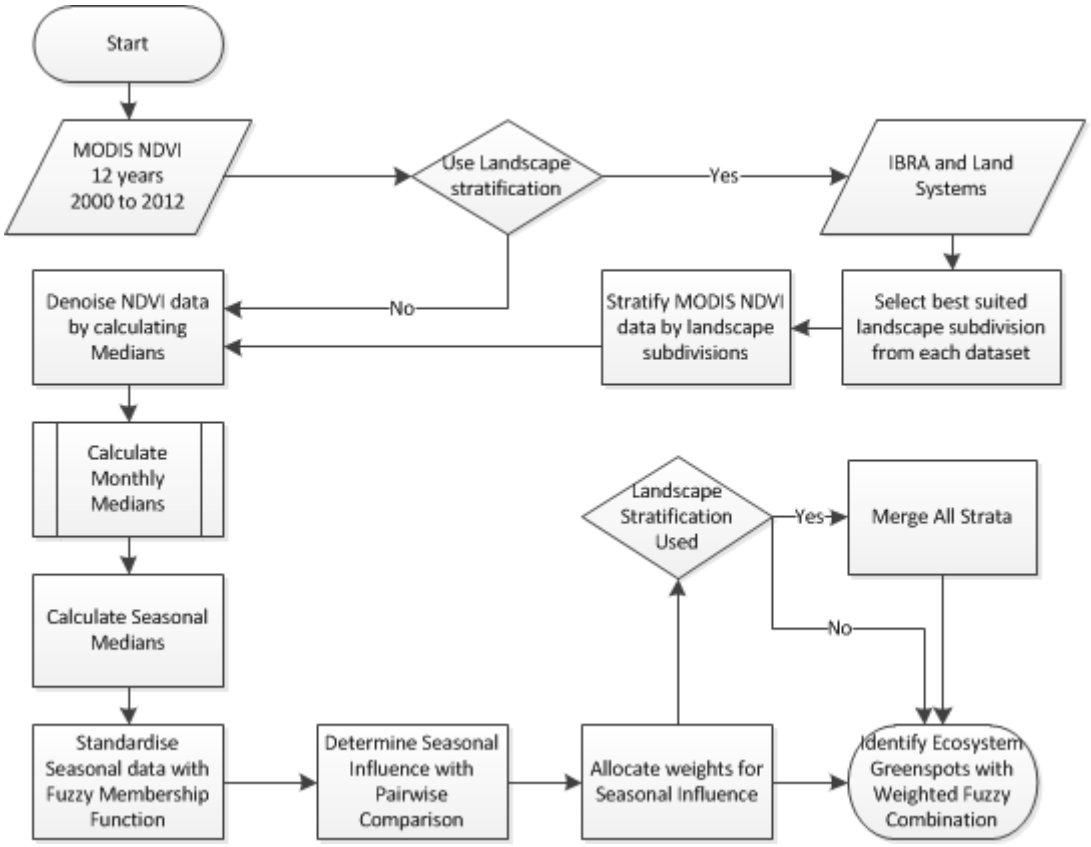

Figure 4.2 *Ecosystem greenspot modelling process diagram.*

4.3.1. MODIS data processing

The processing of the MODIS NDVI data involved the identification and correction of grid cells that were affected by cloud contamination or sensor errors. The dropout cells were determined as those with value that was less than 90% of the value of the corresponding cell in the preceding and subsequent images of the time series. A corrected value was calculated as a weighted average of the values of the preceding and subsequent images of the time series. Following the correction of cells with dropout values through the NDVI time series, cells with spikes were identified by a similar approach but where the value of a grid cell exceeded 110% of the value of the corresponding cell in the preceding and subsequent images. Spike affected cells were then replaced by averages of values of the corresponding cells in the preceding and subsequent images of dropout corrected time series. Following the corrections for dropouts and spikes I generated the complete time series consisting of 23 images per

year at 16 day intervals, where every pixel value is the product of maximum value compositing (Huete & Saleska, 2010). There are 275 datasets in the time series.

4.3.2. Median seasonal NDVI

To derive a typical NDVI response for each season, the time series of NDVI values were first summarised into monthly median images and then combined into seasonal median composite images. The chosen seasonal periods are September-November, December-February, March-May and June-August, corresponding to Spring, Summer, Autumn and Winter (in southern hemisphere terms) following the approach developed by Roy et al. (2010). Seasons are the meteorological breakdown of the year into four three-month periods. Trenberth (1983) gives a detailed discussion of what constitutes a season. Analysis is performed on all seasons and for both land classification systems for the period February 2000 to May 2012.

Initially, stratified four seasonal median composite datasets were used to assess which classification system is better suited to highlight ecosystem greenspots. The stratification was conducted by intersecting the input NDVI images with stratification datasets. 19 IBRA subregions datasets and 39 land zones datasets for each season were produced and then combined into 4 per season median values datasets for each land classification system. The resulting datasets formed the basis for further modelling.

4.3.3. Identify if stratifying the region is needed

A *Z*-test is any statistical test for which the distribution of the test statistic under the null hypothesis can be approximated by a normal distribution (Freund, 1984). A one-tailed test is a directional test and is used for testing whether one mean was higher than the other (Good & Hardin, 2003) rather than to determine whether the first mean was lower than the other. The test is only used to determine one side of the probability distribution.

A one-tailed Z-test of two means (Equation 4.1) was applied to each of the five study sites to test the hypothesis that GOs have a significantly higher seasonal median NDVI response than the surrounding landscape when stratified by available landscape stratification units. One hundred random samples of NDVI were taken from each.

$$Z = \frac{(\overline{x}_1 - \overline{x}_2) - d_0}{\sqrt{\frac{\sigma_1^2}{n_1} + \frac{\sigma_2^2}{n_2}}} \qquad (4.1)$$

Where $\overline{x}_1$ is the median for NDVI of the apron, $\overline{x}_2$ is the median for NDVI of the surrounding landscape, σ_1^2 and σ_2^2 are the variances, and n_1 and n_2 are the sample sizes of sample 1 and 2, respectively.

A cumulative probability of Z-scores was then applied to test if variance on GOs differs to that of wider landscape strata.

$$Z = \frac{x - \mu}{\sigma} \qquad (4.2)$$

Where x is standardised score (given that x has a normal distribution), μ is the population mean, and σ is the population standard deviation.

A cumulative probability refers to the probability that the value of a random variable falls within a specified range where each event needs to be independent of the others (Chiverrell et al., 2011).

Finally Tukey's Honestly Significant Difference (HSD) test was applied to find differences between the medians of all groups (Tukey, 1949). Analysis of Variance (ANOVA) test (Scheffe, 1999) was first conducted to determine if there is any difference between the medians. The differences between the medians of all our groups: GOs, surrounding landscapes and stratifications scores are compared to a critical value to see if the difference is significant. The critical value is the HSD. It is the point when a mean difference becomes honestly significantly different and is calculated using Equation 4.3 (Tukey, 1977):

$$HSD = q\sqrt{\frac{MS_{Within}}{n}} \qquad (4.3)$$

Where q is a value from the Studentized Range Distribution table, MS is the Mean Square value from within a group, and n is number of values in each group.

4.3.4. Identify which landscape stratification is most effective

Receiver Operating Characteristic (ROC) analysis is used to identify which landscape stratification is better suited to map ecosystem greenspots. Firstly, NDVI points were standardised using the weighted fuzzy combination (WFC) method (see 4.3.5 section below), and then a set of optimal cut off pixel values (C) was determined from these standardised NDVI points for samples taken from each of the five GO landscapes.

A perfect classification is at the top left corner (0,1) of the ROC plot. At this point there are no false positives or false negatives (Lobo et al., 2008). Typically, this point is hard to achieve; however, the cut off value closest to this perfect classification is deemed to be the optimal threshold for discriminating between the two classes (Robinson et al., 2009).

An optimal cut off value for each GO landscape was defined with ROC plots. The False Negative Rate (FNR) is a sum of all samples from GO landscape for which standardised NDVI value is greater than or equal to C. Consequently, the False Positive Rate (FPR) is a sum of all samples from the surrounding landscape for which standardised NDVI value is greater than or equal to C.

The FNR and FPR values are computed using confusion matrix derived measures of classification accuracy from Fielding & Bell (1997):

$$FNR = \frac{c}{a + c} \qquad (4.4)$$

$$FPR = \frac{b}{b + d} \qquad (4.5)$$

where *a* is both actual and predicted positively classified sample point, *b* is predicted but not actual, *c* is actual but not predicted, and *d* is neither actual nor predicted sample point.

The ROC plot was also used to generate a summary statistics known as the Area Under the Curve (AUC). The values of AUC are between 0.5 and 1. If the value is 0.5, the classification is no better than that obtained by chance, while a value of 1 indicates no overlap in the distribution of good and poor samples as determined by the modelling; i.e., a perfect discrimination between the two classes (Fielding & Bell, 1997). The AUC makes comparison between models relatively straightforward; the best model will minimise false negatives and false positives and therefore have the highest AUC (Bradley, 1997; Kerekes, 2008). The AUC is calculated using the trapezoidal rule (Pontius Jr & Schneider, 2001):

$$AUC = \sum_{i=1}^{n} [x_{i+1} - x_i] \times \left[\frac{\left(y_i + (y_{i+1} - y_i)\right)}{2} \right] \qquad (4.6)$$

where n is the number of cut off values, x_i is the false positive rate at i, x_{i+1} is the false positive rate at threshold $i+1$, y_i is true positive rate at threshold i, and y_{i+1} is the true positive rate at threshold $i+1$.

For the five GO landscapes AUCs were calculated to assess which landscape subdivision is best suited for greenspot modelling. A 100 random sample points were allocated to each of the five GO landscapes. Further 1000 random sample points were allocated to the surrounding landscapes: a 100 from within a 5 Km radius of the GO landscapes, then a further 100 from within a 10 Km radius, then a further 100 from within a 20 Km radius and so on up to the 80 Km radius of the GO landscapes, but within a land stratification used for modelling the data. The last 100 random sample points were allocated to an area beyond 80 Km radius and within the land stratifications used, totalling a 1000 random sample points for the surrounding landscape covering the entire land subdivision area.

4.3.5. Compare seasonal influence on GO ecosystems

The fuzziness of geographical data is related to the imprecision in the location and boundaries and also to uncertainty and gaps in attribute data (Paegelow & Camacho Olmedo, 2008). Fuzzy set theory was first developed by Zadeh (1965) to deal with uncertainty. Song & Chissom (1993, 1994) successfully modelled a fuzzy forecast by adjusting time series data to the fuzzy sets. According to Saint-Joan and Desachy (1995) fuzzy systems deal with imprecise and uncertain information in a more efficient way than algebra map systems based on boolean logic. Fuzzy logic also allows a standardisation of the original data units in order to process them together. Using fuzzy logic, the aim can be focused onto specific regions of interest. Fuzzy functions standardise multitemporal raster based data and evaluate the possibility of each pixel belonging to a fuzzy set by evaluating any of a series of fuzzy set membership functions (Kasabov, 1996).

The sigmoidal membership function, also called s-shaped function, is the most commonly used function in fuzzy set theory (Duch, 2005), offering a gradual variation for each factor from non-membership, e.g. 0 to complete membership, e.g. 1. The sigmoidal membership function can be specified by four parameters: a) membership rises above 0, b) membership becomes 1, c) membership falls below 1, and d) membership becomes 0. The sigmoidal fuzzy membership functions include a) monotonically increasing, b) monotonically decreasing, c), C-Symmetric, and d) D-symmetric curves.

Fuzzy standardisation was applied to the seasonal NDVI imagery to standardise each to a scale between zero and one (Robinson, 2003). Negative values for ocean in the data were masked, and the four images were stratified by land zones. The sigmoidal monotonically increasing function was calculated using Equation 4.7 (Robertson et al., 2004):

$$\mu = cos^2\left(\left(1 - \frac{x - point\ a}{point\ b - point\ a}\right) * \frac{\pi}{2}\right) \qquad (4.7)$$

Where x is the NDVI response of a pixel, inflection point “a” is the median NDVI value in the stratum; and inflection point “b” is maximum NDVI value in the stratum. Values less than the median were assigned 0.

4.3.5.1. Pairwise comparison

The pairwise comparison method was developed by Saaty (1979) in the context of the analytic hierarchy process (AHP). The method involves pairwise comparisons to create a ratio matrix. It takes as an input the pairwise comparisons and produces the relative weights as output. Specifically, the weights are determined by normalising the eigenvector associated with the maximum eigenvalue of the reciprocal ratio matrix (Merriam et al., 1996). The method employs an underlying scale with values from 1 to 9 to rate the relative preferences for two criteria.

A pairwise comparison matrix (PCM) using a nine point scale (Saaty, 1979) was created to develop a set of weights for each seasonal median. The principal Eigenvector of the matrix is used to derive the weights. The method includes an index called consistency ratio (CR) that indicates the overall consistency of the PCM. According to Saaty (1994), the CR should have a value of less than 10%, indicating consistency of the matrix. The relative importance weights of the evaluation criteria are calculated by using the PCM matrix.

4.3.6. Portray ecosystem greenspots that predict refugia

Weighted fuzzy combination is a final step in the process of fuzzy standardisation required to reduce the risk of including data that may have minimal influence in the fuzzy set (Dubois et al., 1988; Yeung & Tsang, 1997). However, the actual degree of risk is not known, only that the data included are the least risky of the alternatives considered (Nakashima et al., 2007; Schulte et al., 2007).

Weighted fuzzy combination modelling was applied to standardised NDVI values following weight allocations to compensate for varying influences of different seasons on the data. The modelling was first applied to the entire dataset using overall median values. It was then repeated to stratified subsets of data where medians were re-

calculated per strata to compensate for large differences in median values on a regional scale.

4.3.7. ROC slicing validation

Principal applications of Receiver Operating Characteristic (ROC) in spatial studies concern the assessment of raster data models aimed at predicting land cover and land use change over time, among others (Fawcett, 2006). ROC analysis is applied to assess the performance of spatio-temporal models that produce a probability model, which presents the sequence in which the model selects grid cells to determine the occurrence of a certain event, e.g. land cover change (Pontius & Parmentier, 2014).

In the standard ROC approach, the predictive probability model is compared with the map of the true binary event in order to assess the spatial coincidence between the event and the probability values. For raster datasets, input data are simplified by grouping cells with similar probabilities into bins. Strategic thresholds chosen by the user method was used for selecting the slicing thresholds to define the bins on a landscape scale (Peterson et al., 2008). Each threshold of probability is then overlaid with the event map in order to calculate true and false positive rates (Provost & Fawcett, 1998).

A hundred random samples of standardised NDVI values were generated from each GO landscape and a further hundred from the surrounding landscapes to construct an ROC curve to threshold out GOs from non-GOs.

4.4. Results

Ecosystem greenspot locations that may have functioned as refugia across the SWAFR were mapped using weighted fuzzy combination (WFC) method for the 12 year period commencing February 2000. The entire range of ecosystem greenspots was mapped but the focus was on diagnostic analyses and interpretation on the five GOs (Figure 4.1) which cover the rainfall gradient and land subdivisions of the region, and are most likely to function as fire and drought refugia for species threatened by anthropogenic climate change. An automated tool for ArcGIS comprising a set of python scripts was developed to calculate median pixel values per strata, generating monthly and seasonal images,

stratifying study area into different land sub-divisions, and standardise the data with fuzzy standardisation approach (Figure 4.2). Raster calculator tool in ArcGIS was then used to assign appropriate weights to seasons as per pairwise comparison approach described in section 4.3.5 to generate a weighted fuzzy standardised model. The modelled strata images were then combined into a single image covering the whole region by each land sub-division.

4.4.1. Identify if stratifying the region is needed

Initially the data were modelled by WFC with no landscape stratification applied (Figure 4.3), and then the process was repeated with IBRA Subregions and Land Zones stratifications. A hundred random samples were generated from each GO and a further 100 from the surrounding landscapes for each of the five GOs. Medians of the standardised NDVI values for these sites were calculated for each of the three scenarios: a) no stratification, b) region stratified by IBRA subregions, and c) region stratified by Land Zones (Table 4.2).

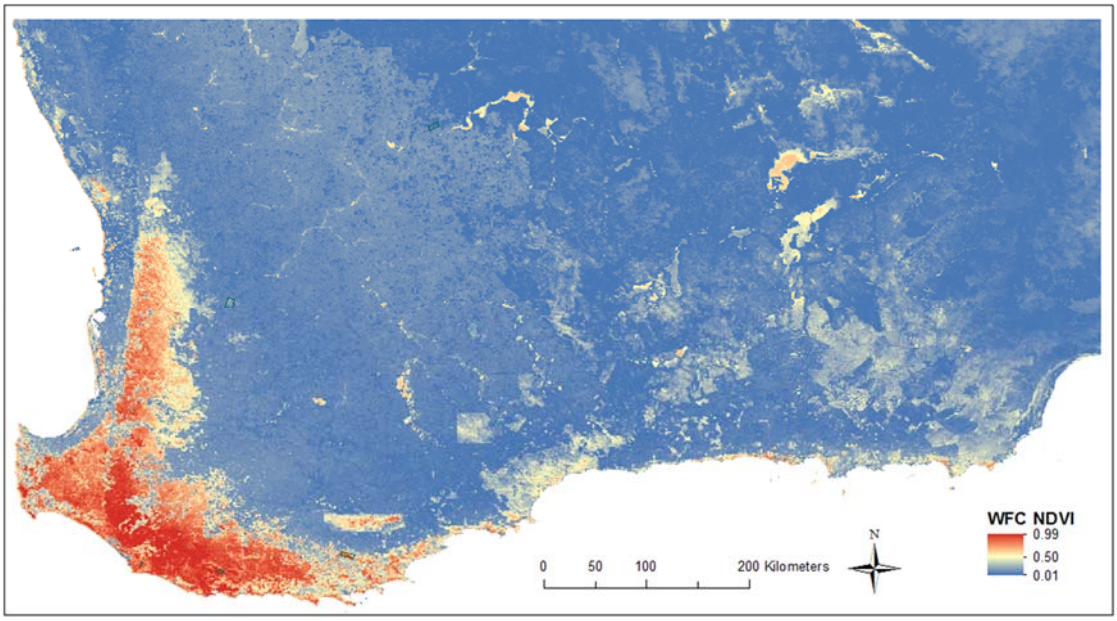

Figure 4.3 *Weighted Fuzzy Standardisation modelled data with no stratification applied.*

The difference between standardised median NDVI values of GOs and surrounding landscape is significantly lower on all sites except Porongurups when no stratification

is applied to data modelling (Table 4.2) resulting in ecosystem greenspots in landscapes surrounding GOs not being well defined from its surroundings (Figure 4.3). This is due to the broader landscape in the mesic end of the gradient to the south and east of the region that lie within the rainfall gradient over the 600 isohyet contour displaying stronger response in vegetation growth on a regional scale which "masks" less prominent localised differences in vegetation growth in semi-arid parts of the OSL. One way to overcome this is by stratifying the SWAFR into more homogenous units which highlights localised differences in vegetation growth and heterogeneity from its homogeneous surroundings in subdued OSL environments.

Table 4.2 *WFC fitted Medians for a) land zone stratification, b) IBRA subregion stratification, and c) no stratification applied with Tukey's test applied to determine which groups differ from each other.*

	Granite Outcrop Medians			**Surrounding Landscape Medians**		
Study Site	Land Zone	IBRA Sub	No strat	Land Zone	IBRA Sub	No strat
Porongurups	$0.644_{a,i}$	$0.453_{a,i}$	$0.800_{a,ii}$	$0.088_{d,iii}$	$0.226_{d,iii}$	$0.281_{d,iv}$
Boyagin	$0.237_{b,i}$	$0.474_{b,i}$	$0.175_{b,ii}$	$0.101_{e,iii}$	$0.059_{e,iii}$	$0.083_{e,iv}$
Chiddarcooping	$0.671_{b,i}$	$0.621_{b,i}$	$0.107_{b,ii}$	$0.008_{e,iii}$	$0.006_{e,iii}$	$0.069_{e,iv}$
Mount Chudalup	$0.479_{c,i}$	$0.275_{c,i}$	$0.914_{c,ii}$	$0.093_{f,iii}$	$0.045_{f,iii}$	$0.825_{f,iv}$
Mount Frankland	$0.491_{c,i}$	$0.629_{c,i}$	$0.971_{c,ii}$	$0.085_{f,iii}$	$0.028_{f,iii}$	$0.827_{f,iv}$

* Median captions in small letters indicate where GOs are not significantly different

** Median captions in Roman numerals indicate significance in stratification difference

Porongurups which are located within the Albany Sandplain Zone stand out from its surroundings regardless of whether the region is stratified or not. This is partly due to its unique geological location on the boundary of the Yilgarn Craton and the Albany-Fraser Orogen. It is also located in close vicinity of the 600 isohyet contour which separates mesic areas from semi-arid parts of the SWAFR. This unique geographic location coupled with its relatively large topographic relief which influences local climate may have contributed to Porongurups extending the range of species from its normal distribution in mesic areas.

From Tukey's HSD test across stratifications (indicated in subscripted Roman numerals in Table 4.3), both Land zone and IBRA subregion stratifications are significantly different from the 'no stratification' mapping approach for both GOs and surrounding landscapes. Tukey's HSD test across GO landscapes (indicated in subscripted small letters in Table 4.2) indicates that Porongurups significantly differ from Boyagin and Chiddarcooping, whilst all these significantly differ from Mount Chudalup and Mount Frankland when grouped by both GO and surrounding landscape medians.

4.4.2. Identify which landscape stratification is most effective

The median NDVI values show less variance between GOs and surrounding landscapes when IBRA subregion stratification is applied compared to land zone stratification. This is due to key differences in ground cover and soil types not being particularly well defined with IBRA subregion stratification. Thus IBRA subregion stratification is inclusive of wider range of vegetation and soils types when compared to land zone stratification. Summary of NDVI responses from GOs vs. surrounding landscape are shown in Table 4.2.

The seasonally averaged mean NDVI values are relatively higher and invariant on the five GOs compared to surrounding landscapes within land zones at all study sites (Figure 4.4). Variance is significantly higher at the surrounding landscapes from season to season peaking at 1852.44 (Table 4.3). Mean NDVI values are also higher in all seasons except in spring and winter at Boyagin. This may be due to heavy agricultural land use in the surrounding areas in these higher rainfall zones, coinciding with the pastures and crops' temporal growth patterns. This further highlights the need for

developing and applying a set of weights for each seasonal median image to reduce the influence of seasonal variation of annual crops on an overall long term vegetation response.

At the more mesic parts of the study area to the south characterised mainly by open forests, low and open vegetation in shallow soils occur only on GOs. However, vegetation is taller and denser in aprons (on-flow areas) at the base of the GOs. Mean NDVI values here are relatively higher and less variant on GO's than in the surrounding landscape with denser and taller vegetation where soil depth increases.

At Porongurups, with its relatively large topographic relief which influences local climate, most dense vegetation is restricted to the highest rainfall and least seasonal end of the high rainfall province.

Boyagin Nature Reserve is located on the Yilgarn Craton beyond the Darling Fault that separates it from the coastal plain. The reserve is diverse with a strong mosaic pattern of terrain, soil and vegetation types with largest areas in the reserve covered by open woodlands. Here too mean NDVI values are higher and less variant on GO's and aprons than at the surrounding landscape.

Chiddarcooping is also located on the Yilgarn Craton but further north-east within the driest part of the study area where only deeper soils along waterways near GOs support relatively dense vegetation. Areas further from streams will only support open shrubs reflecting a much more scattered and open vegetation cover. The proportional changes in vegetation types in the wider landscape are expected to be more pronounced than those directly surrounding GOs. The dense vegetation here is restricted in narrow fringes around the base of GOs. Thus mean NDVI values are significantly lower but are still more stable on GO's than in surrounding landscape.

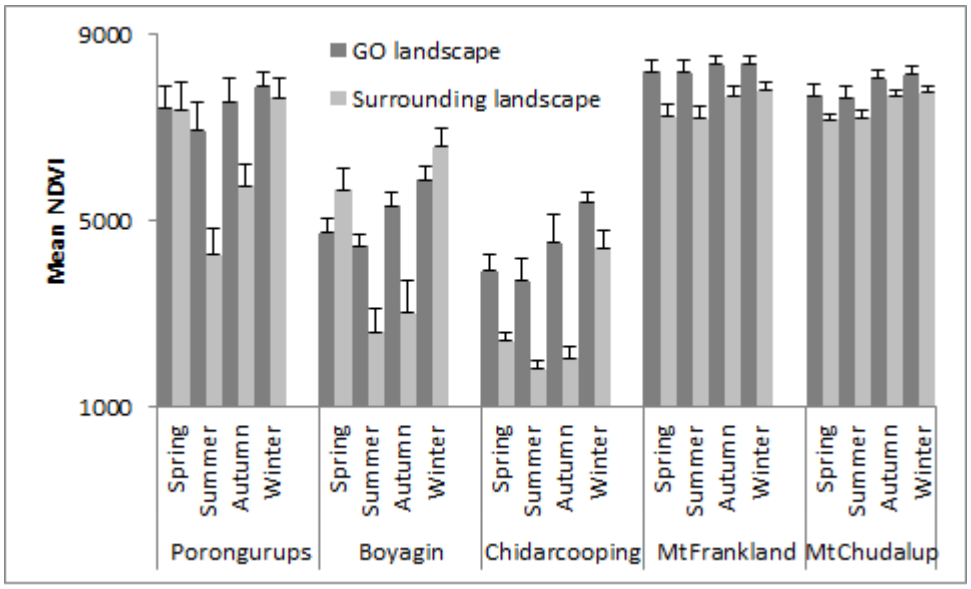

Figure 4.4 *Summary of the mean (and standard error) NDVI responses from GOs vs. surrounding landscape.*

The f-test for equality of variances shows that variance on the GOs is significantly lower than that found further away in their respective land zones (Table 4.3). Much higher F variance found at Boyagin may be due to its proximity to the boundary of the two land zones with significantly different median values.

Table 4.3 *Cumulative probability of variances (1 - P) within GO aprons and surrounding landscapes.*

	Variance_{GO}	Variance_{LS}	$F_{variance}$	P
Porongurups	594.75511	1462.20300	6.04	<0.01
Boyagin	604.67310	1852.43840	9.38	<0.01
Chidarcooping	726.22556	1071.03935	2.17	<0.02
Mt Frankland	154.99055	337.31027	4.74	<0.01
Mt Chudalup	274.07627	296.94334	1.17	<0.02

Table 4.4 *Statistics used to compare standardised NDVI responses from GO landscapes vs. surrounding landscape within a 5 Km radius.*

GO Landscape	Stratification	Optimal Cut-Point	AUC	TPR	FPR	Overall Accuracy (%)
Porongurups	Land Zone	0.345	0.981	0.88	0.01	93.50
	IBRA Subregion	0.183	0.976	0.84	0.24	80.00
	No stratification	0.607	0.843	0.87	0.03	92.00
Boyagin	Land Zone	0.149	0.992	0.99	0.09	95.00
	IBRA Subregion	0.370	0.980	0.97	0.07	95.00
	No stratification	0.098	0.941	0.98	0.31	83.50
Chidarcooping	Land Zone	0.591	0.938	0.90	0.01	94.50
	IBRA Subregion	0.544	0.939	0.90	0.02	94.00
	No stratification	0.044	0.706	0.83	0.24	79.50
Mt Frankland	Land Zone	0.572	0.973	0.96	0.01	97.50
	IBRA Subregion	0.307	0.916	0.98	0.10	94.00
	No stratification	0.899	0.873	0.95	0.12	91.50
Mt Chudalup	Land Zone	0.202	0.981	0.91	0.05	93.00
	IBRA Subregion	0.123	0.897	0.85	0.07	89.00
	No stratification	0.888	0.789	0.73	0.12	80.50

ROC analyses for increasing distance from selected GOs show that mapping without stratifying the region results in greenspots being less separable from surroundings on a landscape scale (Figure 4.5). When the region is stratified into more homogeneous units based on land characteristics GO landscapes differ significantly from its surroundings (Figure 4.5).

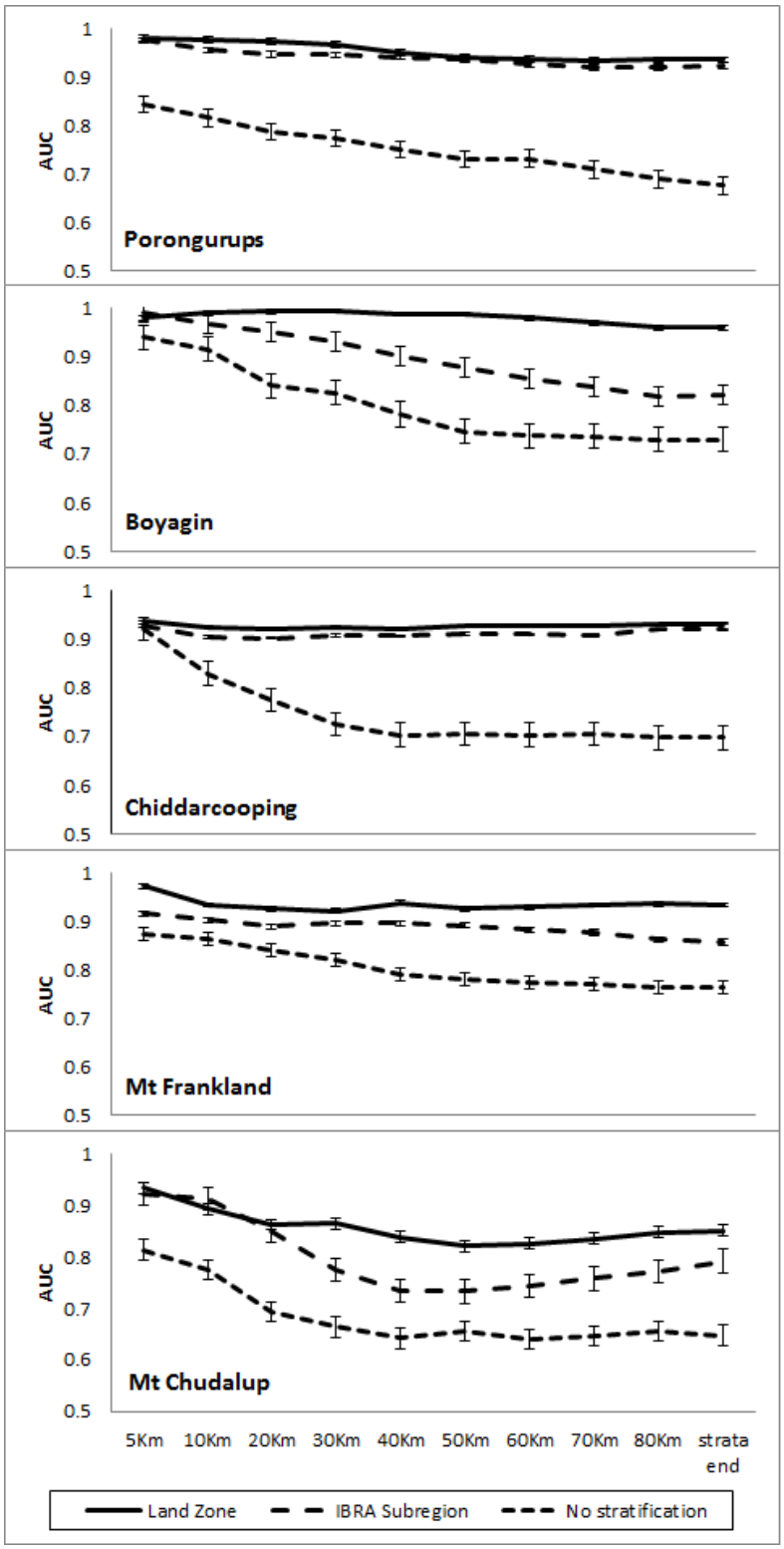

Figure 4.5 *ROC analysis used to compare standardised NDVI responses from GO landscapes vs. surrounding landscape. AUCs were calculated from 100 random sample points on GO landscapes vs. 100 samples from within 5 Km, and then additional 100 samples increments in 10 Km radius succession up to the strata extents where a 1000 sample points were assigned.*

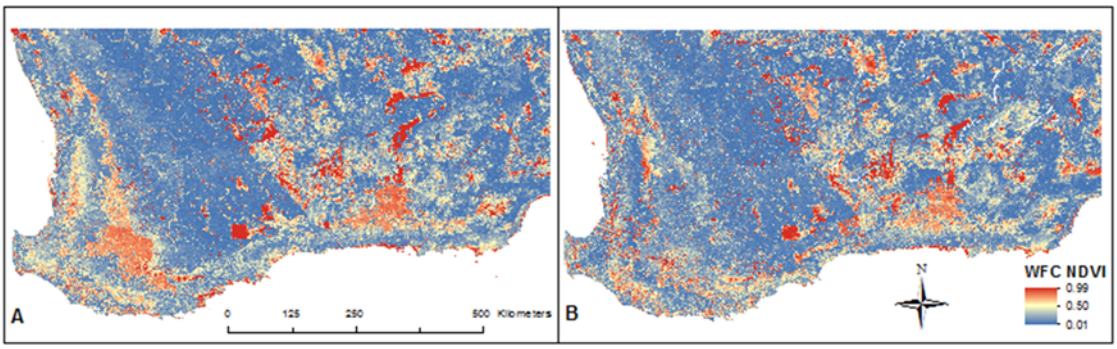

Figure 4.6 *Weighted Fuzzy Standardisation modelled data as stratified by a) IBRA Sub-regions and b) Land Zones.*

4.4.3. Compare seasonal influence on GO ecosystems

NDVI values for all land zones were standardised using a fuzzy membership function as described in section 4.3.5 and per season images were produced for each GO landscape. A monotonically decreasing sigmoidal fuzzy membership function was applied to transform the NDVI values to a 0 to 1 scale to stretch the reflectance values of all 275 datasets onto a same scale. Strongest response on GOs was identified in summer standardised images (Figure 4.7 and Table 4.5).

After standardising all factors to a common 0 to 1 scale using fuzzy membership functions, factor weights were given to all seasons in each group. The weights indicate a season's importance relative to all other factors and control how factors compensate for each other in each factor group.

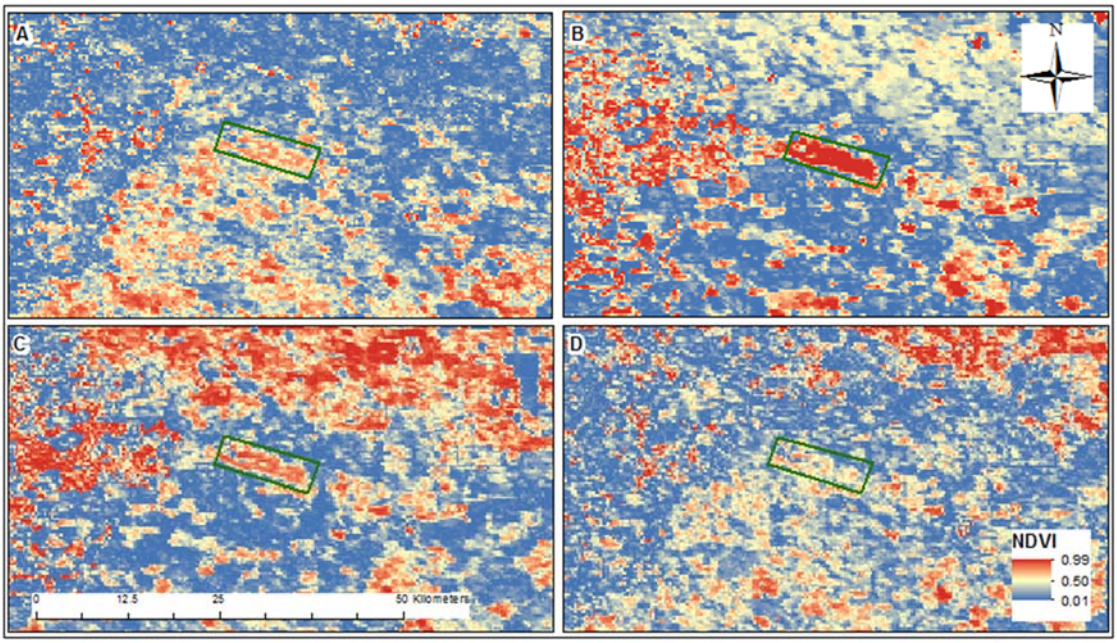

Figure 4.7 *Fuzzy standardised maps for Porongurup National Park (highlighted in green) for four seasons:*
A) Spring; B) Summer; C) Autumn; and D) Winter.

Table 4.5 *Summary of NDVI responses from GOs vs. surrounding landscape for Porongurup National Park. 100 samples were taken from the GO aprons and further 100 from surrounding landscape.*

	Granite Outcrop		**Surrounding Landscape**		
Season	$Median_{GO}$	$SDev_{GO}$	$Median_{LS}$	$SDev_{LS}$	P-value
Spring	0.51	0.24	0.46	0.27	0.21
Summer	0.68	0.21	0.02	0.05	<0.01
Autumn	0.65	0.23	0.02	0.06	<0.01
Winter	0.42	0.19	0.27	0.19	<0.01

4.4.3.1. Pairwise comparison

Summer was considered to be the most important season given the observation that the largest NDVI differences occurred between GOs and the surrounding landscape. This was followed by assigning weights to different seasons from the statistics above to highlight the summer/autumn contrast. The principal Eigenvector of the pairwise comparison matrix was used to derive the weights (Table 4.6). Using this method, the weights are interpreted as the average of all possible ways of comparing the criteria.

From Table 4.6 the criterion weight of 0.58 for summer indicates that summer is the most important criterion, followed by autumn, spring and winter.

The consistency ratio, expressing the degree to which comparisons form a consistent set of relationships was 0.01. Values < 0.1 are considered consistent (Saaty, 1979).

Table 4.6 *Pairwise comparison matrix based on the 9-point scale and derived weights for each season. Consistency ratio is 0.01 (see text).*

	Summer	Autumn	Spring	Winter	Weights
Summer	1	3	5	9	**0.58**
Autumn	1/3	1	2	6	**0.24**
Spring	1/5	1/2	1	4	**0.14**
Winter	1/9	1/6	1/4	1	**0.04**

4.4.4. Portray ecosystem greenspots that predict refugia

The fuzzified layers were multiplied by the weights and summed. Initially, this was done without stratification (Figure 4.3). In this scenario, areas of southern mesic forests, escarpment west of the Darling fault and the Stirling Ranges, which coincide with areas of higher precipitation, show the strongest responses in vegetation vigour. However, locations that have greener and more stable vegetation relative to their surrounds in the subdued parts of the landscape are mostly ignored. This is largely due to the moist forests of the Transitional Rainfall and Southeast Coastal provinces on the Albany-Fraser Orogen overpowering the response of the subdued environments of the Yilgarn Craton when modelled on a same scale of the median values.

To compensate for this, the study area was stratified using land zones and IBRA subregions prior to applying a weighted fuzzy standardisation (Figure 4.6). This way, median values were calculated per strata which vary markedly between mesic and semi-arid land strata, and strata of different soil composition. By stratifying the study area, all GO landscapes showed strong statistical response in terms of vegetation vigour.

All five GO landscapes stand out as areas where vegetation is greener and temporally more stable than that of the surrounding landscape. Stratifying area into land zones allowed GO aprons in semi-arid areas such as Chiddarcooping to show a strong response

(Figure 4.8b), rather than being subdued by high median values further south-west in the mesic southern forests. It also allowed GO aprons in the south-west forests to show a realistic response as it is compared to the median values to its immediate surroundings as in examples of Mount Frankland and Mount Chudalup (Figures 4.8c and 4.8d).

Porongurups (Figure 4.8e) stood out despite a very strong response from vibrant vegetation of the Stirling ranges located to the north. Stirling ranges are the highest mountain ranges in the SWAFR, and even though these are sedimentary formations (largely sandstone) it provides altitudinal refuge for vegetation. Porongurup National Park on the other hand are GOs of significantly lower altitude, but still strongly support vegetation on its aprons when compared to other areas of the Albany Sandplane zone.

Boyagin Nature Reserve (Figure 4.8a) also stood out significantly from its surroundings when the data were modelled based on the Eastern Darling Range zone means it largely occupies. Approximately 20% of the Reserve falls within Southern Zone of Rejuvenated Drainage to the north. This resulted in stronger NDVI response in the northern part of the reserve because of different NDVI means in that zone. However, relative response of both parts of the reserve is proportionally the same on GOs compared to its surroundings. Without stratification Boyagin falls into a background of the stronger response from more mesic areas to the west.

Low and open vegetation associated with shallow and rocky soils on and near GOs are dominant, usually covered with shrubs, lichen or moss mats. Vegetation types with similar structure can be found across the rainfall gradient. Taller and denser vegetation occurs further from GOs in more mesic parts of the region to the south and south-east, but in lower rainfall areas it is confined to narrow fringes near GOs.

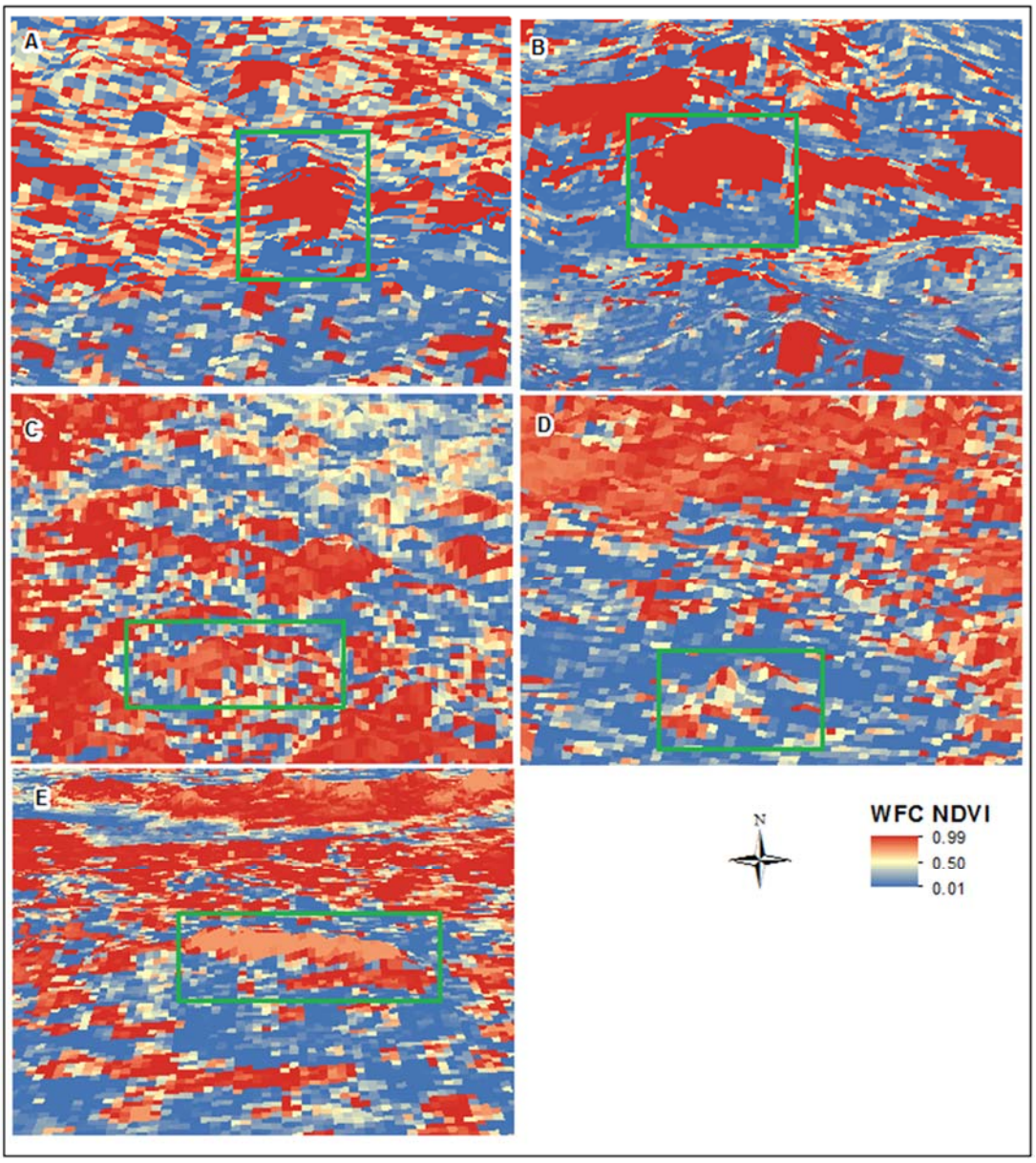

Figure 4.8 *Ecosystem greenspots modelled with weighted fuzzy standardisation technique with topography and land zones boundaries for the five GOs across the SWAFR: a) Boyagin, b) Chiddarcooping, c) Mount Frankland, d) Mount Chudalup, and e) Porongurups. Areas surrounding GOs are shown from a birds-eye view with an elevation exaggeration of four.*

4.4.5. ROC slicing validation

ROC analysis was applied to evaluate the model's performance and to ascertain the NDVI cut off values to threshold out moist stable environments from the wider landscape for both landscape stratifications used. Strategic thresholds of 100 random

samples of the weighted fuzzy combination modelled NDVI values were generated from each of the five GO landscapes and a further 100 from the surrounding landscapes to define the bins on a landscape scale for slicing thresholds. The ROC curves were constructed to threshold out greenspots from non-greenspots. ROC-based NDVI slicing show that threshold values for Land Zone stratification model are higher than those of the IBRA Subregion model for all sites (Table 4.7).

Table 4.7 *ROC-based NDVI slicing of the weighted fuzzy combination data modelled using Land Zone landscape stratification and Overall Kappa for all classes using the optimal cut-off NDVI values from ROC analysis to dichotomise aprons from surrounding landscapes.*

	Optimal cut-off values for Land Zone	**Overall Kappa**
Porongurup National Park	0.34	0.87
Boyagin Nature Reserve	0.15	0.90
Chidarcooping Nature Reserve	0.59	0.89
Mt Frankland National Park	0.57	0.95
Mt Chudalup	0.20	0.86

4.5. Discussion

This study provided a methodology to link long term vegetation vigour with the environment at landscape scale over both mesic and semi-arid climatic regions. The attempt was to objectively identify thresholds that unequivocally delineate refugia from non-refugia across the SWAFR covering the rainfall gradient using existing landscape stratifications. The results of the analysis suggest deterministic controls on the geographical distribution of potential refugia throughout the SWAFR.

GOs have been suggested as refugia during the periods of increased aridity that characterised the Pleistocene (Hopper et al., 1997; Byrne, 2008). Topographic sheltering on GOs, due to some combination of slope, aspect, and horizon shading, creates mesic microhabitats due to reduced potential evaporation as a result of lower levels of direct sun exposure (Laing & Hauck, 1997; Austin & Van Niel, 2011). Thus run-on locations at GO aprons are sites of more reliable surface or subsurface water flow.

If the geographic distribution of potential drought refugia is influenced more by deterministic factors that influence water availability than they are by stochastic factors (Hilbert et al., 2007), then they are more likely to continue to function as such under future climate change predictions (Game et al., 2011). This may be the case where the wetter conditions are due to topographic settings that are relatively stable and less likely to change as a function of climate (Dobrowski, 2011). Should projected climate change result in the surrounding region experiencing increased aridity with respect to average variance, then these sites will remain relatively wetter and continue to function as drought and fire refugia to some extent.

4.5.1. Identify if stratifying the region is needed

Whittaker et al. (2001) proposed a hierarchical framework for discussing the influence of different drivers on patterns of biodiversity. At continental to regional scales, climate is often a primary factor influencing the distribution of species (McGill, 2010). At regional to landscape scales, soils and topography tend to play stronger roles (e.g. Goldblatt, 1997; Ashcroft et al., 2009). At local scale the influences of biotic interactions and abiotic or biotic disturbances tend to become increasingly important (Lawler et al., 2015).

Heterogeneity in the physical environment occurs at a range of spatial and temporal scales, and some factors such as soil moisture, water chemistry and climate can vary even at small spatial scales (Wardell-Johnson & Horwitz, 2000). The forested ecosystems of SWAFR is dominated by three species of regionally distributed eucalyptus (Wardell-Johnson et al., 1997). However, the subdued and ancient SWAFR landscape also harbours pockets of refugial habitat that are dependent on fine-scale hydrological patterns persisting at local scale (Wardell-Johnson & Horwitz, 1996). Portrayal of floristic complexes by Mattiske and Havel (1998) over the Warren and Jarrah Forest Bioregions (Tille & Lantzke, 1990; Thackway & Cresswell, 1995) supports the need to recognise vegetation and environmental patterns at a finer than regional scale currently in use. Ecosystem greenspot modelling highlights this need in both the forested ecosystems in recognition of different vegetation types of floristic complexes within these forests, but also within the subdued semi-arid OSL landscapes.

Ecosystem greenspots were modelled across the SWAFR to predict geographical distribution of potential refugia using standardised NDVI data derived from multitemporal satellite imagery products. The approach is based on varying influences of different seasons, and coupling GIS with multicriteria evaluation techniques and fuzzy logic. Results indicated that stratifying landscape in more homogeneous units of underlying soils and geology is key to identifying ecosystem greenspots in a varied geographical region such as SWAFR on a landscape scale. Stratifying the region into homogeneous units has enabled identification of landscape-scale patterns of vegetation vigour and stability, and potential hotspots for refugia under projected anthropogenic climate change.

There was a direct relationship between rainfall gradient and vegetation vigour, suggesting that water availability is the major driver of vegetation structure in OSL environments. This relationship may be illustrated by the strong crown decline in response to the reduction in rainfall in recent years (Matusick et al., 2013), with a higher incidence of crown dieback on soils with lateritic profiles and low water holding capacity during the recent hot and dry summer seasons (Brouwers et al., 2013).

4.5.2. Identify which landscape stratification is most effective

Mapping of ecosystem greenspot patterns in situ temporal changes can highlight specific areas for potential conservation and protection. This combination of spatial and temporal analysis, particularly when landscape stratification is applied, enabled identification of vegetation patterns within a broader regional context. Ferrier (2002) suggested balancing heterogeneity between classes to improve effectiveness of classifications. Splitting region into classes of different landscape stratifications resulted in lower within-class dissimilarity (Ferrier et al., 2007; Rosauer et al., 2014), and correspondingly higher differential dissimilarity (Lawson et al., 2010).

Ecosystem greenspots mapping based on an index calculated from the fPAR (Mackey et al., 2012) is useful but impractical for landscape classification that include both mesic and semi-arid climatic regions. The approach demonstrated in this study seeks to bridge climatic influence between regions and the need to acquire observable landscape-level

patterns based on underlying geology, geomorphology and soils to more evenly balance dissimilarity levels on a landscape scale.

To examine scale effects in mapping vegetation data, Bedward et al. (1992) have proposed a 'homogeneity analysis' as the basis for determining optimal mapping scale. The approach demonstrated here showed that for vegetation data homogeneity analysis can be used to define the coarsest acceptable scale and to quantity the benefits of mapping at finer scales. Quantification of mapping ecosystems at a range of different scales would provide valuable information for deciding when and where to focus on mapping at a finer scale.

Overall, cumulative AUCs results from the ROC analyses show that subdividing the region into land zones prior to modelling the data provides the most accurate greenspot model (Table 4.6) except for Boyagin and Mount Chudalup. For Boyagin Nature Reserve, GO landscape is more prominent compared its surrounds when the region is stratified by IBRA Subregions. Boyagin is located on the western edge of the Avon Wheatbelt P2 Subregion where majority of the subregion surrounds is to the east of the GO in the semi-arid wheatbelt region. For land systems stratification, Boyagin is located on the western boundary of the Eastern Darling Range Zone where the surrounds are dominated by moist forests of the Darling Ranges.

Mount Chudalup is the most isolated and the smallest of the GO landscapes selected for this study, only 1 x 1.5 Km across. It is located within the Warren subregion and the Warren-Denmark Southland zone. Both strata are dominated by moist southern forests. This has resulted in Mount Chudalup GO landscape being less prominent when land stratifications are applied to data modelling. However, both these GO landscapes stood out from its surrounds with Land Zone stratification.

4.5.3. Compare seasonal influence on GO ecosystems

Strong seasonal oscillations in the vegetation growing season (May-July) across the SWAFR were identified, with maximum median NDVI values observed in winter and seasonal variations ranging from 13 to 28%. These strong relationships between vegetation vigour and climate indicate that the greenspot vegetation map may be used

to identify environmental constraints within the regional context for areas directly surrounding GOs.

As expected, seasonal differences had a significant influence on vegetation vigour and ground cover in areas located at and around GOs (Figure 4.5). This seasonal variation was accounted for when seasonal influence was adjusted with pairwise comparison approach in identification of ecosystem greenspots across the SWAFR.

The results also indicate that NDVI can provide a useful index of vegetation variability on seasonal and inter-annual time-scales. For the five GOs studied here, the results suggest that inter-annual variability of NDVI could show meaningful relationships with inter-annual climate variability, since the 12 year average, seasonal cycle, and inter-annual variability of NDVI reflect characteristics of the regional climate. Such correlations are the subject of a subsequent study (Chapter 5).

4.5.4. Portray ecosystem greenspots that predict refugia

The considerable variety of refugial habitats within the SWAFR have been discussed in detail (e.g. Wardell-Johnson & Horwitz, 1996; Byrne, 2008; Stewart et al., 2010; Keppel et al., 2012). These relatively undisturbed, moist habitats whether coastal flats, headwater streams, unconfined ground water or peat swamps provide conditions for refugial survival. Wardell-Johnson and Horwitz (2000) recognise at least ten types of habitat characteristics within SWAFR.

Currently, there is no substantive understanding of the patterns of biodiversity across the SWAFR (Reside et al., 2014). Thus an ecosystems modelling is needed to provide a map of the area's biogeographical patterns from an ecosystem perspective (Mackey et al., 2012). Mapping ecosystem greenspots using multitemporal satellite imagery across the rainfall gradient has provided a means of understanding spatial patterns within the landscape context that is an essential element of the identification of refugia (Keppel et al., 2012).

Vegetation vigour within the broader landscape in the mesic end of the gradient was more robust whilst more vigorous growth was confined to on-flow areas at the lower

rainfall end of the region. These on-flow areas have access to more water (Laing & Hauck, 1997), and consequently may also have unique microclimates resulting from the topography (Ashcroft & Gollan, 2013). Low and open vegetation is confined to GO aprons in the mesic end of the gradient, but is dominant on GO landscapes in the arid areas of the region.

Numerous stable environments were identified by modelling ecosystem greenspots across the SWAFR. Some of these stable environments can be attributed to the presence of GOs, but a presence of numerous other stable environments was also detected. The approach was applied to derive models for known GOs across the SWAFR that enabled delineation of key potential refugia locations. The five GOs selected for this study, which all fall within the areas of stable environments, are at least one type of ecosystems that provide additional resources for species to survive through periods of unfavourable conditions. This indicates that GOs exhibiting higher water gaining on-flow areas may facilitate biota persistence which is an important characteristic of refugia under projected climate change. However, vegetation at GO aprons in the open forests in the mesic south of the study area have access to moisture from deep, highly weathered lateritic soils that store a large proportion of winter rains (Macfarlane et al., 2010). As the water table further declines, forests on the shallowest soils of the region that have low water holding capacity, will be first affected (Poot & Veneklaas, 2013) further highlighting importance of GOs in supporting long term stability in these seemingly stable landscapes.

Ecosystem greenspots are well spread across major gradients of variation in both mesic and semi-arid climatic regions throughout the SWAFR. These greenspots are therefore likely to include a high proportion of all plant species occurring within the region (Pekin et al., 2012). This finding has important implications for the value of greenspots as priority areas for focusing conservation attention as they may predict as refugia within the region.

The physiographic settings and climatic processes that can potentially support refugia are widespread in areas of varied and complex terrain. Although the climatic processes that support refugia are common (e.g. cold-air drainage), their actual influence on in situ climate patterns may vary in degree and intensity depending on terrain position and

regional climatic context (Poot & Veneklaas, 2013). This means that many locations in landscapes can act as refugia, but the extent to which they maintain relict climates will vary in degree and duration. Areas with pronounced topoclimatic effects that are consistently decoupled from regional climate patterns will maintain relict climates for longer durations than sites that are tightly coupled to the free-air environment. This is evident at the Porongurup National Park where mean NDVI at the apron is similar to the mean NDVI values at GO's located in the mesic open forests indicating that Porongurups are potentially extending the range of the species further east from its normal distribution. It should be noted that further away from GOs, other constraints, such as waterlogging or salinity, may play part in lesser vegetation stability. Consequently, care is needed when extrapolating the relationship between rainfall and standardised vegetation vigour where the response to climate change may be very different.

Other environmental variables that were not considered in this study, e.g. the amount of water influx, soil depth and availability of rock fractures (Poot et al., 2012; Dalmaris et al., 2015), may also be important. The novelty of this approach is that it makes the relationships between environment and vegetation vigour spatially and temporally explicit at landscape scale over both mesic and semi-arid climatic regions, and reveals potential associated patterns in relation to predicted climate change.

Warmer and drier climate projections mean that some ecophysiological thresholds may be reached locally in areas due to spatial variation in topography and radiation (Austin & Van Niel, 2011). Future conservation management is therefore likely to focus on areas such as refugia surrounding GOs (Keppel & Wardell-Johnson, 2012), where biodiversity may be able to persist for longest (Keppel et al., 2012), although further testing of ecophysiological thresholds may be needed to confirm this.

5. DERIVING INTER-ANNUAL PHENOLOGIES TO PORTRAY MOIST REFUGIA ACROSS THE SWAFR

Abstract

Vegetation phenology is the study of plant history traits, such as emergence and senescence and how these relate to climatic variations and habitat characteristics. Vegetation phenology of annual plants corresponds most strongly to light, temperature and water availability. Phenological changes may, therefore, signal important year to year climatic variations or global environmental change. Phenological metrics that focus on the beginning and end of the growing season are related to the vegetation cover types characterised by changes in leaf density that are sufficient to be detected by remote sensing sensors. Here, the hypothesis that aprons near GOs across the SWAFR provide insulation from climatic fluctuations relative to the areas away from them is tested by assessing key phenological metrics. Temporal dynamics of peak and onset of greenness on aprons were compared with the surrounding landscape, and breaks in temperature and rainfall thresholds were identified from chronological clustering of climate data. Inter-annual phenologies of vegetation growth cycles were derived using continental time series of MOD13Q1: 16-day 250 m NDVI data for the first decade of the twenty-first century. MODIS pixels were selected that include *Eucalyptus diversicolor* (Karri) tall open forests from the aprons and *Eucalyptus marginata* (Jarrah) open forests from the non-apron sites. The approach was tested at the Porongurup Range and showed that GO aprons vegetation have longer growing season which starts earlier than at the surrounding landscapes as a direct result of additional resources and protection provided by GOs strongly indicating that spatial and temporal patterns of phenological metrics such as length of growing season and start of growing season are effective indicators of isolated refugia across the SWAFR. Results of chronological clustering showed that the total annual precipitation decreased since 2007 and the mean maximum annual temperature increased since 2005.

5.1. Introduction

Vegetation phenology is the study of plant emergence and senescence events and how these relate to interannual climatic variations and habitat characteristics (e.g. edaphic and altitudinal influences) (Jeganathan et al., 2010; Hmimina et al., 2013). A typical phenological pattern of native vegetation is a low rate of photosynthesis persisting in winter followed by a rapid increase to a maximum by late spring (Jump et al., 2010; Poot & Veneklaas, 2013). Phenological changes may, therefore, signal important year to year climatic variations or global environmental change (Verbesselt et al., 2010; Ma et al., 2013). Such signals are expected to be consistent across climatic zones for similar vegetation types (Prober et al., 2012; Sander & Wardell-Johnson, 2012) and any local differences may be indicative of ecological niches with specific habitat characteristics such as resource availability (Hopper, 2004; Pekin et al., 2012) and topographic protection (Wardell-Johnson & Williams, 1996; Tapper et al., 2014).

Differentiation of seasonal and decadal phenological patterns is an important component of global ecosystem monitoring (Reed et al., 1994; Ivits et al., 2012). Seasonal phenological patterns of plant communities typically follow annual cycles whilst decadal phenological markers are affected by seasonal climate fluctuations (e.g., temperature, rainfall) (Horion et al., 2013; Dalmaris et al., 2015) and/or anthropogenic influence (e.g., groundwater extraction, urbanisation) (White et al., 2002; Elmore et al., 2003). Over decades, seasonal phenologies may shift as a result of climate fluctuations and large scale anthropogenic disturbance (Potter et al., 2003; Bradley et al., 2007; Guerschman et al., 2015).

The use of satellite-derived vegetation indices (VI) is one way to study phenological patterns (Zhang & Goldberg, 2011; Ivits et al., 2013). Moderate resolution satellite remote sensing provides global high temporal frequency measurements of land surface properties and is therefore well suited for monitoring seasonal and decadal patterns and trends in local, regional and global phenology (De Beurs & Henebry, 2005; Fisher & Mustard, 2007). Remote sensing-based studies of phenology began with the Very High Resolution Radiometer (AVHRR) (Schwartz et al., 2002; Zhang et al., 2006) and has been significantly improved with the Moderate Resolution Imaging Spectroradiometer (MODIS) onboard the Earth Observing Systems Terra and Aqua platforms (Huete et al.,

2002; Zhang et al., 2003) in terms of spatial resolution (250 m to 1 km), spectral resolution (36 spectral bands), geolocation accuracy of 50 m at nadir (Wolfe et al., 2002), improved atmospheric correction and cloud screening (Heidinger et al., 2002), and sensor calibration (Justice et al., 1998). Time series of normalised difference vegetation index (NDVI) data have been used extensively for monitoring phenological patterns (e.g. Lloyd, 1990; Cihlar et al., 1996) on local (e.g. Sakamoto et al., 2005; Dobrowski, 2011), regional (e.g. Hill & Donald, 2003; Ahl et al., 2006; Morton et al., 2011) and global scales (e.g. Hutchinson et al., 2005; Heumann et al., 2007).

Phenological metrics are related to the vegetation cover types characterised by changes in leaf density that are sufficient to be detected by remote sensing sensors and have been the impetus for a variety of different studies (Ma & Veroustraete, 2006; Soudani et al., 2008). These metrics focus on the beginning and end of the growing season, that is, the beginning and end of the period of photosynthesis, respectively (Suzuki et al., 2003; Studer et al., 2007). For species that show less seasonal change the noise inherent to satellite based radiance measurements may mask the seasonal variations (Kaduk & Heimann, 1996; Moulin et al., 1997). This interference may explain the fact that few studies have been devoted to evergreen vegetation and that the potential use of remote sensing to monitor the seasonal dynamic of these biomes has not been sufficiently assessed. Despite the significant progress achieved over the last 15 years, there remains a strong need for an effective and unbiased assessment of the potential use of remotely sensed VI data to monitor vegetation phenology.

The first multi decadal continental scale ecosystem phenology study was conducted by Heumann at al. (2007), investigating changes and trends in vegetation phenology using the start and length of growing season. The same phenological metrics complemented by the base level and amplitude were used to monitor changes in vegetation phenology in e.g. northern Scandinavia (Beck et al., 2006), Italian peninsula (Simoniello et al., 2008), Mekong basin (Leinenkugel et al., 2013), or in the Sahel in north Africa (Fensholt et al., 2013). Alcantara et al. (2012) found that six phenology metrics improved classification accuracies of abandoned agricultural areas in eastern Europe when used in conjunction with NDVI time series by more than 8% over the use of NDVI data alone.

The SWAFR is characterised by the ancient granite-based landscapes of the Yilgarn Craton and Albany Fraser Orogen (Twidale, 1997). GOs are topographically complex in comparison to the subdued surrounding landscape (Porembski et al., 1997; Schut et al., 2014), are rich in biodiversity (Hopper et al., 1997; Keppel et al., 2012), and of great conservation importance in the region (Wardell-Johnson & Horwitz, 1996; Withers, 2000). GOs insulate vegetation from harsh climatic extremes across the SWAFR (Porembski & Barthlott, 2000; Byrne & Hopper, 2008). Fringe zones (aprons) that border GOs are thought to be influential in shaping vegetation patterns and contributing to plant survival and regeneration during periods of lower rainfall, high temperatures and fire (Yates et al., 2003).

Water distribution through channels around GOs is thought to be a contributing factor in plant survival (Laing & Hauck, 1997; Keppel & Wardell-Johnson, 2012). This water distribution and lower temperatures on Porongurup Range are linked to the survival of the *Eucalyptus diversicolor* (Karri) tall open forests (Specht, 1970) over a 100 km from their main habitat in the moist southern forests to the south-west of the SWAFR (Coates & Sokolowski, 1989; Inions et al., 1990). However, these observations are mostly inferential (Medail & Quezel, 1997, 1999) and no long-term quantitative study has yet been conducted to identify the influence and magnitude of such topographic protection across the SWAFR.

In this study, I sought to test the hypothesis that aprons near GOs provide insulation from climatic fluctuations relative to the areas away from them by assessing key phenological metrics. To this end, MODIS pixels were selected that include Karri tall open forests from the aprons and *Eucalyptus marginata* (Jarrah) (Boland & Johnston, 1984; Keighery, 1999) open forests from the non-apron sites at the Porongurup Range. Phenological metrics were examined at the regional scale. This longitudinal study provides a unique opportunity to estimate vegetation dynamics using phenological cycles and climate data over the first decade of the twenty-first century. Currently there are no studies focusing on the SWAFR that analysed either spatio-temporal changes in key phenometrics or calculated spatially-explicit trends in these phenometrics. Here I explore three specific aims and associated expectations.

a) Compare the growing season in apron vegetation with that in the surrounding landscapes. I expect the growing season in apron vegetation to start earlier and last longer than in the surrounding landscape.
b) Compare temporal dynamics of peak and onset of greenness on aprons with the surrounding landscape. I expect peak and onset of greenness on aprons to start earlier within years and show less variability with increasing temperature and lower rainfall conditions between years, than in the surrounding landscape.
c) Identify breaks in temperature and rainfall thresholds from chronological clustering. I expect breaks in temperature and rainfall thresholds to be reflected in key phenology metrics.

5.2. Study area and materials

5.2.1. Study area

The Porongurup Range is an ancient and largely weathered GO mountain range at the southern reaches of the SWAFR (Figure 5.1). The Range is 15 km from east to west and consists of granite peaks levelled into domes (Myers, 1997b). The highest point in the Range is 670 m whilst there are several other peaks above 600 metres which is about 400 metres above the surrounding plain. The Karri tall open forests (Specht, 1970) occur in the deep valleys and on the aprons of the range on deep red soils known as "karri loam" (Smith, 1962; Wardell-Johnson et al., 1997), whilst the predominant type of vegetation on lateritic soils downslope in the surrounding landscapes are mixed open forests of Jarrah and *Corymbia calophylla* (Marri) (Boland & Johnston, 1984; Keighery, 1999). The plains surrounding the Range have an annual rainfall of around 800 mm per year to the south and around 600 mm on the northern side (Bureau of Meteorology, 2015). Most of this rain falls between April and October, although light showers are common in the summer months. Summer temperatures on the plains average 26°C, whilst in winter temperatures average 16°C. Temperatures on the peaks are around 3°C lower than on the plains, and snow has occasionally fallen on the ranges (Bureau of Meteorology, 2015).

Karri is a eucalypt native to the wetter regions of the SWAFR (Wardell-Johnson & Williams, 2000). It is the dominant species in tall open-forest, and supports an extensive

ecosystem which is connected to the GOs of the lower south-west and the many subsequent creeks and rivers created from runoff. The understorey of karri forest is dense and may reach a height of 10 m, according to the conditions of the site and time since fire (Wardell-Johnson et al., 1997). Karri are generally confined to and dominate in the deep valleys between GOs surrounding the creeks with nutrient-poor, lateritic or loamy soils (Macfarlane et al., 2010). Jarrah is an endemic species of Eucalyptus within the SWAFR. It is dominant in the high rainfall zone with the trees more widely spread in the transitional rainfall zone towards the east (Boland & Johnston, 1984; Hingston et al., 1989). Because jarrahs are deep-rooted, as much as 40 metres, trees are drought resistant and able to draw water from great depths during dry periods (Wardell-Johnson et al., 1997). Schut et al (2014) established relationships between vegetation structure and environmental variables indicative of local resource availability and growth constraints in topographically complex areas such as Porongurup Range.

The Range has become more arid in the last 30 years, attributed to factors including natural climate variability such as ocean temperatures and atmospheric circulation (Delworth & Zeng, 2014). This trend is predicted to continue throughout the twenty-first century as a result of global climate change (Bureau of Meteorology, 2014). Long-term averages of rainfall allowed the detection of a sudden decrease in autumn and winter precipitation commencing in the 1990s. The region is expected to be drier and warmer with total reductions in autumn and winter precipitation of approximately 40% by the late twenty-first century (Hennessy et al., 2006). The Porongurup Range was selected for this study as the area is large enough to be studied with the MOD13Q1 composite gridded data.

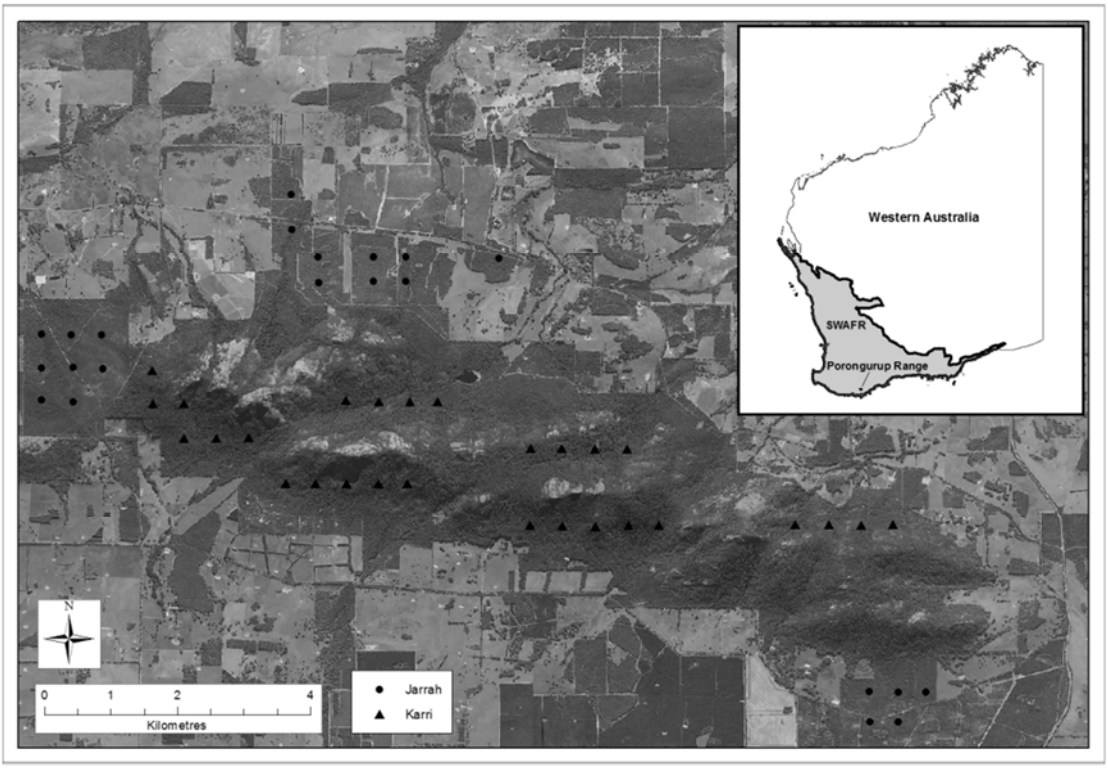

Figure 5.1 *Porongurup Range topography with locations of Karri tall open forest (Apron) and Jarrah open forest (Surrounding landscape).*

5.2.2. MODIS time-series data

Inter-annual phenologies of vegetation growth cycles were derived using time series of MODIS NDVI data. The MODIS Vegetation Index (VI) products are designed to provide consistent, spatial and temporal comparisons of global vegetation conditions that can be used to monitor photosynthetic activity (Justice et al., 1998). The NDVI is successful as a vegetation measure in that it is sufficiently stable to permit meaningful comparisons of seasonal and inter-annual changes in vegetation growth and activity. The continental time series of MOD13Q1: 16-day 250 m NDVI for years 2000 to 2012 were obtained through the Centre for Earth Resources Observation and Science (EROS). The MOD13Q1 NDVI values were built using the CVA-MVC algorithm on a 16-day compositing period described in Huete et al. (2002). The data are at 250 m spatial resolution and in 16-day time intervals resulting in 23 images per year. Each time series consists of a total of 276 observations (over 12 years). The MODIS NDVI data are computed from atmospherically corrected bi-directional surface reflectance that have been masked for water, clouds, heavy aerosols, and cloud shadows.

Externally derived errors in the time-series include cloud cover which persists in composited data (Ganguly et al., 2010) and can partially or fully mask ground reflectance causing lower than expected NDVI values. This is common in winter months when cloud cover is prevalent in mesic areas, but can occur at any time of year. Other errors include long-term NDVI changes due to sensor drift (Hmimina et al., 2013), which are partially accounted for in pre-processing (Roy et al., 2008; Ma et al., 2013), missing data for some dates in the time series, and unknown effects of short and long-term sensor degradation. As a result, a realistic function fitting must account for missing data and discount negative and anomalously low NDVI values. Although the examples shown here apply to MODIS NDVI data across the SWAFR, this function fitting analysis can be applied to any time series of VI data.

5.2.3. Rainfall and temperature

Daily rainfall and temperature records were obtained from the Australian Bureau of Meteorology (BoM) climate database, using the most proximate station to the type sites which had complete or near complete data records (Bureau of Meteorology, 2014, 2015). Only one rainfall and air temperature station in the vicinity of Porongurup Range, that of Mount Barker, had sufficient data for analyses. Rainfall is highly seasonal with up to 80% of the rain being recorded during a 6 month period from May to October. The average annual rainfall is 600 mm, with local maxima on the western escarpment in excess of 1000 mm (Timbal et al., 2006).

5.2.4. Verification sites

Two example landscapes were selected: a) apron landscapes (AL) supported by Karri tall open forests and b) surrounding landscapes (SL) dominated by Jarrah open forests to evaluate the effectiveness of the function fitting to the time series of remotely sensed MODIS NDVI data. Localities for both these landscape systems were determined from high resolution aerial images and in the field during summer season in 2013 and are distributed across and near the Porongurup Range (Figure 5.1). AL localities consist of six Karri locations containing a total of 28 MODIS pixels, and SL localities comprise five Jarrah locations containing a total of 22 pixels. Through the time series of data this

equates to 7728 pixels for AL landscapes and 6072 pixels for SL landscapes. ALs comprise many dependent understory species supported by Karri trees, which may not have a pronounced phenology (Figure 5.2). SLs dominated by Jarrah maintain significant leaf-level transpiration throughout the usually arid summer months in spite of considerable soil water deficit in the upper profile (Hingston et al., 1989) resulting in high amplitude, but asymmetric phenology with prolonged winter data gaps from cloud cover. Cloudiness and sensor noise make phenological markers difficult to identify in these examples.

5.2.5. Software

Idrisi Taiga (Clark Labs, 2012) was used to 1) extract the VI and the pixel reliability data; 2) reproject datasets from the original sinusoidal grid projection to Geocentric Datum of Australia of 1994 (GDA94) by allocating a 7.5 arc seconds to each 250 metres pixel for resampling of data following approach suggested by USGS (Danielson & Gesch, 2011).; 3) concatenate data extents to fit the study area; and 4) create blank files representing the missing data in the time series. Timesat was used to a) generate smooth time series of NDVI and to estimate the vegetation and phenology metrics; b) generate settings files for each metric; c) generate seasonality parameters files; and d) generate seasons to image files. ER Mapper (Hexagon Geospatial, 2015) was used to convert the season to image output files to a georeferenced image format. Command prompt was used to generate the lists of datasets in the time series required for processing in Timesat (Jönsson & Eklundh, 2004), while ArcGIS (ESRI, 2014) suite was used to a) identify and select relevant pixels in the data series; and b) produce final outputs and figures. Excel and SPSS (IBM, 2015) were used to produce comparison graphs of different phenology metrics parameters. Brodgar (Lohr et al., 2014) was used for chronological clustering.

5.3. Methods

A time-series of MODIS NDVI across the SWAFR were analysed and corrected to create a consistent dataset of vegetation phenology. A number of steps were identified to derive “onset of greenness” (a proxy for start of growing season) and “greener for longer” (a proxy for length of growing season) sites using landscape phenology. Firstly

NDVI and pixel reliability data were extracted from the original MODIS time-series (Paget & King, 2008). Then the pixel reliability data were used to remove bad pixels from the NDVI data, and replaced with averaged values from surrounding pixels. Selected NDVI data were then de-projected from the original sinusoidal projection to the GDA94 datum by allocating a 7.5 arc seconds to each 250 m pixel for resampling of data. Time-series of NDVI data were concatenated and clipped to fit the study area. Blank files corresponding to the dates of missing data in the time series were generated and inserted in place of missing data to fill the gaps in the time sequences, as it is needed for Timesat software to read time series data. Image files were generated as 16-bit integers with a little endian byte order. Each image consists of 1874 rows and 3408 columns totalling 6,386,592 pixels each. A list of all 276 datasets in the time series required for temporal analyses was then generated with command prompt.

5.3.1. Phenology patterns as indicators of refugia

The use of function fitting makes it possible to identify inter-annual phenological markers. Here, it is used to identify “onset of greenness” and “greener for longer sites”. Although the function fitting allows for a variety of methods for defining the onset of greenness, the onset and senescence of greenness were set using the timing of half maximum during spring growth because it is stable and consistent across ecosystems (White et al., 1997; Fisher et al., 2006). The half maximum has been used with spatially and temporally composited NDVI data and is defined as the time at which the NDVI value first exceeds the mid-point between minimum and maximum values during spring green-up. Maximum and minimum NDVI values on the inter-annual curve are identified and a half maximum value for each year was calculated. The date at which the half maximum value is exceeded during the spring green-up is set as the onset of greenness.

Following data preparation, Timesat software was used to generate smooth time-series of NDVI and to estimate the vegetation phenology metrics. A smooth continuous curve function with the Savitsky-Golay algorithm (Savitzky & Golay, 1964) was fitted to time series of NDVI data with an adaptive upper envelope to account for negatively biased noise such as cloud (Jönsson & Eklundh, 2002; Jönsson & Eklundh, 2004). These metrics were stored in separate settings files. Number of envelope iterations, adaptation strength, and fitting function window size were then assessed and set. Seasonality

metrics processing generated three outputs: a) seasonality parameters, b) fitted functions, and c) raw data together with corresponding index files for all pixels in all files in the time-series. It should be noted that this is a processing intensive task requiring over 12 hours to complete.

The function fitting method is based on two assumptions that: 1) NDVI time-series follow annual cycle of growth and decline; and 2) clouds and poor atmospheric conditions usually depress NDVI values, requiring that sudden drops in NDVI, which are not compatible with the gradual process of vegetation change, be regarded as noise and removed. The seasonality metrics are required to generate individual seasons to image outputs which are unique for a specific parameter (i.e. start of season) and for a specific time frame (i.e. year 2010). A total of 99 seasons to image files were generated, one for each extracted metric per year in the time series, minus last year in the time-series as the process requires data inputs on both sides of the resulting timeframe. The season to image outputs are generated as the binary grid (BIL) format.

The seasons to image output files were converted to a georeferenced image format (ers) and projected to GDA94 datum. For data conversion, a byte order was set as a little endian where the least significant value in the sequence is stored first to coincide with the original seasons to image output order. For projection, the bounding coordinates for time-series (corresponding to the study area extent) was set as -30, -35 for latitude and 114.5, 124.5 for longitude, and a cell (or pixel) size for both latitude and longitude was set at 0.002935 arc degree which coincides with a 250 m^2 MODIS pixels size to build a raster dataset. The resulting georeferenced images were then adjusted by stretching values with histogram equalise function to highlight phenology patterns to indicate isolated refugia sites.

5.3.2. Temporal dynamics of phenology

The seasonal cycle of plant community photosynthesis is described by the temporal variation of the photosynthetic capacity (PC). The PC is defined as the maximal gross photosynthetic rate when the environmental conditions (e.g. light, moisture, and temperature) are non-limiting for the time of a year under consideration (Gu et al., 2003). This definition takes into account the seasonal variation in climate and generally

assumes that the light intensity is at a saturating level and temperature is about 25°C regardless of the season under consideration. In contrast, the environmental conditions under which a particular value of the PC is realised depend on the time of the year. The composite function adequately representing the PC is given by Gu et al. (2003). The function is flexible and adequately fits the diverse seasonal cycles of plant community photosynthesis. It is capable of representing both the peak and onset of greenness metrics of the growing season.

Daily rainfall and temperature data were combined into Total Annual Rainfall and Mean Maximum Annual Temperature. The dates for the peak and onset of greenness were derived from the phenology metrics as described in section 5.3.1. The phenology graphs were generated for each pixel stack identified as either AL or SL landscape and averaged to produce a single graph for each. The two outputs were combined and graphed on the decadal time scale to identify temporal dynamics of phenology as it relates to annual rainfall and temperature. The graphs are compared with chronologically clustered rainfall and temperature data to reflect temporal response to climate.

5.3.3. Phenological responses to changing rainfall and temperature patterns

Chronological clustering was used to identify statistically significant break-points in the climate data and hence subsets of potentially significant points in the NDVI time-series data. Chronological clustering analysis identifies successional steps in climate data by identifying successional groups of data points (n>1) that are significantly different from other groups of data points occurring immediately before or after the group of interest (Legendre et al., 1985). Significantly different singletons (n=1) are identified as outliers. Results are generated at several significance-levels (α-levels) because continuous climatic succession or a single cluster of data points, rather than separate successional steps, is more likely to be identified at lower α-levels. Larger α-levels allow the identification of less significant chronological changes. The clustered rainfall and temperature climate data were compared with the temporal dynamics of phenology outputs to identify whether the climate change thresholds are reflected in the key phenology metrics.

5.4. Results

5.4.1. Phenology patterns as indicators of refugia

Onset of greenness from the average annual phenology occurs at calendar day 264 ± 6 S.D. in Karri landscapes, and 312 ± 11 S.D. in Jarrah landscapes. Peak NDVI for the AL locality pixels occurs at calendar day 182 ± 4 S.D. in Karri landscapes, and 207 ± 8 S.D. in Jarrah landscapes (Figure 5.2).

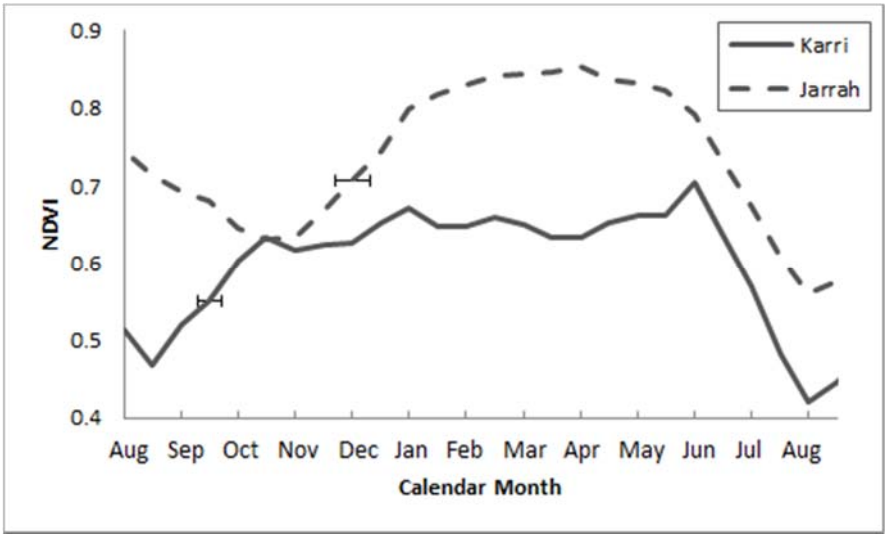

Figure 5.2 *Phenologies: Annual function fitting for Karri tall open forests (apron) and Jarrah open forests (surrounding landscape). The horizontal error bars show the location of onset of greenness and the spatial variability (S.D.) within the AL and SL localities.*

The large degree of spatial variability within the stable heterogeneous Karri supported landscapes (Figure 5.3) is a measure of the local ecosystem responsiveness to microclimatic effects. In sharp contrast, the smaller degree of spatial variability among the Jarrah landscapes SL localities is interpreted as due to the internal consistency of the average annual modelling algorithm. Although the AL and SL localities are distributed across and surrounding the Porongurup Range, in general standard deviations between AL and SL locality pixels are relatively small, indicating that similar land cover types respond similarly in an average year and are fit in a consistent manner.

Inter-annual variability for the length of the growing season (greener for longer sites) is illustrated spatially in Figure 5.4 for Porongurup Range, and Figure 5.5 across the SWAFR. Average length of the growing season for the AL was 186 days ± 16 S.D. in 2001, 178 ± 10 S.D. in 2004, 190 ± 8 S.D. in 2007, and 196 ± 12 S.D. in 2010. Average length of the growing season for the SL was 158 days ± 12 S.D. in 2001, 162 ± 8 S.D. in 2004, 1165 ± 10 S.D. in 2007, and 156 ± 14 S.D. in 2010. Topographic patterns within highly weathered Yilgarn Craton are also apparent (compare with Figure 5.1) with flat landscapes showing a shorter length of the growing season (Figure 5.5).

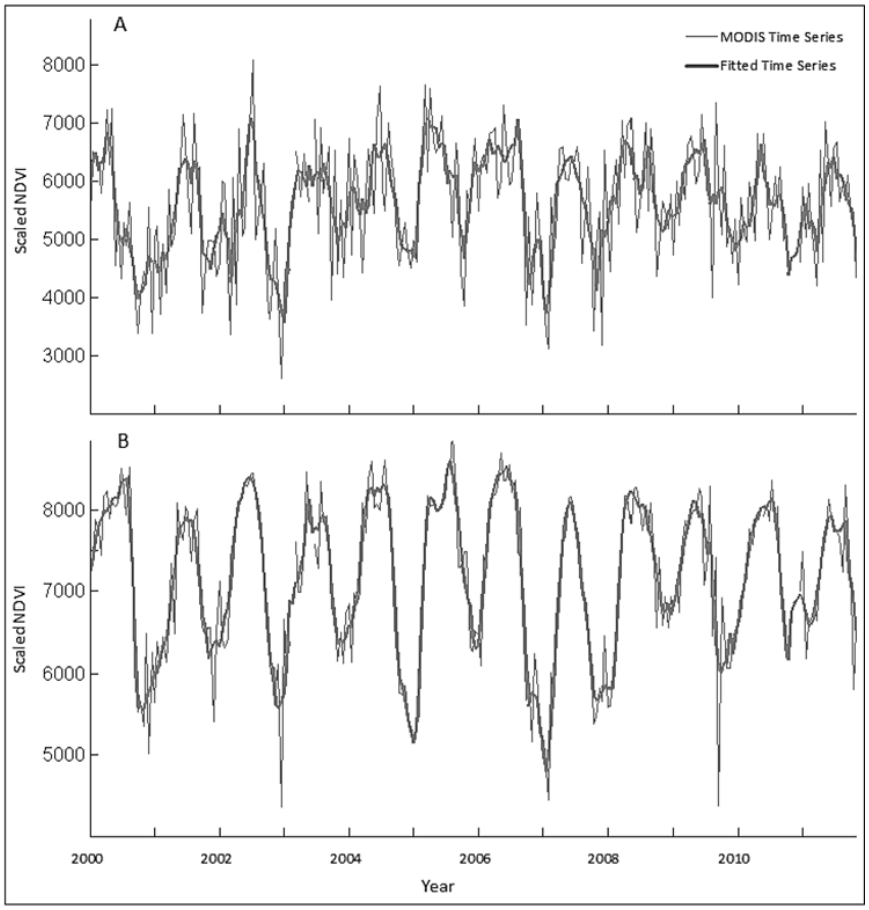

Figure 5.3 *Multi-year fitted MODIS time series at Porongurup Range: A) Karri tall open forest (apron), and B) Jarrah open forest (surrounding landscape).*

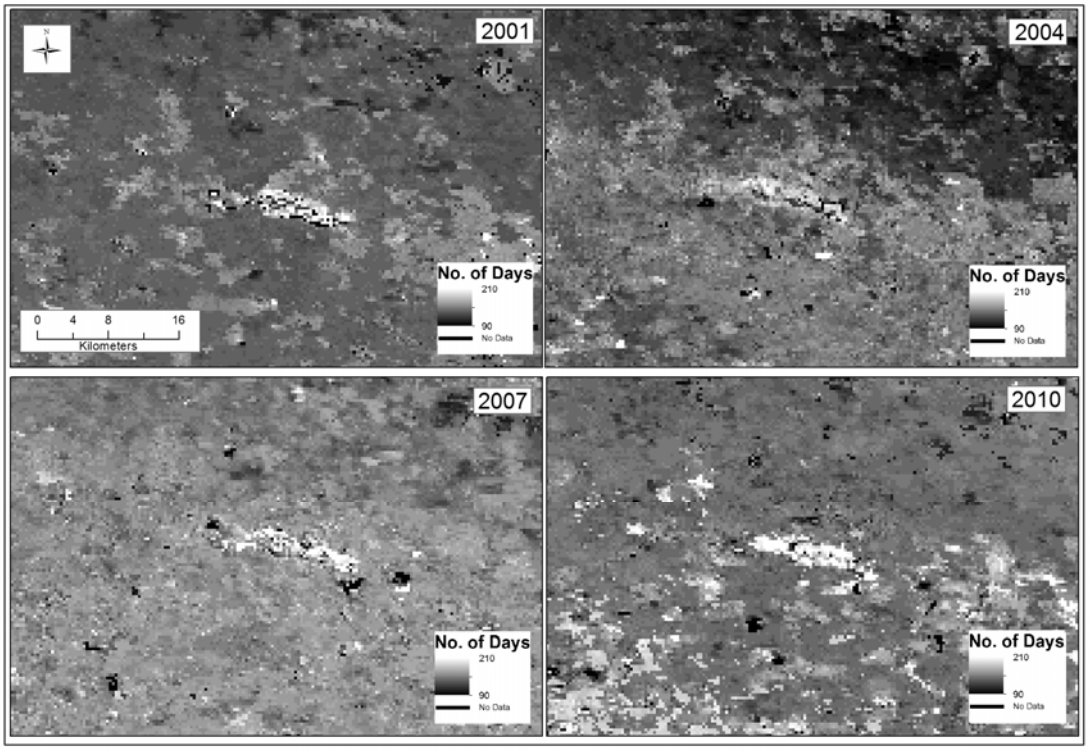

Figure 5.4 *Length of Season in days for 2001, 2004, 2007 and 2010 at Porongurup Range.*

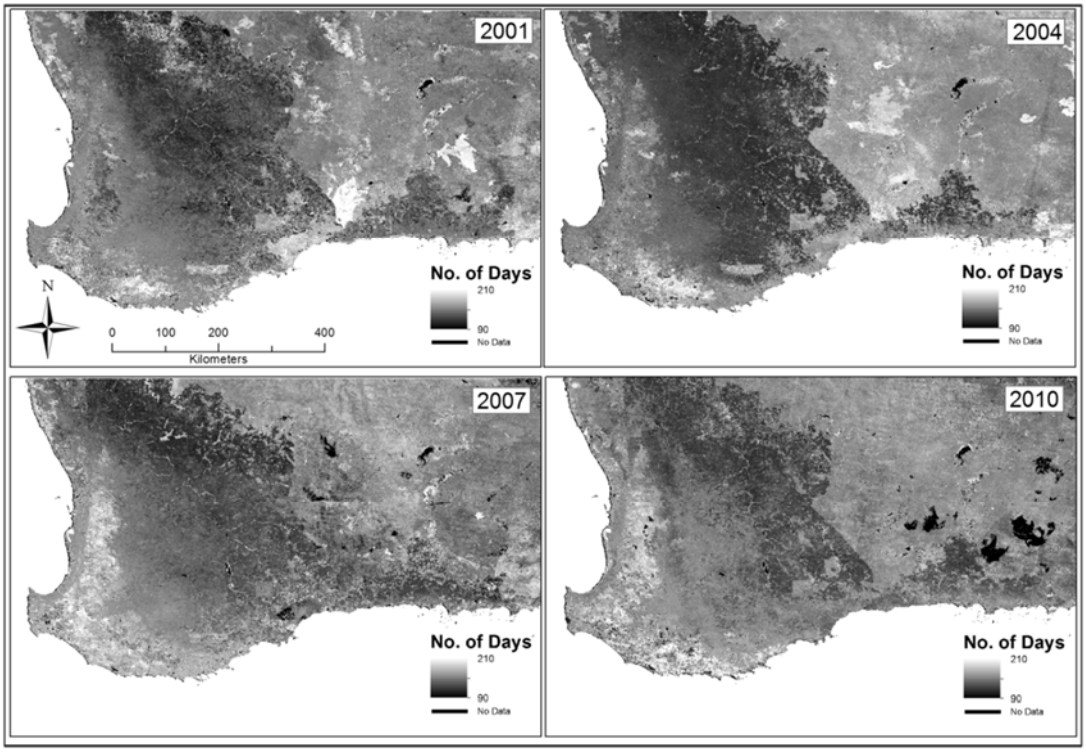

Figure 5.5 *Length of Season in days for 2001, 2004, 2007 and 2010 across SWAFR. Growing season was longest in 2007, while 2010 was so dry that many ecosystems in southern forests and south east had no detectable phenology.*

Inter-annual variability for onset of greenness is illustrated spatially in Figure 5.6 for Porongurup Range, and Figure 5.7 for the SWAFR. Average onset of greenness across the SWAFR was calendar day 278 ± 8 (late September) in 2001, 282 ± 12 (early October) in 2004, 274 ± 10 (late September) in 2007, and 259 ± 9 (mid-September) in 2010. Onset of greenness for the AL was calendar day 256 ± 10 (mid-September) in 2001, 268 ± 7 (late September) in 2004, 271 ± 12 (late September) in 2007, and 252 ± 8 (mid-September) in 2010. Topographic patterns are also apparent (compare with Figure 5.1), with SWAFR flat landscapes showing a later onset of greenness (Figure 5.7). In 2010, the driest of the four years, dry salt lakes and desert shrub systems in the eastern and south-eastern landscapes had such a low phenological response (<0.1 NDVI) that they were classified as unresolvable. The high degree of temporal variability apparent in the example pixels is present throughout the region.

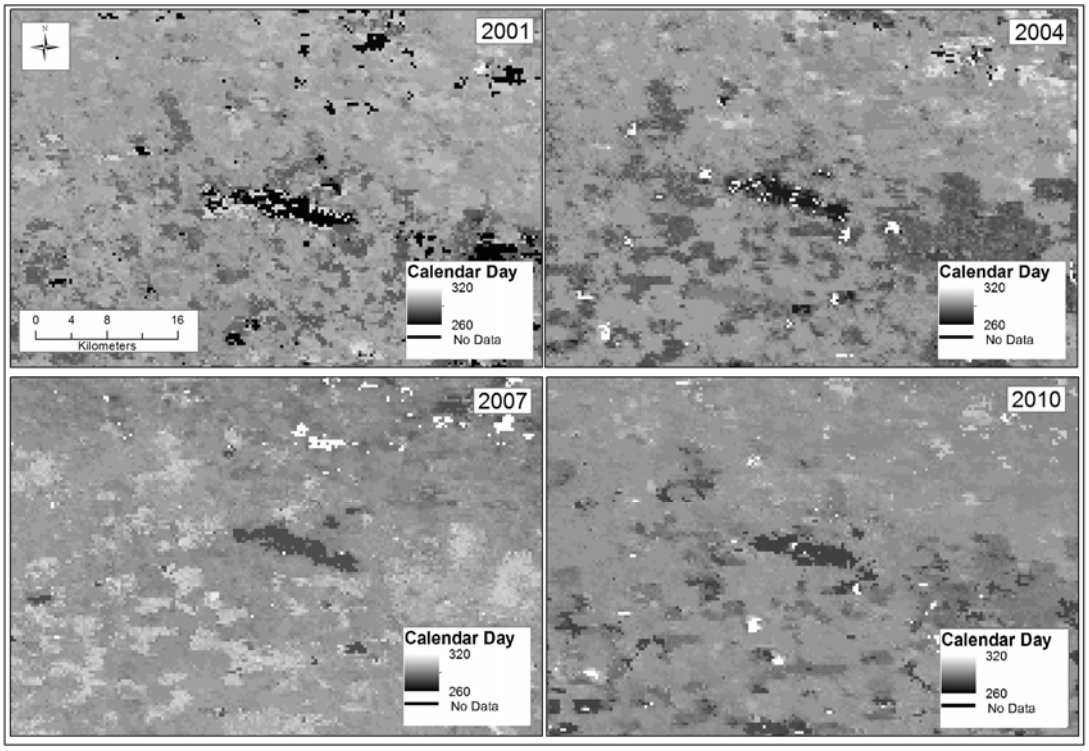

Figure 5.6 *Onset of greenness in calendar day for 2001, 2004, 2007 and 2010 at Porongurup Range.*

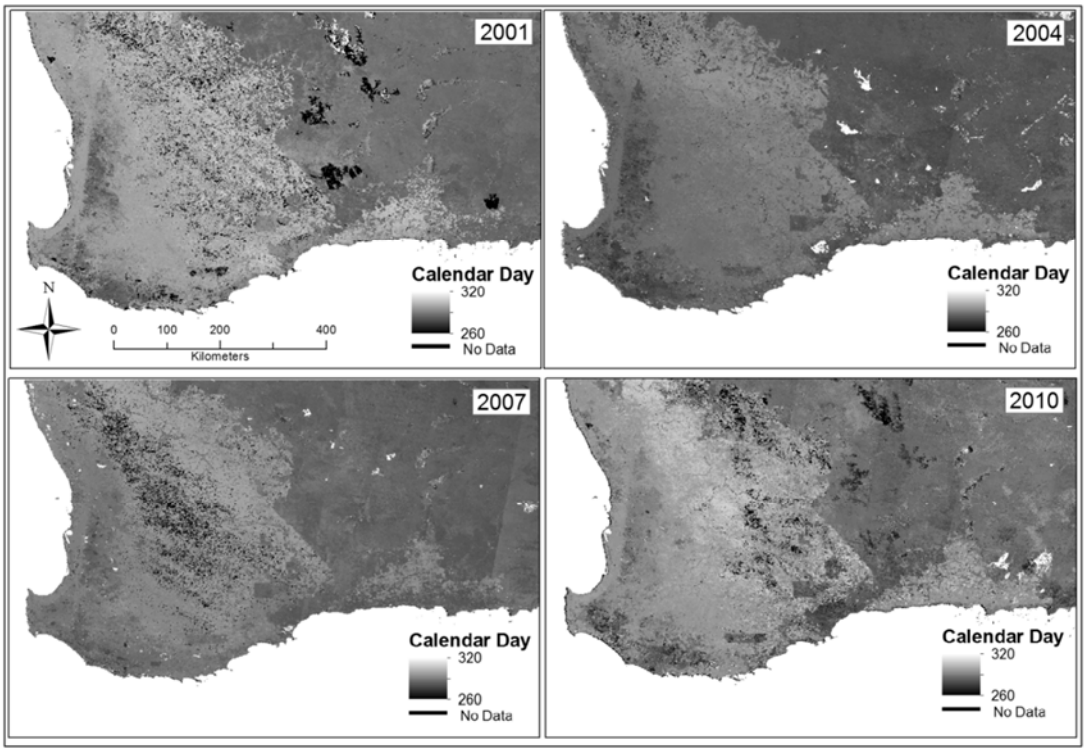

Figure 5.7 *Onset of greenness in calendar day for 2001, 2004, 2007 and 2010. Onset of greenness occurred earlier in 2010 compared to the earlier years.*

5.4.2. Temporal dynamics of phenology

For both Karri and Jarrah landscapes time series, the timing of the peak and onset of greenness are computed for each year as described in section 5.2.6. The results are summarised in Figure 5.8, along with cumulative precipitation and the mean maximum temperature data from the nearby weather station. Within the two example time series, inter-annual onset of greenness occurs respectively at calendar day 268 ± 6 S.D. in Karri landscapes, and 316 ± 8 S.D. in Jarrah landscapes (Figures 5.8A and 5.8B). Peak NDVI occurs at calendar day 186 ± 4 S.D. in Karri landscapes, and 212 ± 13 S.D. in Jarrah landscapes (Figures 5.8C and 5.8D). Clearly, inter-annual phenology is strongly affected by rainfall and to lesser degree temperature patterns in the SL.

Timing of onset of greenness, and the sites that are greener for longer (length of growing season) cannot be compared between original and fitted data because of the difficulty of defining phenological markers on unfitted data without spatial or temporal averaging. However, peak values are more readily identified in the original data and can be compared to the functions fits. Within the two original (observed) single time series, peak NDVI values are 0.72 in Karri landscapes, and 0.81 in Jarrah landscapes. Within the two fitted single time series, peak NDVI values are 0.69 Karri landscapes, and 0.78 in Jarrah landscapes. The similarity between original and fitted peak NDVI values indicates that the Savitzky-Golay function is fitting the upper envelope of data values.

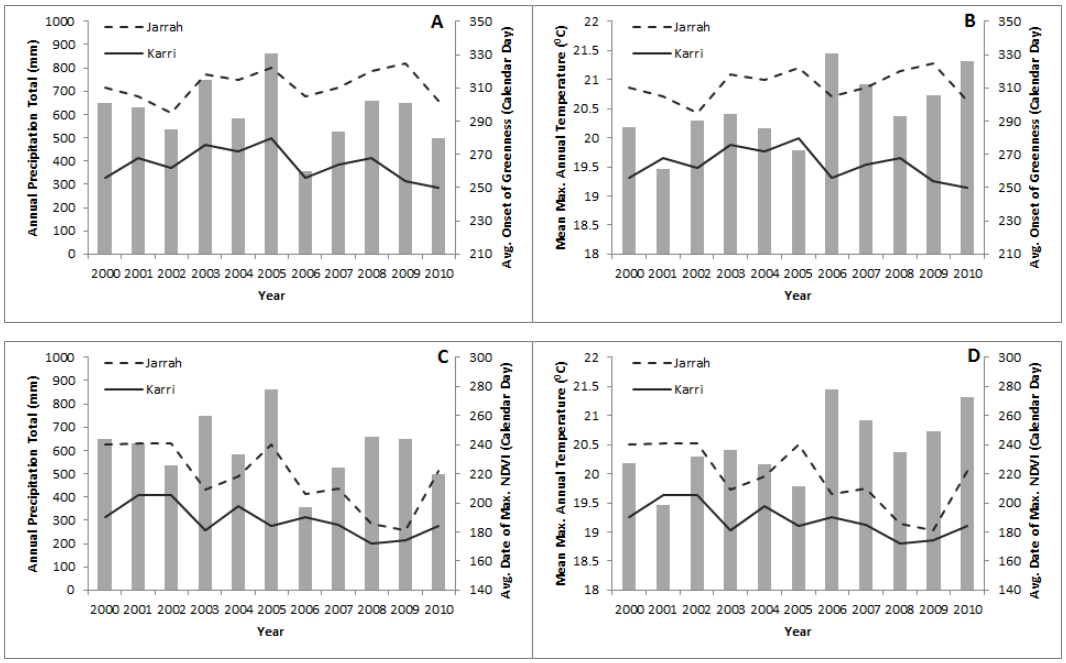

Figure 5.8 *Average onset of greenness with total annual rainfall (A) and mean maximum annual temperature (B); and average date of maximum NDVI with total annual rainfall (C) and mean maximum annual temperature (D) based on the function fitting results during the first decade of 21st century for pixels in the AL and SL locations. SL systems show high degree of temporal variability. Variability in onset of greenness likely reflects a temporal response to climate.*

5.4.3. Phenological responses to changing rainfall and temperature patterns

The chronological clustering analyses outputs were used to define statistically significant break-points in the climate data and hence link the potentially ecologically significant events in the time-series data to changing climate. Chronological clustering identified a break point in 2007 at α-levels 0.2 and 0.3 for total annual precipitation (Figure 5.9A) and a break in the mean maximum annual temperature in 2005 at the most significant α-level of 0.01 (Figure 5.9B), both pointing to a declining decadal trend, i.e. dryer and warmer conditions in the second half of the decade. This coincides with average onset of greenness occurring later in a year (Figures 5.8A and 5.8B) and lower peak NDVI values (Figures 5.8C and 5.8D) since 2005. The dry 2010 year (with below average rainfall) caused further decline in average peak and onset of greenness in SL landscapes (Figure 5.8).

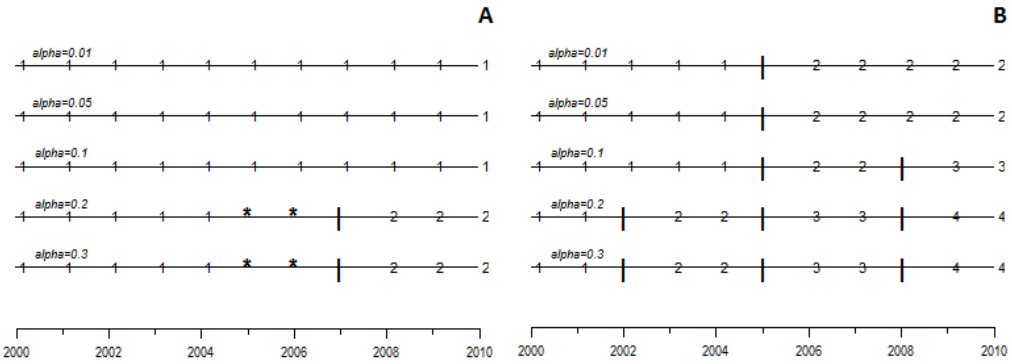

Figure 5.9 *Chronological clustering of a) total annual precipitation, and b) mean maximum annual temperature data at Porongurup Range. Numbers represent temporally similar groups. Vertical bars correspond to the start of a new group. Asterisks represent singletons that do not belong to the group immediately before or after it. Temperature clustering likely reflects response to climate change.*

Temporal variability in timing of both peak and onset of greenness between years in a single time series is much larger than spatial variability between SL localities. That is, similar land cover has a similar phenological pattern in a given year, but year to year phenological variability within a given land cover type may be very high.

5.5. Discussion

5.5.1. Phenology patterns as indicators of refugia

Phenological studies have demonstrated the impacts of climate change on biodiversity (e.g. causing the disturbance of onset of greenness cycles of plants) (Bertin, 2008; Dubovyk et al., 2015). The function fitting methodology presented here focused on deriving phenological markers at the spatial and temporal resolution of the original data by calculating inter-annual onset of greenness across the SWAFR. The methodology is robust to inter-annual variability and is a very effective procedure for focusing on the nature of longer-term trends in seasonality which may lead to improved land cover classification (Eckert et al., 2015). The methodology makes it possible to distinguish land cover trends at native remote sensor resolutions without need for temporal or spatial averaging (Chen et al., 2004). Without spatial or temporal averaging, ecosystem dynamics and long-term change can be more confidently identified and effectively

analysed (Leinenkugel et al., 2013). The results using time series of MODIS NDVI data demonstrate that the method provides realistic results that are geographically and ecologically consistent with the known behaviour of vegetation in this region. In particular, the MODIS-based phenology estimates show strong spatiotemporal patterns that depend on land cover type (Ganguly et al., 2010). As the methodology presented in this work treats each pixel individually without setting thresholds or empirical constants, the method is globally applicable.

An approach to fitting a function curve to time-series data has been shown to be effective across a range of land cover (White et al., 1997). The methodology presented here has the added advantages of modelling unequally spaced data and reducing the influence of no-value NDVI data during winter months. In the Porongurup Range, the Savitzky-Golay function fitting (Savitzky & Golay, 1964) used in this study is spatially consistent within land cover types. In an average year the fitted curve is similar between distributed landscapes of the same ecosystem. The standard deviations for timing of peak NDVI and onset of greenness for both the AL and SL localities were within the temporal resolution of the MODIS vegetation product (16 days) in both cases except Karri landscapes onset of greenness. The broader range of values in the Karri landscapes case can be attributed to earlier onset of greenness at two of the five Karri landscapes localities situated at the foot of the slopes. The small spatial variability observed for onset of greenness within particular land cover types at the Porongurup Range supports the utility of the function fitting as a tool for single-year phenology based land cover classifications.

Remote sensing derived vegetation phenological indicators can capture the spatial patterns of vegetation dynamics repetitively over vast areas (Jönsson & Eklundh, 2004), are directly related to key aspects of vegetation dynamism such as seasonality, productivity and inter-annual variation (Ma et al., 2013) and have a tremendous potential for the monitoring of the status and change of ecosystems (Chmielewski & Rötzer, 2001). Results show that remote sensing derived phenological metrics have a large potential in improving classifications that mostly rely on the spectral properties of the land covers because the functional information inherit in them supply additional details on the dynamism of these land covers (Leinenkugel et al., 2013).

5.5.2. Temporal dynamics of phenology

The function fitting is flexible enough to allow for shifts in timing of annual phenology (Bradley & Mustard, 2005). This point is illustrated by fluctuations in onset of greenness at the AL and SL localities (Figures 5.8A and 5.8B) as well as changes in the regional onset of greenness (Figures 5.6 and 5.7), which shifts by 29 days from as late as day 278 (5th October) in 2010 to as early as day 249 (6th September) in 2005. Local and regional shifts in phenology are likely a result of weather patterns. Heavy rains in 2005 enhanced and extended the growing season in Porongurup Range, while additional cloud cover delayed onset of greenness in SL. Temporal flexibility is also apparent in the range of onset of greenness and peak NDVI dates through time in the example pixels. Standard deviations of these phenological markers through time range from 8 to 12 days, a high degree of inter-annual variability compared to spatial variability estimated with the fitted function.

The high degree of phenological variability between years demonstrates the necessity of understanding the underlying cause of inter-annual variability when analysing land cover dynamics (Lunetta et al., 2006). The function fitting makes phenological variability easier to identify and thus is an effective tool for distinguishing temporal variability from land cover change (Soudani et al., 2008). The value of a function fitting result for regional studies cannot be overemphasised, as it allows for land cover change analysis at the native spatial and temporal resolutions of the sensor (Schwartz et al., 2002; Beck et al., 2008). Although the function fitting was applied to fit the variety of systems across the SWAFR, it has not been tested in systems with lower amounts of annual rainfall (below 500 mm). The application of this function fitting in other regions may require additional tuning of the function fitting metrics.

MODIS NDVI data were used to construct a phenological profile of and extract key phonological event dates from vegetation (Zhang et al., 2003; Dubovyk et al., 2015) across the SWAFR during a period of known climatic anomalies. Overall, the research findings support the use of the MODIS NDVI for this purpose, principally due to its sensitivity to chlorophyll content, a vegetation property that is a proxy for the physical and chemical alterations associated with change to phenological event timing (Heumann et al., 2007).

The use of satellite sensor data in phenological studies is increasingly recognised as a key component for understanding of the response of vegetation systems to climatic change (Bertin, 2008). Repeat observations from satellite-borne multispectral sensors provide a mechanism to move from plant-specific to regional scale studies of phenology (Ganguly et al., 2010). Here, it is advocated that the readily available MODIS NDVI and other multispectral sensors data should be considered for use along with understanding of the physical processes and computational approaches that determine the index values and how these may vary from those obtained using other vegetation indices.

The methodology presented here for function fitting long-term time series data models both average annual and inter-annual phenologies (Horion et al., 2013). In addition, the approach can accommodate irregularly spaced data with substantial data gaps. Further, the same function fitting metrics effectively model a range of land cover types (Hmimina et al., 2013). Although it is difficult to quantitatively compare fitted data to original data, the method clearly achieves the stated goals of fitting local maxima, capturing interannual variability, and remaining stable through data gaps and winter months. This approach can be applied to any time series of remotely sensed data and allows for consistent identification of phenological metrics (Tuanmu et al., 2010; Verbesselt et al., 2010). The function fitting modelling presented here, which provides identification of inter-annual phenological characteristics and defined average annual phenology, has significant potential for studies of local and regional phenology and long term land cover change as the south west of Western Australia has observed a drying climate trend.

5.5.3. Phenological responses to changing rainfall and temperature patterns

The results agree with findings of other authors (e.g. Badeck et al., 2004; Bertin, 2008; Ivits et al., 2012), concerning the influence of rising temperature on the timing of onset of greenness. In recent studies, an advanced timing of start of growing season between 2 and 4 days per degree was found (Beaubien & Freeland, 2000; Kramer et al., 2000). The result that an increase in mean maximum annual temperature of 1^0C is associated with an extension of growing season by 5 days in Europe coincide exactly with the

findings of White et al. (1999) for US stations. There is no doubt that a global warming will lead to changes in the length of growing season within certain limits (Chmielewski & Rötzer, 2001). This modelling showed that the extension of growing season was mainly influenced by an earlier onset of greenness. The end of growing season showed a lower variability across the SWAFR.

SWAFR is drying faster than other parts of the country and it will have a transforming effect on the habitats, and there will be an increased risk of bushfires (CSIRO et al., 2007; Smith et al., 2007). The driest year to date was 2010, however trends indicate that most years of this decade will exceed the dryness of 2010 (Trewin, 2013; Bureau of Meteorology & CSIRO, 2014). The region has become markedly drier, with a 15% reduction in rainfall since the mid-1970s (Macfarlane et al., 2010) which is attributed to increased greenhouse gases, natural climate variability, and land-use change (Wardell-Johnson et al., 2011).

In conclusion the phenological observations from multi-temporal NDVI measurements data allow for deriving information that is significant for i) assessment of inter and intra-annual vegetation dynamics across environmental gradients, ii) detection of the impact of precipitation and temperature variability, and iii) mapping of spatial patterns of productivity trends. Follow-up work in the region should investigate the relationship between climate and human-induced change using spatially-explicit reference data on known land-use activities.

6. SUMMARY AND RECOMMENDATIONS

6.1. Introduction

Remote sensing has considerable potential as a source of information on biodiversity at landscape and regional scales as it offers an inexpensive means of deriving complete spatial coverage of environmental information for large areas in a consistent manner that may be updated regularly. It therefore offers a contemporary way in which to derive the necessary information for spatial and temporal characterisation of landscapes surrounding GO's. Three kinds of information products that can be derived from temporal sequences of remote sensing data are demonstrated in the research of this thesis:

i) Multispectral imagery can be used to effectively map GOs masked with low growth cover across the SWAFR;
ii) Multitemporal imagery can assist with mapping greenspots across the landscape to isolate refugia; and
iii) Phenological metrics derived from multitemporal imagery can assist in separating GO apron from non-apron vegetation.

Discussions of these three modules of research are presented in this chapter, followed by conclusions and recommendations for further research and management implications.

6.2. Mapping GOs abundance

Chapter 3 studied the ways to develop a methodology for the rapid differentiation of GOs from other habitats at the regional scale of the southern Yilgarn Craton and western Albany-Fraser Orogen in south-west Western Australia. A novel methodology was developed that successively eliminates non-granite land covers (e.g. vegetated areas, bare soil) from further classification process using winter and summer imagery until only the granite class remains.

Previously developed methods for mapping rock types with remote sensing indicate that GOs have a distinct spectral reflectance when compared to other rock types (Rowan & Mars, 2003; Watts et al., 2005) and can be separated from native vegetation (Campbell et al., 2000). However, reflectance of granite is masked by a surface coverage of lichen, algae and mosses (Schut et al., 2010). Spectral characteristics of GOs are therefore dominated by this low growth cover in the visible and near infrared, and in the mid infrared range masking granite absorption features (Schut et al., 2010), and strongly reduces reflectance (Satterwhite et al., 1985).

Major advantage of this methodology over other approaches to map GOs is that it allows for separation of granite from both native and seasonal vegetation as well as bare sandy soil. The methodology is robust, relatively easy technique for mapping GOs that can be easily adapted to GOs with distal locations and thus is likely to be useful globally.

6.2.1. Conclusions and recommendations

There are NDVI changes on GOs due to the presence of lichen, algae and mosses growing on areas with granite at the surface. The methodology developed successfully used this characteristic to differentiate bare rock areas from its surroundings with a high accuracy (Kc > 0.77 in all tested areas). This is an improvement on findings from Campbell et al. (2000) who demonstrated that granite can be separated from native vegetation, but not sand and bare areas.

A multispectral ASTER data are widely used in geological studies to map different lithological units (Rowan & Mars, 2003). Most of these approaches rely on a large spectral Library which is available for ASTER data (Baldridge et al., 2009). ASTER data proved to be successful for identifying and mapping lithological units in well exposed areas (Rowan et al., 2005; van Ruitenbeek et al., 2006; Massironi et al., 2008). However, the availability of ASTER data over large areas and over different seasons is limited.

To separate granite from other cover types using the data from thermal sensors, the data acquisition needs to be targeted at periods when there are differences in the temperature of granite from its surroundings (Ninomiya et al., 2006). This approach could be very

effective for mapping granite on or near the surface but it would restrict image acquisition to a very specific window of opportunity in terms of temperature differences and cloud presence.

The methods presented in this study make it possible to map exposed granite surfaces not covered by vascular plants effectively, and with minimal cost. Using imagery from summer and winter, the majority of seasonal and native vegetation was masked. The maximum likelihood classifier was able to differentiate with only two classes, in line with findings of other binary classifiers (better classified than multiclass classifier). Initial thresholds were identified visually by assessing histograms, while the optimum thresholds required to separate vegetation from granitic and sandy surfaces were identified using ROC curves (Kerekes, 2008). The major advantage of this methodology is that it allows the differentiation of GOs from other environments, and hence enables low-cost and accurate mapping of GOs across the region. It has potential to be used to provide a more accurate and contemporary inventory of GOs at the landscape scale (Landsat TM) for the SWAFR than currently exists. This may enable more effective planning for the conservation of refugia in the areas surrounding GOs across the SWAFR.

A limitation of this approach is that potentially the margins of outcrops are excluded due to scattered vegetation coverage, and smaller outcrops are missed as insufficient bare granite areas are present. The potential improvement to overcome this shortcoming of the areas with dense cover on the outcrops that were missed out could be overcome by deploying a “grow region” algorithm where highlighted outcropping areas could be grown to the base where the outcrop flattens to show the full extent of outcrops with dense cover. The other approach that could potentially resolve the issue where smaller outcrops are being missed out could possibly be developed using an “object based image analysis” methodology which employs two main processes, segmentation and classification (Duro et al., 2012).

6.3. Ecosystem greenspots modelling to predict refugia in landscapes surrounding GOs

Chapter 4 implemented a novel approach for modelling greenspots by mapping of vegetation response over a twelve year period using multi-temporal MODIS NDVI data to identify potential refugia. The model implemented in this study revealed that:

i) Stratifying the region into available landscape subdivisions such as Land Zones or IBRA Subregions improves ecosystem greenspots mapping;
ii) Landscape stratification into Land Zones is better suited to map ecosystem greenspots than IBRA Subregions; and
iii) Landscape subdivisions enable data from localised context to be assessed on a landscape scale.

Previously developed methods on the east coast of Australia have identified potential ecosystem greenspots within the Great Eastern Ranges based on the fPAR over a ten year time period, stratified by major vegetation types (Mackey et al., 2012). This approach was tested in the region encompassing subtropical, temperate, and alpine thermal regimes, including ecosystems such as coastal forests and heathland, rainforests, alpine herbfields, and woodlands. The approach demonstrated in this study focused on the region that has become more arid in the last 30 years to bridge the climatic influence between landscapes and the need to acquire observable landscape-level patterns based on underlying geology, geomorphology and soils to more evenly balance dissimilarity levels on a landscape scale.

6.3.1. Conclusions and recommendations

This study demonstrates the utility of enabling standardised NDVI data derived from multitemporal satellite imagery products for identifying and mapping potential climate change refugia. Here, 39 distinct land zones strata (geophysical settings) were comprehensively mapped based on underlying geology, geomorphology and soil types (Tille et al., 1998). Within each geophysical setting, sites that had relatively more microclimates indicated by diverse topography and high standardised NDVI values were identified. High NDVI scoring sites had the greatest resilience to climate change,

and captured significantly more of the biodiversity sites than expected by chance ($p < 0.01$).

Vegetation around GOs is more stable compared to the surrounding landscape reflecting differences in geomorphology, additional resources linked to water influx and microclimates that can be associated with biodiversity found on GOs (Porembski et al., 1997). This enabled identification of areas where vegetation may be likely to persist for longest across the OSLs and not only limited to GO aprons, but including other fragmented landscapes such as wetlands, estuaries and groundwater dependent ecosystems, which provide safe havens for the biota under projected climate change. Because for every strata mapped the method identified sites that are most likely to retain species under a changing climate, it reveals natural strongholds for future conservation that would also capture substantial existing biodiversity.

Current recommendations for addressing climate change in conservation planning largely focus on predicting future habitats for individual species based on global environmental change modelling (Heller & Zavaleta, 2009; Austin & Van Niel, 2011). Many models assume that climatic conditions alone set range limits at both high and low extremes (Svenning & Condit, 2008) and fail to account for biogeographic factors such as persistence and spread from isolated refugia (Schauffler & Jacobson, 2002). The results from this study indicate that adding geology, geomorphology and soil types to the models might allow for more realistic results and in many cases narrower predictions of suitable habitat. This approach may be more effective in conserving biodiversity over long time scales.

The importance of microhabitats within old infertile soils for the biodiversity of south-west Australia's OSL has been previously demonstrated by Sander and Wardell-Johnson (2011a, 2011b). The findings from this study emphasise the role of GOs, in maintaining plant diversity within biodiversity hotspots. Although the climatic conditions differ between outcrops in this study from mesic to semi-arid, the results indicate that outcrops across the region have supported greater persistence of plant species throughout climatic changes, accentuating the value of these habitats to biodiversity conservation under future changing climate.

The role of refugia in the persistence of species during prolonged isolation in fragmented landscapes has been recognised across the world's arid zones, and in particular for the old, highly weathered Gondwanan landscapes of Australia, southern Africa, and South America (Morton et al., 2011). Fragmented refugia networks may play an important role in maintaining beta-diversity (Whittaker, 1977) over a broader geographic area, hence contributing to the resilience, stability and adaptive capacity of ecosystems (Thompson et al., 2009) facing anthropogenic climate change.

The approach demonstrated here provides a consistent and comprehensive means by which ecosystem greenspot mapping can predict refugia in OSLs globally in both mesic and semi-arid climatic regions at a landscape scale. This is useful in prioritising the allocation of conservation planning resources to these areas focusing on conserving threatened biogeographical regions rather than the individual species.

Vegetation dynamics monitoring from satellite measurements could lead to a better understanding of space-time variability in the OSLs ecosystems. Further work is needed to discriminate between these stable environments and to potentially further separate GO refugia from other environments that provide resources and shelter for species survival.

6.4. Deriving inter-annual phenologies to portray moist refugia across the SWAFR

Chapter 5 examined the hypothesis that aprons near GOs provide insulation from climatic fluctuations relative to the areas away from them by assessing key phenological metrics of environments on the Porongurup Range. The results revealed that:

i) The growing season in apron vegetation starts earlier and lasts longer than in the surrounding landscape;
ii) Peak and onset of greenness on aprons start earlier within years and show less variability with increasing temperature and lower rainfall conditions between years, than in the surrounding landscape; and
iii) Breaks in temperature and rainfall thresholds are reflected in key phenology metrics.

Phenology is a dominant and often overlooked aspect of plant ecology, from the scale of individuals to whole ecosystems. Global climate change could significantly alter plant phenology because temperature influences the timing of development. In areas that lack long-term ground-based phenological observations, deriving robust phenological models from multi-temporal NDVI measurements could be used to simulate past, present and future species phenology over wide areas, and these predictions could be compared with other remotely sensed data.

The function fitting modelling presented here illustrates techniques that can be used to evaluate the variability or stability of the phenology of land cover types. Further studies may experiment with different smoothing algorithms, use a longer time series of satellite data, assess effects of fire on NDVI between SL and AL environments and incorporate further climate data as they become available as the south west of Western Australia is observing a drying climate trend.

6.4.1. Conclusions and recommendations

Projections of climate change in Western Australia are indicating hotter and drier conditions. However, distribution of rainfall may be, as or more important than amount and is directly reflected in phenological changes, and alterations in the timing of phenological events are among the first responses at plant and ecosystem levels to climate change (Badeck et al., 2004).

Vegetation on the GO aprons have a longer growing season which starts earlier than at the surrounding landscapes as a direct result of additional resources and protection provided by GOs (Hill & Donald, 2003; Ganguly et al., 2010). This strongly indicates that spatial and temporal patterns of phenological metrics such as length of growing season and start of growing season are effective indicators of isolated refugia across the SWAFR.

The SWAFR is threatened by climate changes that are projected to have significant impacts on the quantity and variability of rainfall and affect key ecosystem drivers (e.g. fire regimes). Effective monitoring of the impact of climate change on biodiversity

(rather than individual species) requires a cross-disciplinary, coordinated, focused and integrated approach. Those refugia estimated capable of buffering climate change were mapped as likely areas to persist under future climate. The isolated persistent refugia may be flagged for conservation management as valuable areas providing landscape stepping stones and anchors to ecosystem resilience under climate change.

6.5. Conclusions and future directions

Remote sensing can be used to understand patterns and processes in relation to refugia on GOs by deriving multispectral views of the environment at multiple spatio-temporal scales, readily integrated with other forms of data (e.g., GIS layers and georeferenced observational data). It provides a means to characterise ecosystem dynamics and indicators to quantify ecosystem, habitat and microhabitat diversity. From this, in combination with ecosystem and niche modelling approaches, habitats and micro-habitats that are more likely to foster refugia can be identified, mapped, studied and monitored.

Climate change vulnerability is aggravated by the subdued topography of the SWAFR, further limiting opportunities for plant species to migrate to more favourable climatic conditions. Due to fine-scale associations with the environment, floristic diversity within the region appears to be highly vulnerable to future climate changes. This is confirmed by evidence of historical contractions of the Mediterranean-climate region of the SWAFR (Hopper & Gioia, 2004; Byrne & Hopper, 2008). Further contractions have been predicted within a recent global study (Klausmeyer & Shaw, 2009).

The findings of this study highlighted the conservation significance of GOs as valuable refugial habitats, reaffirming propositions by Byrne & Hopper (2008). GO habitats within the semi-arid and mesic zones are characterised by unique geographic and hydrological properties and could possibly continue to provide refugial habitat for the highly diverse flora in the future (Horwitz et al., 2008). Because of significant correlations between GO habitats and high diversity of species, these environments are highly vulnerable to future climatic changes.

REFERENCES

Ahl, D. E., Gower, S. T., Burrows, S. N., Shabanov, N. V., Myneni, R. B., & Knyazikhin, Y. (2006). Monitoring spring canopy phenology of a deciduous broadleaf forest using MODIS. *Remote Sensing of Environment, 104*(1), 88-95.

Alcantara, C., Kuemmerle, T., Prishchepov, A. V., & Radeloff, V. C. (2012). Mapping abandoned agriculture with multi-temporal MODIS satellite data. *Remote Sensing of Environment, 124*, 334-347.

Alibegovic, G., Schut, A. G. T., Wardell-Johnson, G. W., & Robinson, T. P. (2014). Seasonal differences assist in mapping granite outcrops using Landsat TM imagery across the Southwest Australian Floristic Region. *Journal of Spatial Science*, 1-13.

Allen, A., & Beetson, B. (1999). The Land Monitor Project; A multi-agency project of the Western Australian Salinity Action. *WALIS Forum*, 74-77.

Ashcroft, M. B. (2010). Identifying refugia from climate change. *Journal of Biogeography, 37*(8), 1407-1413.

Ashcroft, M. B., Chisholm, L. A., & French, K. O. (2009). Climate change at the landscape scale: predicting fine-grained spatial heterogeneity in warming and potential refugia for vegetation. *Global Change Biology, 15*(3), 656-667.

Ashcroft, M. B., & Gollan, J. R. (2013). Moisture, thermal inertia, and the spatial distributions of near-surface soil and air temperatures: Understanding factors that promote microrefugia. *Agricultural and Forest Meteorology, 176*(0), 77-89.

Ashcroft, M. B., Gollan, J. R., Warton, D. I., & Ramp, D. (2012). A novel approach to quantify and locate potential microrefugia using topoclimate, climate stability, and isolation from the matrix. *Global Change Biology, 18*(6), 1866-1879.

Austin, M. P., & Van Niel, K. P. (2011). Improving species distribution models for climate change studies: variable selection and scale. *Journal of Biogeography, 38*(1), 1-8.

Badeck, F.-W., Bondeau, A., Böttcher, K., Doktor, D., Lucht, W., Schaber, J., & Sitch, S. (2004). Responses of spring phenology to climate change. *New Phytologist, 162*(2), 295-309.

Baird, A. K. (1984). Rapid Discrimination of Granitic Rock Compositions by Low-Resolution Near-Infrared Reflectance. *J. Geophys. Res., 89*(B4), 2491-2496.

Baldridge, A. M., Hook, S. J., Grove, C. I., & Rivera, G. (2009). The ASTER spectral library version 2.0. *Remote Sensing of Environment, 113*(4), 711-715.

Barbosa, H. A., Huete, A. R., & Baethgen, W. E. (2006). A 20-year study of NDVI variability over the Northeast Region of Brazil. *Journal of Arid Environments, 67*(2), 288-307.

Bates, B. C., Hope, P., Ryan, B., Smith, I., & Charles, S. (2008). Key findings from the Indian Ocean Climate Initiative and their impact on policy development in Australia. *Climatic Change, 89*(3-4), 339-354.

Beard, J. S. (1984). Biogeography of the Kwongan. In: Pate, J.S. & Beard, J.S. (eds) Kwongan - plant life of the sandplain: biology of a south-west Australian shrubland ecosystem. (University of Western Australia Press: Nedlands, Western Australia), pp. 1–26.

Beard, J. S., Chapman, A. R., & Gioia, P. (2000). Species richness and endemism in the Western Australian flora. *Journal of Biogeography, 27*(6), 1257-1268.

Beaubien, E. G., & Freeland, H. J. (2000). Spring phenology trends in Alberta, Canada: links to ocean temperature. *International Journal of Biometeorology, 44*(2), 53-59.

Beck, P. S. A., Atzberger, C., Høgda, K. A., Johansen, B., & Skidmore, A. K. (2006). Improved monitoring of vegetation dynamics at very high latitudes: A new method using MODIS NDVI. *Remote Sensing of Environment, 100*(3), 321-334.

Beck, P. S. A., Wang, T. J., Skidmore, A. K., & Liu, X. H. (2008). Displaying remotely sensed vegetation dynamics along natural gradients for ecological studies. *International Journal of Remote Sensing, 29*(14), 4277-4283.

Bedward, M., Keith, D. A., & Pressey, R. L. (1992). Homogeneity analysis: Assessing the utility of classifications and maps of natural resources. *Australian Journal of Ecology, 17*(2), 133-139.

Bertin, R. I. (2008). Plant phenology and distribution in relation to recent climate change. *The Journal of the Torrey Botanical Society, 135*(1), 126-146.

Bishop, Y. M., Fienberg, S. E., & Holland, P. W. (1975). *Discrete Multivariate Analysis: Theory and Practice*. Cambridge, MA: MIT Press.

Blatt, H., & Tracy, R. (1997). *Petrology, Second Edition: Igneous, Sedimentary, and Metamorphic* (2 ed.). New York: W. H. Freeman.

Boland, D. J., & Johnston, R. D. (1984). *Forest Trees of Australia*. Melbourne: CSIRO Publishing.

Bradley, A. P. (1997). The use of the area under the ROC curve in the evaluation of machine learning algorithms. *Pattern Recognition, 30*(7), 1145-1159.

Bradley, B. A., Jacob, R. W., Hermance, J. F., & Mustard, J. F. (2007). A curve fitting procedure to derive inter-annual phenologies from time series of noisy satellite NDVI data. *Remote Sensing of Environment, 106*(2), 137-145.

Bradley, B. A., & Mustard, J. F. (2005). Identifying land cover variability distinct from land cover change: Cheatgrass in the Great Basin. *Remote Sensing of Environment, 94*(2), 204-213.

Brouwers, N., Matusick, G., Ruthrof, K., Lyons, T., & Hardy, G. (2013). Landscape-scale assessment of tree crown dieback following extreme drought and heat in a Mediterranean eucalypt forest ecosystem. *Landscape Ecology, 28*(1), 69-80.

Brown, A. P., Thompson-Dans, C., & Marchant, N. G. (1998). Western Australia's Threatened Flora. In D. o. C. a. L. Management (Ed.). Perth.

Bureau of Meteorology. (2014). Australian climate variability & change - Time series graphs. *Commonwealth of Australia, Canberra*.

Bureau of Meteorology. (2015). Climate Data Online. *http://www.bom.gov.au/climate/data/, (accessed 17.02.2015)*.

Bureau of Meteorology, & CSIRO. (2014). The State of the Climate report. *Commonwealth of Australia, Canberra*.

Burke, A. (2002). Properties of soil pockets on arid Nama Karoo inselbergs–the effect of geology and derived landforms. *Journal of Arid Environments, 50*(2), 219-234.

Byrne, M. (2008). Evidence for multiple refugia at different time scales during Pleistocene climatic oscillations in southern Australia inferred from phylogeography. *Quaternary Science Reviews, 27*(27–28), 2576-2585.

Byrne, M., & Hopper, S. D. (2008). Granite outcrops as ancient islands in old landscapes: evidence from the phylogeography and population genetics of Eucalyptus caesia (Myrtaceae) in Western Australia. *Biological Journal of the Linnean Society, 93*(1), 177-188.

Campbell, N. A., Hopper, S. D., & Caccetta, P. A. (2000). Mapping granite outcrops in the Western Australian wheatbelt using Landsat TM data. *Journal of the Royal Society of Western Australia, 83*, 109-113.

Charles, S. P., Silberstein, R., Teng, J., Fu, G., Hodgson, G., Gabrovsek, C., Crute, J., Chiew, F. H. S., Smith, I. N., Kirono, D. G. C., Bathols, J. M., Li, L. T., Yang, A., Donohue, R. J., Marvanek, S. P., McVicar, T. R., Van Niel, T. G., & Cai, W. (2010). Climate analyses for south-west Western Australia. *A report to the Australian Government from the CSIRO South-West Western Australia Sustainable Yields Project, CSIRO, Australia*, 83.

Chen, J., Jönsson, P., Tamura, M., Gu, Z., Matsushita, B., & Eklundh, L. (2004). A simple method for reconstructing a high-quality NDVI time-series data set based on the Savitzky-Golay filter. *Remote Sensing of Environment, 91*(3–4), 332-344.

Chiverrell, R. C., Thorndycraft, V. R., & Hoffmann, T. O. (2011). Cumulative probability functions and their role in evaluating the chronology of geomorphological events during the Holocene. *Journal of Quaternary Science, 26*(1), 76-85.

Chmielewski, F.-M., & Rötzer, T. (2001). Response of tree phenology to climate change across Europe. *Agricultural and Forest Meteorology, 108*(2), 101-112.

Christian, C. S., & Stewart, G. A. (1953). General Report on Survey of Katherine-Darwin Region. *CSIRO Land Research Series, 1*.

Cihlar, J., Ly, H., & Xiao, Q. (1996). Land cover classification with AVHRR multichannel composites in northern environments. *Remote Sensing of Environment, 58*(1), 36-51.

Cingolani, A. M., Renison, D., Zak, M. R., & Cabido, M. R. (2004). Mapping vegetation in a heterogeneous mountain rangeland using landsat data: an alternative method to define and classify land-cover units. *Remote Sensing of Environment, 92*(1), 84-97.

Clark Labs. (2012). IDRISI Taiga GIS and image processing software. *Clark University, Worcester, Massachusetts*.

Clark, R. N. (1999). Spectroscopy of Rocks and Minerals, and Principles of Spectroscopy, Manual of Remote Sensing. *Remote Sensing for the Earth Sciences, 3*, 3-58.

Coates, D. J., & Sokolowski, R. E. (1989). Geographic Patterns of Genetic Diversity in Karri (Eucalyptus diversicolor F. Muell.). *Australian Journal of Botany, 37*(2), 145-156.

Congalton, R. G. (1991). A review of assessing the accuracy of classifications of remotely sensed data. *Remote Sensing of Environment, 37*(1), 35-46.

Cowling, R. M., Rundel, P. W., Lamont, B. B., Kalin Arroyo, M., & Arianoutsou, M. (1996). Plant diversity in mediterranean-climate regions. *Trends in Ecology & Evolution, 11*(9), 362-366.

Cracknell, M. J., & Reading, A. M. (2014). Geological mapping using remote sensing data: A comparison of five machine learning algorithms, their response to variations in the spatial distribution of training data and the use of explicit spatial information. *Computers & Geosciences, 63*(0), 22-33.

CSIRO. (1983). Soils: an Australian viewpoint. *CSIRO Division of Soils, Melbourne*.

CSIRO, Bureau of Meteorology, & Department of Climate Change and Energy Efficiency. (2007). Climate change in Australia: technical report 2007. In CSIRO (Ed.), *Australian Climate Change Science Program* (pp. 148). Melbourne: Australian Climate Change Science Program.

Dalmaris, E., Ramalho, C. E., Poot, P., Veneklaas, E. J., & Byrne, M. (2015). A climate change context for the decline of a foundation tree species in south-western Australia: insights from phylogeography and species distribution modelling. *Annals of Botany*.

Danielson, J. J., & Gesch, D. B. (2011). Global Multi-resolution Terrain Elevation Data 2010 (GMTED2010) (Vol. 2011-1073). U. S. Department of the Interior: U. S. Geological Survey.

De Beurs, K. M., & Henebry, G. M. (2005). Land surface phenology and temperature variation in the International Geosphere–Biosphere Program high-latitude transects. *Global Change Biology, 11*(5), 779-790.

Dean, C., & Wardell-Johnson, G. (2010). Old-growth forests, carbon and climate change: Functions and management for tall open-forests in two hotspots of temperate Australia. *Plant Biosystems - An International Journal Dealing with all Aspects of Plant Biology: Official Journal of the Societa Botanica Italiana, 144*(1), 180-193.

Delworth, T. L., & Zeng, F. (2014). Regional rainfall decline in Australia attributed to anthropogenic greenhouse gases and ozone levels. [Letter]. *Nature Geoscience, 7*(8), 583-587.

Dobrowski, S. Z. (2011). A climatic basis for microrefugia: the influence of terrain on climate. *Global Change Biology, 17*(2), 1022-1035.

Dowling, T. I., Brooks, M., & Read, A. M. (2011). *Continental hydrologic assessment using the 1 second (30m) resolution Shuttle Radar Topographic Mission DEM of Australia*. Paper presented at the 19th International Congress on Modelling and Simulation, Perth.

Dubois, D., Prade, H., & Testemale, C. (1988). Weighted fuzzy pattern matching. *Fuzzy Sets and Systems, 28*(3), 313-331.

Dubovyk, O., Landmann, T., Erasmus, B. F. N., Tewes, A., & Schellberg, J. (2015). Monitoring vegetation dynamics with medium resolution MODIS-EVI time series at sub-regional scale in southern Africa. *International Journal of Applied Earth Observation and Geoinformation, 38*(0), 175-183.

Duch, W. (2005). Uncertainty of data, fuzzy membership functions, and multilayer perceptrons. *Neural Networks, IEEE Transactions on, 16*(1), 10-23.

Duro, D. C., Franklin, S. E., & Dubé, M. G. (2012). A comparison of pixel-based and object-based image analysis with selected machine learning algorithms for the classification of agricultural landscapes using SPOT-5 HRG imagery. *Remote Sensing of Environment, 118*, 259-272.

Eckert, S., Hüsler, F., Liniger, H., & Hodel, E. (2015). Trend analysis of MODIS NDVI time series for detecting land degradation and regeneration in Mongolia. *Journal of Arid Environments, 113*(0), 16-28.

Elmore, A. J., Mustard, J. F., & Manning, S. J. (2003). Regional patterns of plant community response to changes in water: Owens Valley, California. *Ecological Applications, 13*(2), 443-460.

ESRI. (2014). ArcMap 10.2. *ESRI (Environmental Systems Research Institute), Redlands, California*.

Fawcett, T. (2006). An introduction to ROC analysis. *Pattern Recognition Letters, 27*(8), 861-874.

Fensholt, R., Rasmussen, K., Kaspersen, P., Huber, S., Horion, S., & Swinnen, E. (2013). Assessing Land Degradation/Recovery in the African Sahel from Long-Term Earth Observation Based Primary Productivity and Precipitation Relationships. *Remote Sensing, 5*(2), 664-686.

Ferrier, S. (2002). Mapping Spatial Pattern in Biodiversity for Regional Conservation Planning: Where to from Here? *Systematic Biology, 51*(2), 331-363.

Ferrier, S., Manion, G., Elith, J., & Richardson, K. (2007). Using generalized dissimilarity modelling to analyse and predict patterns of beta diversity in regional biodiversity assessment. *Diversity and Distributions, 13*(3), 252-264.

Fielding, A. H., & Bell, J. F. (1997). A review of methods for the assessment of prediction errors in conservation presence/absence models. *Environmental Conservation, 24*(01), 38-49.

Fisher, J. I., & Mustard, J. F. (2007). Cross-scalar satellite phenology from ground, Landsat, and MODIS data. *Remote Sensing of Environment, 109*(3), 261-273.

Fisher, J. I., Mustard, J. F., & Vadeboncoeur, M. A. (2006). Green leaf phenology at Landsat resolution: Scaling from the field to the satellite. *Remote Sensing of Environment, 100*(2), 265-279.

Freund, J. E. (1984). Modern Elementary Statistics, Significance Tests (sixth edition ed., pp. 289). London: Prentice-Hall International.

Friedl, M. A., & Brodley, C. E. (1997). Decision tree classification of land cover from remotely sensed data. *Remote Sensing of Environment, 61*(3), 399-409.

Gallant, J. C. (2011). *The ground beneath your feet: digital elevation data for today and tomorrow*. Paper presented at the 19th International Congress on Modelling and Simulation, Perth.

Gallant, J. C., Read, A. M., & Dowling, T. I. (2012). *Removal of tree offsets from SRTM and other digital surface modles*. Paper presented at the International Archives of the Photogrammetry, Remote Sensing and Spatial Information Sciences, XXII ISPRS Congress, Melbourne.

Gallant, J. C., Wilson, N., Dowling, T. I., Read, A. M., & Inskeep, C. (2011). SRTM-derived 1 Second Digital Elevation Models Version 1.0. In G. Australia (Ed.). Canberra.

Game, E. T., Lipsett-Moore, G., Saxon, E., Peterson, N., & Sheppard, S. (2011). Incorporating climate change adaptation into national conservation assessments. *Global Change Biology, 17*(10), 3150-3160.

Ganguly, S., Friedl, M. A., Tan, B., Zhang, X., & Verma, M. (2010). Land surface phenology from MODIS: Characterization of the Collection 5 global land cover dynamics product. *Remote Sensing of Environment, 114*(8), 1805-1816.

Gentilli, J. (1972). *Australian climate patterns*. Melbourne: Thomas Nelson (Australia).

Geological Survey of Western Australia. (2008). ANZLIC Core Metadata Elements - Directory Item Report. 1:250 000 geological map - PERTH (SH50-14 and part SH50-13), first edition. *Geological Survey of Western Australia, Department of Minerals and Energy, East Perth*.

Gillespie, T. W., Foody, G. M., Rocchini, D., Giorgi, A. P., & Saatchi, S. (2008). Measuring and modelling biodiversity from space. *Progress in Physical Geography, 32*(2), 203-221.

Goldblatt, P. (1997). Floristic diversity in the Cape Flora of South Africa. *Biodiversity & Conservation, 6*(3), 359-377.

Good, P. I., & Hardin, J. W. (2003). Common errors in statistics (and how to avoid them) (pp. 254): John Wiley & Sons, Inc.

Gould, S. F., Hugh, S., Porfirio, L. L., & Mackey, B. (2014). Ecosystem greenspots pass the first test. *Landscape Ecology*, 1-11.

Gu, L., Post, W. M., Baldocchi, D., Black , T. A., Verma, S. B., Vesala, T., & Wofsy, S. C. (2003). *Phenology of vegetation photosynthesis. In: Schwartz , M. D. (Ed.) Phenology: An Integrated Environmental Science*. Dordecht.

Guerschman, J. P., Scarth, P. F., McVicar, T. R., Renzullo, L. J., Malthus, T. J., Stewart, J. B., Rickards, J. E., & Trevithick, R. (2015). Assessing the effects of site heterogeneity and soil properties when unmixing photosynthetic vegetation, non-photosynthetic vegetation and bare soil fractions from Landsat and MODIS data. *Remote Sensing of Environment, 161*, 12-26.

Hansen, J., Sato, M., Kharecha, P., Russell, G., Lea, D. W., & Siddall, M. (2007). Climate change and trace gases. *Philosophical Transactions of the Royal Society A: Mathematical, Physical and Engineering Sciences, 365*(1856), 1925-1954.

Heidinger, A. K., Venkata Rao, A., & Dean, C. (2002). Using MODIS to estimate cloud contamination of the AVHRR data record. *Journal of Atmospheric and Oceanic Technology, 19*(5), 586-601.

Heller, N. E., & Zavaleta, E. S. (2009). Biodiversity management in the face of climate change: A review of 22 years of recommendations. *Biological Conservation, 142*(1), 14-32.

Hennessy, K. J., Macadam, I., & Whetton, P. H. (2006). Climate Change Scenarios for Initial Assessment of Risk in Accordance with Risk Management Guidance (pp. 35): CSIRO, Canberra.

Heumann, B. W., Seaquist, J. W., Eklundh, L., & Jönsson, P. (2007). AVHRR derived phenological change in the Sahel and Soudan, Africa, 1982-2005. *Remote Sensing of Environment, 108*(4), 385-392.

Hexagon Geospatial. (2015). ERDAS ER Mapper. *Norcross, GA*.

Highland Statistics Ltd. (2013). Software Package for Data Exploration, Univariate Analysis, Multivariate Analysis and Time Series Analysis. *Newburgh, United Kingdom*.

Hilbert, D. W., Graham, A., & Hopkins, M. S. (2007). Glacial and interglacial refugia within a long-term rainforest refugium: The Wet Tropics Bioregion of NE Queensland, Australia. *Palaeogeography, Palaeoclimatology, Palaeoecology, 251*(1), 104-118.

Hill, M. J., & Donald, G. E. (2003). Estimating spatio-temporal patterns of agricultural productivity in fragmented landscapes using AVHRR NDVI time series. *Remote Sensing of Environment, 84*(3), 367-384.

Hingston, F. J., O'Connell, A. M., & Grove, T. S. (1989). Nutrient cycling in jarrah forest. In B. Dell, J. J. Havel & N. Malajczuk (Eds.), *The Jarrah Forest* (Vol. 13, pp. 155-177): Springer Netherlands.

Hmimina, G., Dufrêne, E., Pontailler, J. Y., Delpierre, N., Aubinet, M., Caquet, B., de Grandcourt, A., Burban, B., Flechard, C., Granier, A., Gross, P., Heinesch, B., Longdoz, B., Moureaux, C., Ourcival, J. M., Rambal, S., Saint André, L., & Soudani, K. (2013). Evaluation of the potential of MODIS satellite data to predict vegetation phenology in different biomes: An investigation using ground-based NDVI measurements. *Remote Sensing of Environment, 132*, 145-158.

Hoffmann, H., & Boehner, J. (1999). Spatial pattern recognition by means of representativeness measures. *Geoscience and Remote Sensing Symposium, 1999. IGARSS '99 Proceedings. IEEE 1999 International, 1*, 110-112 vol.111.

Hopper, S. D. (1979). Biogeographical Aspects of Speciation in the Southwest Australian Flora. *Annual Review of Ecology and Systematics, 10*(1), 399-422.

Hopper, S. D. (1992). Patterns of plant diversity at the population and species levels in south-west Australian mediterranean ecosystems. *In R.J. Hobbs (ed.). Biodiversity of Mediterranean Ecosystems in Australia*(Surrey Beattey & Sons, Sydney), 27-46.

Hopper, S. D. (2004). South-western Australia, Cinderella of the world's temperate floristic regions, 2. *Curtis's Botanical Magazine, 21*(2), 132-180.

Hopper, S. D. (2009). OCBIL theory: towards an integrated understanding of the evolution, ecology and conservation of biodiversity on old, climatically buffered, infertile landscapes. *Plant and Soil, 322*(1-2), 49-86.

Hopper, S. D., Brown, A. P., & Marchant, N. G. (1997). Plants of Western Australian granite outcrops. *Journal of the Royal Society of Western Australia, 80*, 141-158.

Hopper, S. D., & Gioia, P. (2004). The Southwest Australian Floristic Region: evolution and conservation of a global hotspot of biodiversity. *Annual Review of Ecology, Evolution, and Systematics, 35*(1), 623-650.

Horion, S., Cornet, Y., Erpicum, M., & Tychon, B. (2013). Studying interactions between climate variability and vegetation dynamic using a phenology based approach. *International Journal of Applied Earth Observation and Geoinformation, 20*(0), 20-32.

Horwitz, P., Bradshaw, D., Hopper, S. D., Davies, P., Froend, R., & Bradshaw, F. (2008). Hydrological changes escalates risk of ecosystem stress in Australia's threatened biodiversity hotspot. *Journal of the Royal Society of Western Australia 80*, 141-158.

Huete, A. R., Didan, K., Miura, T., Rodriguez, E. P., Gao, X., & Ferreira, L. G. (2002). Overview of the radiometric and biophysical performance of the MODIS vegetation indices. *Remote Sensing of Environment, 83*(1-2), 195-213.

Huete, A. R., & Saleska, S. R. (2010). Remote Sensing of Tropical Forest Phenology: Issues and Controversies. *International Archives of the Photogrammetry, 38*(8).

Hutchinson, M. F., McIntyre, S., Hobbs, R. J., Stein, J. L., Garnett, S., & Kinloch, J. (2005). Integrating a global agro-climatic classification with bioregional boundaries in Australia. *Global Ecology and Biogeography, 14*(3), 197-212.

IBM. (2015). R and SPSS software: Everyone wins. *Business Analytics, IBM Corporation, Software Group, Somers, NY*.

Inions, G., Wardell-Johnson, G., & Annels, A. (1990). Classification and evaluation of sites in karri (Eucalyptus diversicolor) regeneration 2. Floristic attributes. *Forest Ecology and Management, 32*(2–4), 135-154.

Ivits, E., Cherlet, M., Sommer, S., & Mehl, W. (2013). Addressing the complexity in non-linear evolution of vegetation phenological change with time-series of remote sensing images. *Ecological Indicators, 26*(0), 49-60.

Ivits, E., Cherlet, M., Tóth, G., Sommer, S., Mehl, W., Vogt, J., & Micale, F. (2012). Combining satellite derived phenology with climate data for climate change impact assessment. *Global and Planetary Change, 88–89*(0), 85-97.

Jeganathan, C., Dash, J., & Atkinson, P. M. (2010). Characterising the spatial pattern of phenology for the tropical vegetation of India using multi-temporal MERIS chlorophyll data. *Landscape Ecology, 25*(7), 1125-1141.

Jongman, R. H. G., Bunce, R. G. H., Metzger, M. J., Mücher, C. A., Howard, D. C., & Mateus, V. L. (2006). Objectives and Applications of a Statistical Environmental Stratification of Europe. *Landscape Ecology, 21*(3), 409-419.

Jönsson, P., & Eklundh, L. (2002). Seasonality extraction by function fitting to time-series of satellite sensor data. *Geoscience and Remote Sensing, IEEE Transactions on, 40*(8), 1824-1832.

Jönsson, P., & Eklundh, L. (2004). TIMESAT- a program for analyzing time-series of satellite sensor data. *Computers & Geosciences, 30*(8), 833-845.

Jump, A. S., Cavin, L., & Hunter, P. D. (2010). Monitoring and managing responses to climate change at the retreating range edge of forest trees. [10.1039/B923773A]. *Journal of Environmental Monitoring, 12*(10), 1791-1798.

Justice, C. O., Vermote, E., Townshend, J. R. G., DeFries, R., Roy, D. P., Hall, D. K., Salomonson, V. V., Privette, J. L., Riggs, G., Strahler, A., Lucht, W., Myneni, R. B., Knyazikhin, Y., Running, S. W., Nemani, R. R., Zhengming, W., Huete, A. R., Van Leeuwen, W., Wolfe, R. E., Giglio, L., Muller, J. P., Lewis, P., & Barnsley, M. J. (1998). The Moderate Resolution Imaging Spectroradiometer (MODIS): land remote sensing for global change research. *Geoscience and Remote Sensing, IEEE Transactions on, 36*(4), 1228-1249.

Kaduk, J., & Heimann, M. (1996). A prognostic phenology scheme for global terrestrial carbon cycle models. *Climate Research, 06*(1), 1-19.

Kasabov, N. K. (1996). Foundations of neural networks, fuzzy systems, and knowledge engineering (pp. 566). Cambridge, MA: MIT Press.

Keighery, G. (1999). A checklist of the vascular flora of the Porongurup National Park, Western Australia. *The Western Australian Naturalist, 22*(3), 137–158.

Keppel, G., Van Niel, K. P., Wardell-Johnson, G. W., Yates, C. J., Byrne, M., Mucina, L., Schut, A. G. T., Hopper, S. D., & Franklin, S. E. (2012). Refugia: identifying and understanding safe havens for biodiversity under climate change. *Global Ecology and Biogeography, 21*(4), 393-404.

Keppel, G., & Wardell-Johnson, G. W. (2012). Refugia: keys to climate change management. *Global Change Biology, 18*(8), 2389-2391.

Kerekes, J. (2008). Receiver Operating Characteristic Curve Confidence Intervals and Regions. *Geoscience and Remote Sensing Letters, IEEE, 5*(2), 251-255.

Klausmeyer, K. R., & Shaw, M. R. (2009). Climate Change, Habitat Loss, Protected Areas and the Climate Adaptation Potential of Species in Mediterranean Ecosystems Worldwide. *PLoS ONE, 4*(7), e6392.

Klein, C., Wilson, K., Watts, M., Stein, J., Berry, S., Carwardine, J., Smith, M. S., Mackey, B., & Possingham, H. (2009). Incorporating ecological and evolutionary processes into continental-scale conservation planning. *Ecological Applications, 19*(1), 206-217.

Kramer, K., Leinonen, I., & Loustau, D. (2000). The importance of phenology for the evaluation of impact of climate change on growth of boreal, temperate and Mediterranean forests ecosystems: an overview. *International Journal of Biometeorology, 44*(2), 67-75.

Laing, I. A. F., & Hauck, E. J. (1997). Water harvesting from granite outcrops in Western Australia. *Journal of the Royal Society of Western Australia, 80*, 181-184.

Lambers, H., Brundrett, M. C., Raven, J. A., & Hopper, S. D. (2010). Plant mineral nutrition in ancient landscapes: high plant species diversity on infertile soils is linked to functional diversity for nutritional strategies. *Plant and Soil, 334*(1-2), 11-31.

Lawler, J. J., Ackerly, D. D., Albano, C. M., Anderson, M. G., Dobrowski, S. Z., Gill, J. L., Heller, N. E., Pressey, R. L., Sanderson, E. W., & Weiss, S. B. (2015). The theory behind, and the challenges of, conserving nature's stage in a time of rapid change. *Conservation Biology, 29*(3), 618-629.

Lawley, E. F., Lewis, M. M., & Ostendorf, B. (2011). Environmental zonation across the Australian arid region based on long-term vegetation dynamics. *Journal of Arid Environments, 75*(6), 576-585.

Lawson, B. E., Ferrier, S., Wardell-Johnson, G., Beeton, R. J. S., & Pullar, D. V. (2010). Improving the assessment of species compositional dissimilarity in a "priori" ecological classifications: evaluating map scale, sampling intensity and improvement in a hierarchical classification. *Applied Vegetation Science, 13*(4), 473-484.

Legendre, P., Dallot, S., & Legendre, L. (1985). Succession of Species within a Community: Chronological Clustering, with Applications to Marine and Freshwater Zooplankton. *The American Naturalist, 125*(2), 257-288.

Leinenkugel, P., Kuenzer, C., Oppelt, N., & Dech, S. (2013). Characterisation of land surface phenology and land cover based on moderate resolution satellite data in cloud prone areas - A novel product for the Mekong Basin. *Remote Sensing of Environment, 136*, 180-198.

Lloyd, D. (1990). A phenological classification of terrestrial vegetation cover using shortwave vegetation index imagery. *International Journal of Remote Sensing, 11*(12), 2269-2279.

Lobo, J. M., Jiménez-Valverde, A., & Real, R. (2008). AUC: A Misleading Measure of the Performance of Predictive Distribution Models. *Global Ecology and Biogeography, 17*(2), 145-151.

Lohr, C., Van Dongen, R., Huntley, B., Gibson, L., & Morris, K. (2014). Remotely Monitoring Change in Vegetation Cover on the Montebello Islands, Western Australia, in Response to Introduced Rodent Eradication. *PLoS ONE, 9*(12), e114095.

Lunetta, R. S., Knight, J. F., Ediriwickrema, J., Lyon, J. G., & Worthy, L. D. (2006). Land-cover change detection using multi-temporal MODIS NDVI data. *Remote Sensing of Environment, 105*(2), 142-154.

Ma, M., & Veroustraete, F. (2006). Reconstructing pathfinder AVHRR land NDVI time-series data for the Northwest of China. *Advances in Space Research, 37*(4), 835-840.

Ma, X., Huete, A., Yu, Q., Coupe, N. R., Davies, K., Broich, M., Ratana, P., Beringer, J., Hutley, L. B., Cleverly, J., Boulain, N., & Eamus, D. (2013). Spatial patterns and temporal dynamics in savanna vegetation phenology across the North Australian Tropical Transect. *Remote Sensing of Environment, 139*(0), 97-115.

Macfarlane, C., Bond, C., White, D. A., Grigg, A. H., Ogden, G. N., & Silberstein, R. (2010). Transpiration and hydraulic traits of old and regrowth eucalypt forest in southwestern Australia. *Forest Ecology and Management, 260*(1), 96-105.

Mackey, B., Berry, S., Hugh, S., Ferrier, S., Harwood, T. D., & Williams, K. J. (2012). Ecosystem greenspots: identifying potential drought, fire, and climate-change micro-refuges. *Ecological Applications, 22*(6), 1852-1864.

Malatesta, L., Attorre, F., Altobelli, A., Adeeb, A., De Sanctis, M., Taleb, N. M., Scholte, P. T., & Vitale, M. (2013). Vegetation mapping from high-resolution satellite images in the heterogeneous arid environments of Socotra Island (Yemen). *Journal of Applied Remote Sensing, 7*(1), 073527-073527.

Massironi, M., Bertoldi, L., Calafa, P., Visonà, D., Bistacchi, A., Giardino, C., & Schiavo, A. (2008). Interpretation and processing of ASTER data for geological mapping and granitoids detection in the Saghro massif (eastern Anti-Atlas, Morocco). *Geosphere, 4*(4), 736-759.

Mattiske, E. M., & Havel, J. J. (1998). *Vegetation Complexes of the Southwest Forest Region of Western Australia*. Department of Conservation and Land Management. Perth, Western Australia.

Matusick, G., Ruthrof, K., Brouwers, N., Dell, B., & Hardy, G. J. (2013). Sudden forest canopy collapse corresponding with extreme drought and heat in a mediterranean-type eucalypt forest in southwestern Australia. *European Journal of Forest Research, 132*(3), 497-510.

McGill, B. J. (2010). Matters of Scale. *Science, 328*(5978), 575-576.

Medail, F., & Quezel, P. (1997). Hot-Spots Analysis for Conservation of Plant Biodiversity in the Mediterranean Basin. *Annals of the Missouri Botanical Garden, 84*(1), 112-127.

Medail, F., & Quezel, P. (1999). Biodiversity Hotspots in the Mediterranean Basin: Setting Global Conservation Priorities. *Conservation Biology, 13*(6), 1510-1513.

Merriam, D. F., Herzfeld, U. C., & Forster, A. (1996). Pairwise Comparison of spatial map data *Geologic Modeling and Mapping* (pp. 215-228): Springer US.

Michael, D. R., Lindenmayer, D. B., & Cunningham, R. B. (2010). Managing rock outcrops to improve biodiversity conservation in Australian agricultural landscapes. *Ecological Management & Restoration, 11*(1), 43-50.

Monserud, R. A., & Leemans, R. (1992). Comparing global vegetation maps with the Kappa statistic. *Ecological Modelling, 62*(4), 275-293.

Morgan, G., & Terrey, J. (1992). Nature conservation in western New South Wales. In N. P. Association (Ed.). Sydney.

Morton, S. R., Stafford Smith, D. M., Dickman, C. R., Dunkerley, D. L., Friedel, M. H., McAllister, R. R. J., Reid, J. R. W., Roshier, D. A., Smith, M. A., Walsh, F. J., Wardle, G. M., Watson, I. W., & Westoby, M. (2011). A fresh framework for the ecology of arid Australia. *Journal of Arid Environments, 75*(4), 313-329.

Moulin, S., Kergoat, L., Viovy, N., & Dedieu, G. (1997). Global-Scale Assessment of Vegetation Phenology Using NOAA/AVHRR Satellite Measurements. *Journal of Climate, 10*(6), 1154-1170.

Mücher, C. A., Klijn, J. A., Wascher, D. M., & Schaminée, J. H. J. (2010). A new European Landscape Classification (LANMAP): A transparent, flexible and user-oriented methodology to distinguish landscapes. *Ecological Indicators, 10*(1), 87-103.

Mucina, L., & Wardell-Johnson, G. W. (2011). Landscape age and soil fertility, climatic stability, and fire regime predictability: beyond the OCBIL framework. *Plant and Soil, 341*(1-2), 1-23.

Mulder, V. L., de Bruin, S., Schaepman, M. E., & Mayr, T. R. (2011). The use of remote sensing in soil and terrain mapping - A review. *Geoderma, 162*(1–2), 1-19.

Myers, J. S. (1997a). Geology of Granite. *Journal of the Royal Society of Western Australia, 80*, 87-100.

Myers, J. S. (1997b). Tectonic evolution of deep crustal structures in the mid-Proterozoic Albany-Fraser Orogen, Western Australia. In S. Sengupta (Ed.), *Evolution of Geological Structures in Micro- to Macro-scales* (pp. 473-485): Springer Netherlands.

Myers, N., Mittermeier, R. A., Mittermeier, C. G., da Fonseca, G. A. B., & Kent, J. (2000). Biodiversity hotspots for conservation priorities. *Nature, 403*(6772), 853-858.

Nagendra, H. (2001). Using remote sensing to assess biodiversity. *International Journal of Remote Sensing, 22*(12), 2377 - 2400.

Nakashima, T., Schaefer, G., Yokota, Y., & Ishibuchi, H. (2007). A weighted fuzzy classifier and its application to image processing tasks. *Fuzzy Sets and Systems, 158*(3), 284-294.

Neigh, C. S. R., Tucker, C. J., & Townshend, J. R. G. (2008). North American vegetation dynamics observed with multi-resolution satellite data. *Remote Sensing of Environment, 112*(4), 1749-1772.

Ninomiya, Y., Fu, B., & Cudahy, T. J. (2006). Corrigendum to "Detecting lithology with Advanced Spaceborne Thermal Emission and Reflection Radiometer (ASTER) multispectral thermal infrared "radiance-at-sensor" data" [Remote Sensing of Environment 99(1–2):127–139 (2005), ASTER special issue]. *Remote Sensing of Environment, 101*(4), 567.

Paegelow, M., & Camacho Olmedo, M. T. (2008). *Modelling environmental dynamics*. Berlin: Springer-Verlag.

Paget, M. J., & King, E. A. (2008). MODIS land data sets for the Australian region. *CSIRO Marine and Atmospheric Research Canberra*.

Pekin, B. K., Boer, M. M., Wittkuhn, R. S., Macfarlane, C., & Grierson, P. F. (2012). Plant diversity is linked to nutrient limitation of dominant species in a world biodiversity hotspot. *Journal of Vegetation Science, 23*(4), 745-754.

Peterson, A. T., Papes, M., & Soberon, J. (2008). Rethinking receiver operating characteristic analysis applications in ecological niche modeling. *Ecological Modelling, 213*(1), 63-72.

Pontius Jr, R. G., & Schneider, L. C. (2001). Land-cover change model validation by an ROC method for the Ipswich watershed, Massachusetts, USA. *Agriculture, Ecosystems & Environment, 85*(1–3), 239-248.

Pontius, R. G., & Parmentier, B. (2014). Recommendations for using the relative operating characteristic (ROC). *Landscape Ecology, 29*(3), 367-382.

Poot, P., Hopper, S. D., & van Diggelen, J. M. H. (2012). Exploring rock fissures: does a specialized root morphology explain endemism on granite outcrops? *Annals of Botany, 110*(2), 291-300.

Poot, P., & Veneklaas, E. J. (2013). Species distribution and crown decline are associated with contrasting water relations in four common sympatric eucalypt species in southwestern Australia. *Plant and Soil, 364*(1-2), 409-423.

Porembski, S., & Barthlott, W. (2000). Granitic and gneissic outcrops (inselbergs) as centers of diversity for desiccation-tolerant vascular plants. *Plant Ecology, 151*(1), 19-28.

Porembski, S., Seine, R., & Barthlott, W. (1997). Inselberg vegetation and the biodiversity of granite outcrops. *Journal of the Royal Society of Western Australia, 80*, 193-199.

Potter, C., Tan, P.-N., Steinbach, M., Klooster, S., Kumar, V., Myneni, R., & Genovese, V. (2003). Major disturbance events in terrestrial ecosystems detected using global satellite data sets. *Global Change Biology, 9*(7), 1005-1021.

Pressey, R. L., Cabeza, M., Watts, M. E., Cowling, R. M., & Wilson, K. A. (2007). Conservation planning in a changing world. *Trends in Ecology & Evolution, 22*(11), 583-592.

Prober, S. M., Thiele, K. R., Rundel, P. W., Yates, C. J., Berry, S. L., Byrne, M., Christidis, L., Gosper, C. R., Grierson, P. F., Lemson, K., Lyons, T., Macfarlane, C., O'Connor, M. H., Scott, J. K., Standish, R. J., Stock, W. D., van Etten, E. J. B., Wardell-Johnson, G. W., & Watson, A. (2012). Facilitating adaptation of biodiversity to climate change: a conceptual framework applied to the world's largest Mediterranean-climate woodland. *Climatic Change, 110*(1-2), 227-248.

Provost, F., & Fawcett, T. (1998). Robust classification systems for imprecise environments. *In: Proc. AAAI-98*, 706–713.

Reed, B. C., Brown, J. F., VanderZee, D., Loveland, T. R., Merchant, J. W., & Ohlen, D. O. (1994). Measuring Phenological Variability from Satellite Imagery. *Journal of Vegetation Science, 5*(5), 703-714.

Reside, A. E., Welbergen, J. A., Phillips, B. L., Wardell-Johnson, G. W., Keppel, G., Ferrier, S., Williams, S. E., & VanDerWal, J. (2014). Characteristics of climate change refugia for Australian biodiversity. *Austral Ecology, 39*(8), 887-897.

Richards, J. A. (1993). *Remote Sensing Digital Image Analysis: An Introduction*. Heidelberg: Springer-Verlag.

Robertson, M. P., Villet, M. H., & Palmer, A. R. (2004). A fuzzy classification technique for predicting species' distributions: applications using invasive alien plants and indigenous insects. *Diversity and Distributions, 10*(5-6), 461-474.

Robinson, T. P., Novelly, P. E., Watson, I. W., Corner, R., Thomas, P., Schut, A. G. T., Jansen, S., & Shepherd, D. (2009). *Towards an approach for remote sensing-based rangeland condition assessment in north western Australia.* Paper presented at the Surveying & Spatial Sciences Institute Biennial International Conference, Adelaide.

Robinson, V. B. (2003). A Perspective on the Fundamentals of Fuzzy Sets and their Use in Geographic Information Systems. *Transactions in GIS, 7*(1), 3-30.

Rollin, E. M., Milton, E. J., & Roche, P. (1994). The influence of weathering and lichen cover on the reflectance spectra of granitic rocks. *Remote Sensing of Environment, 50*(2), 194-199.

Rosauer, D. F., Ferrier, S., Williams, K. J., Manion, G., Keogh, J. S., & Laffan, S. W. (2014). Phylogenetic generalised dissimilarity modelling: a new approach to analysing and predicting spatial turnover in the phylogenetic composition of communities. *Ecography, 37*(1), 21-32.

Rowan, L. C., & Mars, J. C. (2003). Lithologic mapping in the Mountain Pass, California area using Advanced Spaceborne Thermal Emission and Reflection Radiometer (ASTER) data. *Remote Sensing of Environment, 84*(3), 350-366.

Rowan, L. C., Mars, J. C., & Simpson, C. J. (2005). Lithologic mapping of the Mordor, NT, Australia ultramafic complex by using the Advanced Spaceborne Thermal Emission and Reflection Radiometer (ASTER). *Remote Sensing of Environment, 99*(1–2), 105-126.

Roy, D. P., Ju, J., Kline, K., Scaramuzza, P. L., Kovalskyy, V., Hansen, M., Loveland, T. R., Vermote, E., & Zhang, C. (2010). Web-enabled Landsat Data (WELD): Landsat ETM+ composited mosaics of the conterminous United States. *Remote Sensing of Environment, 114*(1), 35-49.

Roy, D. P., Ju, J., Lewis, P., Schaaf, C., Gao, F., Hansen, M., & Lindquist, E. (2008). Multi-temporal MODIS-Landsat data fusion for relative radiometric normalization, gap filling, and prediction of Landsat data. *Remote Sensing of Environment, 112*(6), 3112-3130.

Saaty, T. L. (1979). Applications of analytical hierarchies. *Mathematics and Computers in Simulation, 21*(1), 1-20.

Saaty, T. L. (1994). Fundamentals of decision making with the Analytic Hierarchy Process (Vol. 6, pp. 473). Pittsburgh: RWS Publications.

Saint-Joan, D., & Desachy, J. (1995, 20-24 Mar 1995). *A fuzzy expert system for geographical problems: an agricultural application.* Paper presented at the Fuzzy Systems, International Joint Conference of the Fourth IEEE International Conference on Fuzzy Systems and The Second International Fuzzy Engineering Symposium, Proceedings of 1995 IEEE Int.

Sakamoto, T., Yokozawa, M., Toritani, H., Shibayama, M., Ishitsuka, N., & Ohno, H. (2005). A crop phenology detection method using time-series MODIS data. *Remote Sensing of Environment, 96*(3-4), 366-374.

Sander, J., & Wardell-Johnson, G. (2011a). Fine-scale patterns of species and phylogenetic turnover in a global biodiversity hotspot: Implications for climate change vulnerability. *Journal of Vegetation Science, 22*(5), 766-780.

Sander, J., & Wardell-Johnson, G. (2011b). Impacts of soil fertility on species and phylogenetic turnover in the high - rainfall zone of the Southwest Australian global biodiversity hotspot. *Plant and Soil, 345*(1-2), 103-124.

Sander, J., & Wardell-Johnson, G. (2012). Defining and characterizing high-rainfall Mediterranean climates. *Plant Biosystems, 146*(2), 451-460.

Satterwhite, M. B., Henley, P. J., & Carney, J. M. (1985). Effects of lichens on the reflectance spectra of granitic rock surfaces. *Remote Sensing of Environment, 18*(2), 105-112.

Savitzky, A., & Golay, M. J. E. (1964). Smoothing and Differentiation of Data by Simplified Least Squares Procedures. *Analytical Chemistry, 36*(8), 1627-1639.

Schauffler, M., & Jacobson, G. L. (2002). Persistence of Coastal Spruce Refugia during the Holocene in Northern New England, USA, Detected by Stand-Scale Pollen Stratigraphies. *Journal of Ecology, 90*(2), 235-250.

Scheffe, H. (1999). *The Analysis of Variance* (Wiley Classics Library ed.). New York: Wiley-Interscience.

Schoknecht, N. (1997). Soil groups of Western Australia. A simple guide to the main soils of Western Australia. In A. W. Australia (Ed.), *Resource Management Technical Report 171*. Perth.

Schoknecht, N. (2002). Soil Groups of Western Australia - a guide to the main soils of Western Australia, Edition 3 *Resource Management Technical Report 246*. Department of Agriculture, Western Australia.

Schoknecht, N., Tille, P., & Purdie, B. (2004). Soil-landscape mapping in south-western Australia. An overview of methodology and outputs *Resource Management Technical Report*: Department of Agriculture, State of Western Australia.

Schulte, S., De Witte, V., Nachtegael, M., Van der Weken, D., & Kerre, E. E. (2007). Fuzzy random impulse noise reduction method. *Fuzzy Sets and Systems, 158*(3), 270-283.

Schut, A. G. T., Stephens, D. J., Stovold, R. G. H., Adams, M., & Craig, R. L. (2009). Improved wheat yield and production forecasting with a moisture stress index, AVHRR and MODIS data. *Crop and Pasture Science, 60*(1), 60-70.

Schut, A. G. T., Wardell-Johnson, G. W., Yates, C. J., Keppel, G., Baran, I., Franklin, S. E., Hopper, S. D., Van Niel, K. P., Mucina, L., & Byrne, M. (2014). Rapid Characterisation of Vegetation Structure to Predict Refugia and Climate Change Impacts across a Global Biodiversity Hotspot. *PLoS ONE, 9*(1), e82778.

Schut, A. G. T., Wardell-Johnson, G. W., Yates, C. J., Keppel, G., Earls, C., & Franklin, S. E. (2010). Characterizing ecosystem habitats on granite outcrops. *The 15th Australasian Remote Sensing and Photogrammetry Conference*.

Schwartz, M. D., Reed, B. C., & White, M. A. (2002). Assessing satellite-derived start-of-season measures in the conterminous USA. *International Journal of Climatology, 22*(14), 1793-1805.

Simoniello, T., Lanfredi, M., Liberti, M., Coppola, R., & Macchiato, M. (2008). Estimation of vegetation cover resilience from satellite time series. *Hydrol. Earth Syst. Sci., 12*(4), 1053-1064.

Smith, G. T. (1962). The Flora of the Granite Rocks of the Porongurup Range, South-Western Australia. *Journal of the Royal Society of Western Australia, 45*(1), 18-23.

Smith, R., Adams, M., Maier, S., Craig, R., Kristina, A., & Maling, I. (2007). Estimating the area of stubble burning from the number of active fires detected by satellite. *Remote Sensing of Environment, 109*(1), 95-106.

Smith, R. L., Kolenikov, S., & Cox, L. H. (2003). Spatiotemporal modeling of PM2.5 data with missing values. *Journal of Geophysical Research, 108*, 9004-9015.

Song, Q., & Chissom, B. S. (1993). Forecasting enrollments with fuzzy time series - Part I. *Fuzzy Sets and Systems, 54*(1), 1-9.

Song, Q., & Chissom, B. S. (1994). Forecasting enrollments with fuzzy time series - part II. *Fuzzy Sets and Systems, 62*(1), 1-8.

Sonnenschein, R., Kuemmerle, T., Udelhoven, T., Stellmes, M., & Hostert, P. (2011). Differences in Landsat-based trend analyses in drylands due to the choice of vegetation estimate. *Remote Sensing of Environment, 115*(6), 1408-1420.

Soudani, K., le Maire, G., Dufrêne, E., François, C., Delpierre, N., Ulrich, E., & Cecchini, S. (2008). Evaluation of the onset of green-up in temperate deciduous broadleaf forests derived from Moderate Resolution Imaging Spectroradiometer (MODIS) data. *Remote Sensing of Environment, 112*(5), 2643-2655.

Specht, R. L. (1970). Vegetation, In: Australian Environment (ed. G. W. Leeper), 4th Edn (pp. 44–67). CSIRO and Melbourne University Press, Melbourne.

Stewart, J. R., Lister, A. M., Barnes, I., & Dalén, L. (2010). Refugia revisited: individualistic responses of species in space and time. *Proceedings of the Royal Society B: Biological Sciences, 277*(1682), 661-671.

Studer, S., Stöckli, R., Appenzeller, C., & Vidale, P. L. (2007). A comparative study of satellite and ground-based phenology. *International Journal of Biometeorology, 51*(5), 405-414.

Suzuki, R., Nomaki, T., & Yasunari, T. (2003). West-east contrast of phenology and climate in northern Asia revealed using a remotely sensed vegetation index. *International Journal of Biometeorology, 47*(3), 126-138.

Svenning, J.-C., & Condit, R. (2008). Biodiversity in a Warmer World. *Science, 322*(5899), 206-207.

Takhtajan, A. (1986). Floristic Regions of the World (pp. 544). Berkeley: University of California Press.

Tapper, S.-L., Byrne, M., Yates, C. J., Keppel, G., Hopper, S. D., Niel, K. V., Schut, A. G. T., Mucina, L., & Wardell-Johnson, G. W. (2014). Prolonged isolation and persistence of a common endemic on granite outcrops in both mesic and semi-arid environments in south-western Australia. *Journal of Biogeography, 41*(11), 2032-2044.

Thackway, R., & Cresswell, I. D. (1995). *An Interim Biogeographic Regionalisation for Australia: a framework for establishing the national system of reserves*. Australian Nature Conservation Agency, (4). Canberra.

Thackway, R., & Cresswell, I. D. (1997). A bioregional framework for planning the national system of protected areas in Australia. *Natural Areas Journal, 17*(3), 241-247.

Thompson, I., Mackey, B., McNulty, S., & Mosseler, A. (2009). Forest Resilience, Biodiversity, and Climate Change. A synthesis of the biodiversity/resilience/stability relationship in forest ecosystems. *Technical Series 43* (pp. 67). Montreal: Secretariat of the Convention on Biological Diversity.

Tille, P., & Lantzke, N. (1990). *The Busselton-Margaret River-Augusta land capability study*. Land Resources Series No. 5, Department fo Agriculture. Perth, Western Australia.

Tille, P. J. (2006). Soil-landscapes of Western Australia's Rangelands and Arid Interior. In D. o. A. a. Food (Ed.), *Resource Management Technical Report 313*. Perth.

Tille, P. J., Moore, G., & Griffin, E. (1998). Soils and landscapes of south-western Australia. In: 'Soilguide - A handbook for understanding and managing agricultural soils'. *Agriculture Western Australia, Bulletin 4343*, 31-42.

Timbal, B., Arblaster, J. M., & Power, S. (2006). Attribution of the Late-Twentieth-Century Rainfall Decline in Southwest Australia. *Journal of Climate, 19*(10), 2046-2062.

Townshend, J., Justice, C., Li, W., Gurney, C., & McManus, J. (1991). Global land cover classification by remote sensing: present capabilities and future possibilities. *Remote Sensing of Environment, 35*(2–3), 243-255.

Trenberth, K. E. (1983). What are the Seasons? *Bulletin of the American Meteorological Society, 64*(11), 1276-1282.

Trewin, B. (2013). A daily homogenized temperature data set for Australia. *International Journal of Climatology, 33*(6), 1510-1529.

Tuanmu, M.-N., Viña, A., Bearer, S., Xu, W., Ouyang, Z., Zhang, H., & Liu, J. (2010). Mapping understory vegetation using phenological characteristics derived from remotely sensed data. *Remote Sensing of Environment, 114*(8), 1833-1844.

Tucker, C. J. (1979). Red and photographic infrared linear combinations for monitoring vegetation. *Remote Sensing of Environment, 8*(2), 127-150.

Tukey, J. W. (1949). Comparing Individual Means in the Analysis of Variance. *Biometrics, 5*(2), 99-114.

Tukey, J. W. (1977). *Exploratory Data Analysis*: Addison-Wesley.

Turcotte, K. M., Lulla, K., & Venugopal, G. (1993). Mapping small-scale vegetation changes of Mexico. *Geocarto International, 8*(4), 73-85.

Twidale, C. R. (1997). The great age of some Australian landforms: examples of, and possible explanations for, landscape longevity. *Geological Society, London, Special Publications, 120*(1), 13-23.

U.S. Geological Survey. (2012). U.S. Geological Survey's Earth Resources Observation and Science (EROS) Center. from U.S. Department of the Interior http://earthexplorer.usgs.gov

van Ruitenbeek, F. J. A., Debba, P., van der Meer, F. D., Cudahy, T., van der Meijde, M., & Hale, M. (2006). Mapping white micas and their absorption wavelengths using hyperspectral band ratios. *Remote Sensing of Environment, 102*(3–4), 211-222.

Verbesselt, J., Hyndman, R., Newnham, G., & Culvenor, D. (2010). Detecting trend and seasonal changes in satellite image time series. *Remote Sensing of Environment, 114*(1), 106-115.

Verboom, W. H., & Pate, J. S. (2003). Relationships between cluster root-bearing taxa and laterite across landscapes in southwest Western Australia: an approach using airborne radiometric and digital elevation models. *Plant and Soil, 248*(1-2), 321-333.

Wardell-Johnson, G., & Horwitz, P. (1996). Conserving biodiversity and the recognition of heterogeneity in ancient landscapes: a case study from south-western Australia. *Forest Ecology and Management, 85*(1–3), 219-238.

Wardell-Johnson, G., & Horwitz, P. (2000). The recognition of heterogeneity and restricted endemism in the management of forested ecosystems in south-western Australia. *Australian Forestry, 63*(3), 218-225.

Wardell-Johnson, G., & Roberts, J. D. (1993). Biogeographic Barriers in a Subdued Landscape: The Distribution of the Geocrinia rosea (Anura: Myobatrachidae) Complex in South-Western Australia. *Journal of Biogeography, 20*(1), 95-108.

Wardell-Johnson, G., Wardell-Johnson, A., Bradby, K., Robinson, T., Bateman, P. W., Williams, K., Keesing, A., Braun, K., Beckerling, J., & Burbridge, M. (2016). Application of a Gondwanan perspective to restore ecological integrity in the south-western Australian global biodiversity hotspot. *Restoration Ecology*, n/a-n/a.

Wardell-Johnson, G., Williams, J., Hill, K., & Cummings, R. (1997). Evolutionary biogeography and contemporary distribution of eucalypts. In Eucalypt Ecology: Individuals to Ecosystems. (Eds. Williams, J. and Woinowski, J.) *Cambridge University Press*, 92-128.

Wardell-Johnson, G., & Williams, M. (1996). A floristic survey of the Tingle Mosaic, south-western Australia: applications in land use planning and management. *Journal of the Royal Society of Western Australia, 79*, 249-264.

Wardell-Johnson, G., & Williams, M. (2000). Edges and gaps in mature karri forest, south-western Australia: logging effects on bird species abundance and diversity. *Forest Ecology and Management, 131*(1–3), 1-21.

Wardell-Johnson, G. W., Keppel, G., & Sander, J. (2011). Climate change impacts on the terrestrial biodiversity and carbon stocks of Oceania. *Pacific Conservation Biology, 17*(3), 220-240.

Wardell-Johnson, G. W., Van Niel, K. P., Yates, C. J., Byrne, M., Hopper, S. D., Mucina, L., & Franklin, S. E. (2009). Protecting the safe havens: will granite outcrop environments serve as refuges for flora threatened by anthropogenic climate change (pp. 109). Perth: ARC linkage project description (LP0990914).

Warner, T. A., & Campagna, D. J. (2013). Remote Sensing with IDRISI. *Geocarto Internacional Centre Ltd., Hong Kong*.

Watts, D. R., Harris, N. B., & Group, T. N. G. S. W. (2005). Mapping granite and gneiss in domes along the North Himalayan antiform with ASTER SWIR band ratios. *Geological Society of America, 117*(7-8), 879-886.

White, M. A., Nemani, R. R., Thornton, P. E., & Running, S. W. (2002). Satellite Evidence of Phenological Differences between Urbanized and Rural Areas of the Eastern United States Deciduous Broadleaf Forest. *Ecosystems, 5*(3), 260-273.

White, M. A., Running, S. W., & Thornton, P. E. (1999). The impact of growing-season length variability on carbon assimilation and evapotranspiration over 88 years in the eastern US deciduous forest. *International Journal of Biometeorology, 42*(3), 139-145.

White, M. A., Thornton, P. E., & Running, S. W. (1997). A continental phenology model for monitoring vegetation responses to interannual climatic variability. *Global Biogeochemical Cycles, 11*(2), 217-234.

Whittaker, R. H. (1977). Evolution of species diversity in land communities. *Evolutionary Biology, 10*, 1-67.

Whittaker, R. J., Willis, K. J., & Field, R. (2001). Scale and species richness: towards a general, hierarchical theory of species diversity. *Journal of Biogeography, 28*(4), 453-470.

Withers, P. C. (2000). Overview of granite outcrops in Western Australia. *Journal of the Royal Society of Western Australia, 83*, 103-108.

Wolfe, R. E., Nishihama, M., Fleig, A. J., Kuyper, J. A., Roy, D. P., Storey, J. C., & Patt, F. S. (2002). Achieving sub-pixel geolocation accuracy in support of MODIS land science. *Remote Sensing of Environment, 83*(1–2), 31-49.

Yates, C. J., Elith, J., Latimer, A. M., Le Maitre, D., Midgley, G. F., Schurr, F. M., & West, A. G. (2010). Projecting climate change impacts on species distributions in megadiverse South African Cape and Southwest Australian Floristic Regions: Opportunities and challenges. *Austral Ecology, 35*(4), 374-391.

Yates, C. J., Hopper, S. D., Brown, A., & Leeuwen, S. v. (2003). Impact of Two Wildfires on Endemic Granite Outcrop Vegetation in Western Australia. *Journal of Vegetation Science, 14*(2), 185-194.

Yates, C. J., Ladd, P. G., Coates, D. J., & McArthur, S. (2007). Hierarchies of cause: understanding rarity in an endemic shrub Verticordia staminosa (Myrtaceae) with a highly restricted distribution. *Australian Journal of Botany, 55*(3), 194-205.

Yeung, D. S., & Tsang, E. C. C. (1997). Weighted fuzzy production rules. *Fuzzy Sets and Systems, 88*(3), 299-313.

Zadeh, L. A. (1965). Fuzzy sets. *Information and Control, 8*(3), 338-353.

Zhang, L., Li, X., Yuan, Q., & Liu, Y. (2014). Object-based approach to national land cover mapping using HJ satellite imagery. *Journal of Applied Remote Sensing, 8*(1), 083686-083686.

Zhang, X., Friedl, M. A., & Schaaf, C. B. (2006). Global vegetation phenology from Moderate Resolution Imaging Spectroradiometer (MODIS): Evaluation of global patterns and comparison with in situ measurements. *Journal of Geophysical Research: Biogeosciences, 111*(G4).

Zhang, X., Friedl, M. A., Schaaf, C. B., Strahler, A. H., Hodges, J. C. F., Gao, F., Reed, B. C., & Huete, A. (2003). Monitoring vegetation phenology using MODIS. *Remote Sensing of Environment, 84*(3), 471-475.

Zhang, X., & Goldberg, M. D. (2011). Monitoring fall foliage coloration dynamics using time-series satellite data. *Remote Sensing of Environment, 115*(2), 382-391.